NATIONAL TECHNICAL UNIVERSITY OF ATHENS
SCHOOL OF NAVAL ARCHITECTURE & MARINE ENGINEERING
DIVISION OF MARINE ENGINEERING

Diploma Thesis

Elastic Shaft Alignment of a Container Vessel

Stavros Siamantas

Thesis Committee:

Supervisor:	**C. I. Papadopoulos,**	**Assistant Professor NTUA**
Members:	**L. Kaiktsis,**	**Associate Professor NTUA**
	G. Papalambrou,	**Assistant Professor NTUA**

Athens, March 2018

ΕΘΝΙΚΟ ΜΕΤΣΟΒΙΟ ΠΟΛΥΤΕΧΝΕΙΟ
ΣΧΟΛΗ ΝΑΥΠΗΓΩΝ ΜΗΧΑΝΟΛΟΓΩΝ ΜΗΧΑΝΙΚΩΝ
ΤΟΜΕΑΣ ΝΑΥΤΙΚΗΣ ΜΗΧΑΝΟΛΟΓΙΑΣ

Διπλωματική Εργασία

Ελαστική Ευθυγράμμιση Αξονικού Συστήματος Πλοίου Μεταφοράς Εμπορευματοκιβωτίων

Σταύρος Σιαμαντάς

Εξεταστική επιτροπή:

Επιβλέπων:	**Χ. Ι. Παπαδόπουλος,**	**Επίκουρος Καθηγητής ΕΜΠ**
Μέλη:	**Λ. Καϊκτσής,**	**Αναπληρωτής Καθηγητής ΕΜΠ**
	Γ. Παπαλάμπρου,	**Επίκουρος Καθηγητής ΕΜΠ**

Αθήνα, Μάρτιος 2018

Acknowledgements

After an intensive period, today is the day: writing this note of gratitude is the finishing touch on my thesis. It has been a period of intense learning for me, not only in the scientific arena, but also on a personal level. I would like to reflect on the people who have supported and helped me so much throughout this period.

I would first like to thank my thesis advisor Assistant Professor Christos Papadopoulos. The door to Prof. Papadopoulos' office was always open whenever I ran into a trouble spot or had a question about my research or writing. He consistently allowed this paper to be my own work, but steered me in the right direction whenever he thought I needed it.

Special thanks goes out to Anastassis Charitopoulos for the vital support and relentless encouragement he showed to me during the preparation of my Diploma Thesis. The end result of my Diploma Thesis wouldn't be at this level, if it hadn't been for him.

At this point, I would like to thank my friends and classmates for their friendship and assistance throughout our studies in NTUA. I cannot express how grateful I am towards my fellow classmates, Spyridon Antonopoulos and Sotirios Nanopoulos for their assistance, advice and company over the last year.

Last, but surely not least, I must express my deepest gratitude to my parents, my brothers and to my partner in crime. This journey would not have been possible without their support. I am extremely grateful to my parents for their love, caring and sacrifices for raising, educating and preparing me for my future. I am very thankful to my brothers, for their continuing support and understanding throughout my entire life till this very moment. To be honest, there are no words to express my gratitude to my partner in crime; thank you for everything.

Abstract

Proper shaft alignment is vital for safe operation and performance of a vessel. Until recently, a static analysis of propulsion systems, taking into consideration bearing stiffness foundation, dynamic loading of the propeller and cold and hot conditions of the main engine have been common practice in the maritime sector. In 2015, Classification Societies BV and ABS released rule notations concerning the shaft alignment procedure onboard large cargo ships. Both methodologies of shafting alignment take into consideration hull deformations, oil film characteristics and stiffness of the bearings' foundation. The regulations are applicable to a wide range of cargo ships, in particular to ships of all types having propulsion power per shaft line greater or equal to 30 MW, to container ships having propulsion power per shaft line greater or equal to 15 MW, and to liquefied gas carriers having propulsion power per shaft line greater or equal to 10 MW.

In the present work, the shafting system of a typical 10K containership driven by a two-stroke low-speed Diesel engine is studied. The propulsion shaft of the ship is modelled as a statically indeterminate multi-supported beam. For a reference shaft alignment plan, the static equilibrium of the shaft is calculated using matrix analysis, taking elasticity of the bearing foundations into account. A detailed finite element model of the ship, extending from the aft-end to the fore engine room bulkhead, is generated. The generated mesh is characterized by quality that is in compliance with the requirements set by Classification Societies. The FE model is utilised to accurately calculate hull deflections for a series of representative loading conditions of the vessel.

The aforementioned hull deflections are used for calculation of the additional vertical offsets of the bearings due to hull bending, and the corresponding effect on shaft equilibrium and bearing reactions. In those calculations, a quasi-static loading of the propulsion shaft is considered, taking into account bearing foundation stiffness and oil film characteristics of the bearings. Several operational parameters of bearing operation, such as bearing load, minimum film thickness, maximum pressure and power loss are calculated for each loading condition of the vessel.

Based on the above, conclusions are drawn regarding the effects of hull deflections on (a) the shaft alignment plan of the vessel, (b) the bearing hydrodynamic lubrication characteristics, and (c) on friction power loss of the system. Additionally, a comparative analysis of the key parameters affecting shaft alignment is conducted. The present results demonstrate that bearing foundation stiffness has to be accounted for in the shaft alignment calculations, for obtaining accurate and valid results. Further, in cases where shaft alignment is applied before installation of the accommodation block, the results show that the corresponding hull deflections after block installation affect moderately the bearing reactions, and therefore, this effect should not be disregarded in the design stage. Finally, the effect of shaft rigidity on hull deformation has been assessed; the results demonstrate that shaft rigidity affects substantially bearing offsets at different loading conditions and the corresponding bearing loads, therefore, it should be included in the finite element model of the vessel structure.

Σύνοψη

Η σωστή ευθυγράμμιση του αξονικού συστήματος ενός πλοίου είναι ζωτικής σημασίας για την ασφαλή λειτουργία και απόδοση αυτού. Μέχρι προσφάτως, η συνήθης διαδικασία υπολογισμού συμπεριελάμβανε τη χρήση ενός μοντέλου στατικής ισορροπίας του άξονα, λαμβάνοντας υπόψη την ελαστικότητα της βάσης των εδράνων, τη δυναμική φόρτιση της έλικας, καθώς και την ψυχρή και θερμή κατάσταση της κύριας μηχανής. Το 2015, ο Γαλλικός και ο Αμερικανικός νηογνώμονας (BV και ABS) εξέδωσαν κανόνες σχετικούς με τη διαδικασία ευθυγράμμισης των αξόνων επί μεγάλων φορτηγών πλοίων. Καί οι δύο κανονισμοί ευθυγράμμισης άξονα λαμβάνουν υπόψη τις παραμορφώσεις της γάστρας, τα χαρακτηριστικά του λιπαντικού φιλμ των εδράνων και την ακαμψία της βάσης στήριξής τους. Οι κανονισμοί αφορούν σε ένα ευρύ φάσμα μεγάλων φορτηγών πλοίων, ειδικότερα σε πλοία παντός τύπου με ισχύ πρόωσης ανά άξονα ίση ή μεγαλύτερη των 30 MW, σε πλοία μεταφοράς εμπορευματοκιβωτίων με ισχύ πρόωσης ανά άξονα ίση ή μεγαλύτερη των 15 MW και σε πλοία μεταφοράς υγροποιημένου αερίου με ισχύ πρόωσης ανά άξονα ίση ή μεγαλύτερη των 10 MW.

Στην παρούσα εργασία, μελετήθηκε το αξονικό σύστημα ενός τυπικού πλοίου μεταφοράς εμπορευματοκιβωτίων, με κύρια διάταξη πρόωσης αποτελούμενη από βραδύστροφο δίχρονο κινητήρα Diesel. Το αξονικό σύστημα του σκάφους αναπαρεστήθη ως υπερστατική δοκός πολλαπλών στηρίξεων. Η επίλυση του φορέα πραγματοποιήθηκε με χρήση μητρωικής ανάλυσης, ενώ ελήφθη υπόψη η ελαστικότητα των βάσεων των εδράνων. Συγκεκριμένα, δημιουργήθηκε ένα λεπτομερές μοντέλο πεπερασμένων στοιχείων της γάστρας του πλοίου, το οποίο εκτείνεται από το πρυμναίο άκρο έως και την πρωραία φρακτή του μηχανοστασίου. Το παραχθέν πλέγμα χαρακτηρίζεται από υψηλή ποιότητα, σύμφωνη με τις απαιτήσεις που έχουν καθορίσει οι νηογνώμονες. Το μοντέλο πεπερασμένων στοιχείων χρησιμοποιήθηκε για τον ακριβή υπολογισμό των παραμορφώσεων της γάστρας, για μια σειρά αντιπροσωπευτικών καταστάσεων φόρτωσης του σκάφους.

Οι προαναφερθείσες παραμορφώσεις της γάστρας χρησιμοποιήθηκαν για τον υπολογισμό επιπρόσθετων κατακόρυφων μετατοπίσεων των εδράνων λόγω κάμψης του πλοίου. Οι επιπρόσθετες μετατοπίσεις χρησιμοποιήθηκαν για τον υπολογισμό των αντιδράσεων των εδράνων σε διαφορετικές καταστάσεις φόρτωσης. Στο πλαίσιο αυτό, θεωρήθηκε ψευδο-στατική φόρτιση του αξονικού συστήματος, λαμβάνοντας υπόψη την ελαστικότητα της βάσης των εδράνων καθώς και τα χαρακτηριστικά του λιπαντικού φιλμ των εδράνων. Για κάθε κατάσταση φόρτωσης του πλοίου, υπολογίστηκαν διάφορες παράμετροι λειτουργίας του εδράνου, όπως το φέρον φορτίο, το ελάχιστο πάχος του λιπαντικού φιλμ, η μέγιστη πίεση του λιπαντικού και οι απώλειες ισχύος.

Με βάση τα παραπάνω, εξήχθησαν συμπεράσματα σχετικά με τις επιδράσεις των παραμορφώσεων της γάστρας (α) στο πλάνο ευθυγράμμισης του αξονικού συστήματος του σκάφους, (β) στα χαρακτηριστικά υδροδυναμικής λίπανσης των εδράνων, και (γ) στην απώλεια ισχύος λόγω τριβής του συστήματος. Επιπρόσθετα, διεξήχθη μια συγκριτική ανάλυση των βασικών παραμέτρων που επηρεάζουν την

ευθυγράμμιση του άξονα. Καταδείχθηκε ότι, για να εξαχθούν ακριβή και έγκυρα αποτελέσματα, η ελαστικότητα της βάσης των εδράνων πρέπει να ληφθεί υπόψη στους υπολογισμούς ευθυγράμμισης του αξονικού συστήματος. Επιπλέον, για τις περιπτώσεις που το πλάνο ευθυγράμμισης του αξονικού συστήματος εφαρμόζεται πριν την τοποθέτηση της υπερκατασκευής του πλοίου, τα αποτελέσματα κατέδειξαν ότι οι επιπρόσθετες μετατοπίσεις της γάστρας μετά την εγκατάσταση της υπερκατασκευής επηρεάζουν τις αντιδράσεις των εδράνων, επομένως, ο παράγοντας αυτός δεν θα πρέπει να αγνοείται στο στάδιο του σχεδιασμού. Τέλος, αξιολογήθηκε η επίδραση της ακαμψίας του άξονα στις παραμορφώσεις της γάστρας στο πρυμναίο άκρο του πλοίου. Τα αποτελέσματα κατέδειξαν ότι η ακαμψία του άξονα επηρεάζει σημαντικά τις παραμορφώσεις της γάστρας σε διαφορετικές καταστάσεις φόρτωσης, καθώς και τα αντίστοιχα φορτία των εδράνων, και συνεπώς η ακαμψία του άξονα πρέπει να συμπεριλαμβάνεται στο μοντέλο πεπερασμένων στοιχείων του πλοίου.

Table of Contents

Nomenclature

A	Admiralty coefficient
c	Bearing radial clearance [m]
D	Inner bearing diameter [m]
d	Outer shaft diameter [m]
e	Bearing eccentricity [m]
E	Young's modulus of elasticity [Pa]
f	Generalised load [N, N m]
f*	Bearing friction coefficient
F	Friction force [N]
h	Lubricant film thickness [m]
h_{min}	Minimum lubricant film thickness [m]
H	Wave height [m]
L	Bearing length [m]
p	Pressure [Pa]
P_{loss}	Friction power loss [W]
R	Bearing inner radius [m]
S	Sommerfeld number
U	Tangential velocity of the shaft
W	Bearing external load [N]
θ	Hydrodynamic film angle [degrees]
λ	Wave length [m]
μ	Dynamic Viscosity [Pa s]
σ	Influence factor
ϕ, phi	Attitude angle [degrees]
ω	Angular velocity [s^{-1}]

List of Figures

List of Tables

1. Introduction

The propulsion system of cargo vessels typically comprises a two-stroke diesel engine and a shafting system transmitting power to the propeller. In ships with a four-stroke diesel engine installed, a reduction gearbox is required to transmit the generated power to the propeller in the most efficient rotational speed range (**Figure 1.1**). Radial shaft loads (propeller/shaft/engine weights) need to be supported by journal bearings (stern tube bearings, line bearings, crankshaft bearings), while axial loads are transmitted to the ship's structure by the main engine thrust bearing [1]. Nowadays maritime industry demands larger and lighter ships to maximize the carrying capacity, while keeping the building and operational costs relatively low. Larger ships translates to larger power plants and consequently greater torsional loads applied to the shafting system. To overcome that threat, a shaft with increased diameter is installed, which in return increases the overall weight and stiffness of the system. On the other hand, hull structure is more flexible due to the reduced thickness of high tensile strength steel. We can observe that the synergy of the flexible hull structure and the stiff shafting system is an important issue for reliable operation of the vessel, which needs to be addressed in the design stage by means of detailed shaft alignment analysis.

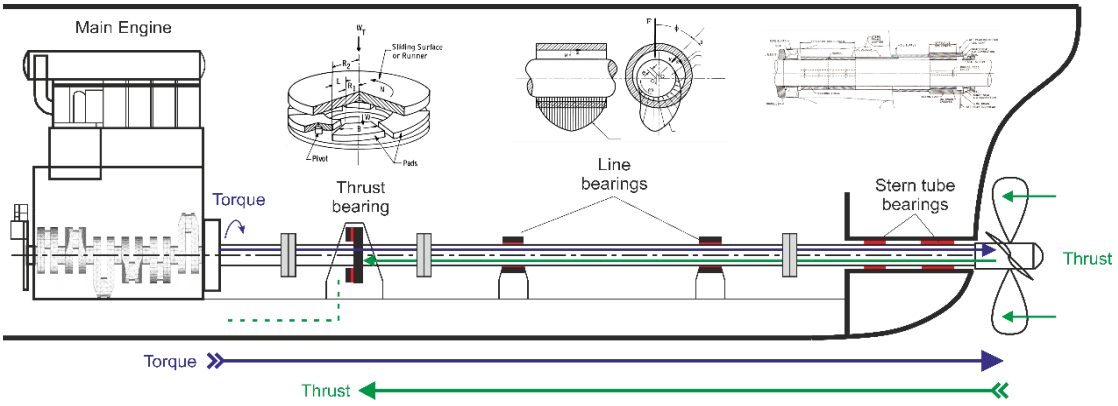

FIGURE 1.1: Typical arrangement of the propulsion system of a cargo vessel.

Shaft alignment is concerned with the determination of the number of bearings, their longitudinal position and their vertical offset, with the ultimate goal of an optimized shafting system complying to bearing loading criteria. The successful application of a shaft alignment plan is essential for stable and efficient operation of the propulsion system with decreased bearing wear, increased lifetime and decreased maintenance costs.

A key influence factor of the shaft alignment is the hull deformation of the vessel. Until recently, shaft alignment calculations were performed for the condition in which the alignment would be conducted. However, the ship operates in a wide range of different loading conditions throughout its lifetime. As mentioned above, ships are getting larger, thus more flexible. It is imperative that the designer takes into account the hull deflections for all the anticipated loading conditions to ensure a fully

optimized shaft alignment plan. To this extent, detailed Finite Element Analysis (FEA) are to be utilized for the accurate prediction of hull deflections.

Another factor playing an important role in the shaft alignment process is the stiffness of the bearing foundation. The shafting system is modelled as an assembly of beam elements supported at the bearing locations. Contrary to that modelling assumption, all supporting points are very stiff, not completely rigid though. The bearings' foundation is expected to deform elastically under the weight of the shaft and all the other components of the system. Elastic deformation of the bearings' foundation should be taken into consideration in the design stage of the shaft alignment plan to approximate more accurately the performance of the shafting system.

During operation of the main engine, the engine components near the combustion chambers generally have a higher temperature (approximately 80-90 °C) in comparison to the components near the foundation of the engine (approximately 30-40 °C). Thermal expansion of the engine components is generally three-dimensional, but only the vertical component affects the alignment of the shafting system. The overall offsets of the main engine bearings, due to thermal expansion, can be assumed to be the composition of two components; a parallel vertical offset and a non-uniform parabolic offset. The parallel vertical offset is attributed mainly to the increased mean temperature of the main engine's foundation, whereas the parabolic is attributed to the larger expansion of the components near the combustion chambers, in comparison to the smaller expansion of the components near the engine foundation. Shaft alignment calculations need to incorporate vertical offsets of the M/E bearings due to thermal expansion to achieve a shaft alignment plan optimized for operational characteristics of the vessel as well.

Last but not least, the Marine Engineer must keep in mind the operating principle of the journal bearings, namely hydrodynamic lubrication. The existence of a thick lubricating oil film on which the shaft floats is another key parameter that contributes to the final vertical offsets of the bearings. Oil film thickness is dependent on a set of operational parameters such as oil temperature, oil viscosity and rotational speed of the shaft. It is obvious that the wide range of loading conditions and the uncertainty of shaft loads due to engine and propeller operation affect oil film formation and may alter all relevant calculations of shaft equilibrium.

1.1. Literature Review

Numerous concerns about the capability of a shafting system to operate at a satisfactory level under different vessel loading conditions have been raised in related literature. Devanney and Kennedy (2003) [2] have highlighted the drastic deterioration of tanker newbuilding standards in the 90's, and specifically, the effect on the reliability of the shafting system. They emphasized on the severity of stern tube bearing failures in modern VLCCs and ULCCs, which may lead to loss of propulsion and vessel immobilisation. According to the authors, the main reason of this failure is the design of propulsion shafts with decreased diameters, followed by improper shafting alignment. They suggested that (a) hull deflections should be taken into consideration for a wide range of loading conditions of the ship, (b) time varying loads on the stern tube bearing should be incorporated in the relevant calculations, (c) heat dissipation in the lubricant domain should be considered, and (d) the engine room structure should be reinforced, to minimise additional offset of the bearings.

In his work, Šverko (2003) [3] has underlined several design concerns in propulsion shafting, especially for VLCC and large bulk carriers. He suggested that shaft alignment of these vessels is very sensitive to hull deflections; such behavior is attributed to increased hull flexibility of such ships (due to increased length and scantling optimization) and increased stiffness of the propulsion shaft (due to increased power output and therefore larger shaft diameters). It was concluded an optimal set of bearing offsets for the vessel on even keel may exhibit a reasonably good performance at other loading conditions of the vessel, should the actual hull deformations be predicted accurately; however, since hull deflections cannot be easily calculated with such accuracy, a practical solution could be to complete the alignment at dry dock conditions, and make provisions to correct (if needed) bearing vertical offsets when the reactions are verified afloat. Based on calculations computed with the shaft alignment software developed by American Bureau of Shipping (ABS) [4], Šverko made key remarks about the stern tube bearing. Specifically, he claimed the maximum absolute bearing - shaft allowed misalignment is 0.3 mrad; further misalignment imposes the necessity of slope boring application at the aft stern tube bearing. Moreover, due to some misalignment being inevitable, the single point equivalent of an aft stern tube bearing should be longitudinally positioned closer to the aft end of the bearing at about a third of the bearing's diameter away. Last, oil film characteristics of the bearing were studied, as Šverko used bearing reaction forces as input to calculate bearing behavior. In a later paper, Šverko (2006) [5] proposed a solution to the problem of accurately predicting hull deflections by analyzing a series of collected real world data. Bending gauges were utilized to measure shaft deflections and subsequently estimate hull deflections. Utmost goal of this study was to extrapolate hull deflections from a pool of data of similar vessel types based on the main parameters of the ship in study.

In their study, Dahler et al. (2004) [6] presented their findings of an industrial project between DNV, MAN B&W and DAEWOO regarding shaft deflections and bearing loads in large ships propelled by two-stroke Diesel engines. They utilized a complete

FEM of a VLCC, which exhibited a fine mesh at the aft end of the ship hull (engine room). They focused on engine and crankshaft deflections and the corresponding bearing loads. To this end, FEAs were performed taking into account the real crankshaft geometry, and the results were compared with simulations using simplified crankshaft models. Simulation results were also compared to experimental measurements. They concluded FEAs capture the general trend of hull deflections reasonably well, but fail to account for local variations in the curvature of the shaft, leading to inaccurate predictions of bearing loads.

In his work, Murawski (2005) [7] also utilized a FEM of a 2,000 TEU containership. He underlined the importance of (a) hull deformations under different loading conditions, (b) stiffness and damping characteristics of the journal bearings' oil film, and (c) stiffness characteristics of the bearing foundations on the shaft alignment problem. Firstly, he recommended all bearings should be equally loaded and Sommerfeld number of intermediate bearing(s) should be 30-50% greater than the rest to endure loading scenarios where these bearings will have to support bigger loads. Another key point underlined by Muraski was that stern tube bearings should be modelled as a continuous support, intermediate bearings and main engine bearings support can be modelled as points. He concluded that, in a holistic approach to the shaft alignment problem, bearing stiffness and oil film characteristics of each bearing should be taken into account in the design stage.

Another relevant work was conducted by Korbetis et al. (2015) [8]. They utilized a detailed FEM of a VLCC taking into account the contribution of shaft rigidity and the foundation of the main propulsion engine. Hull deformations were calculated for a set of typical loading conditions of the vessel. Furthermore, they fed these deformations into a software developed at NTUA as additional bearing offsets due to hull bending. Last, they took into consideration bearing foundation stiffness and oil film characteristics. The authors concluded differences in bearing reaction forces at different loading conditions are not very pronounced with the intermediate shaft bearing exhibiting the most pronounced deviations in reaction forces and tending to be lightly loaded, whereas in one case it was negatively loaded. To this extent, they advise designers to consider all the parameters described in their study to ensure safe and stable operation of the shafting system.

Recently, BV (2015) [9] and ABS (2015) [10] released rule notations concerning the shaft alignment procedure onboard large vessels. Both methodologies of shafting alignment take into account hull deformations, oil film characteristics and stiffness of the bearings' foundation. ESA notation (Elastic Shaft Alignment for BV and Enhanced Shaft Alignment for ABS) is optional but deemed necessary for several ship types. BV's rule is mainly applicable to: (a) ships of all types having propulsion power per shaft line greater or equal to 30 MW, (b) container ships having propulsion power per shaft line greater or equal to 15 MW, and (c) liquefied gas carriers having propulsion power per shaft line greater or equal to 10 MW. On the contrary, ABS considers large tankers (such as Suezmax, VLCC, ULCC, LNGC), large bulk carriers (such as Capesize and VLOC) and large container vessels (above 9,000 TEU) to be shaft alignment sensitive vessels. As can be seen, the release of ESA makes the

importance of proper shaft alignment in modern ships evident and detailed calculations at the stage of vessel design imperative.

1.2. Goals of the Present Study - Outline

In the present work, a typical 10,000 TEU container ship driven by a two-stroke Diesel engine is considered. The vessel is shaft alignment sensitive and within the scope of the ESA rules of both BV and ABS, taking into consideration the following data:

- Power output: 51,000 kW x 84 RPM
- Shafting system length: Over 50 meters
- Number of intermediate bearings: Three (3)
- Propeller shaft diameter: 990 mm

First a 3D representation of the ship's hull and compartmentation of the aft end structure was generated through digitization of the ship construction plans. Further, a detailed FEM was generated utilizing the ANSA meshing software (quality criteria and other meshing requirements set by Classification Societies were met). By conducting FEM simulations, hull deflections were calculated as additional bearing offsets, for later use in the shaft alignment software developed at NTUA, in the course of the diploma thesis of Mr. O. Vlachos [11].

Next, the propulsion shaft of the vessel was modelled as a statically indeterminate multi support beam consisting of 78 elementary beams. Bearing characteristics and bearing foundation stiffness were taken into account, and static equilibrium of the shaft was calculated using matrix analysis. Next task was the replication of the yard's shaft alignment plan in terms of jack up loads validation. Last, a series of different loading conditions (docking, ballast, design, scantling) were considered, relevant vertical offsets were incorporated to the shaft alignment plan, and corresponding reaction forces for every bearing were calculated. For each bearing, performance indices, such as minimum oil film thickness, maximum pressure and friction power losses have been calculated.

Finally, a comparative analysis of the key parameters affecting shaft alignment has been conducted. In particular, the effects (a) of shaft rigidity on hull deflection, (b) of accommodation block installation on bearing offsets, and (c) of bearing foundation stiffness on bearing loads have been assessed by performing additional simulations. The results have demonstrated that bearing foundation stiffness has to be accounted for in the shaft alignment calculations, for obtaining accurate and valid results. Further, hull deflections after installation of the accomodation block affect moderately the bearing reactions, and therefore, this effect should not be disregarded in the design stage. Finally, the effect of shaft rigidity on hull deformation has been assessed; the results have demonstrated that shaft rigidity affects substantially bearing offsets at different loading conditions and the corresponding bearing loads, therefore, it should be included in the finite element model of the vessel structure.

2. FEM Generation of Ship Structures

A vessel underway is subjected to numerous loads. One can identify three major types of loads; lightship, deadweight and buoyancy. Lightship weight comprises hull and superstructure weight, outfitting and machinery installation. Lightship weight is constant throughout the operational life of a vessel. Deadweight, on the other hand, contains consumables and payload. Last, buoyancy is the balancing force, to lightship and deadweight, created by the pressure of the surrounding sea water.

For each and every different loading condition, an equilibrium is achieved meaning that hull reacts to the external loads application in terms of deflections. As expected, these deflections depend heavily on the rigidity of the construction, globally and locally. It is also reasonable that different loading conditions produce different hull deformations.

The aft end construction of a vessel, where the main engine and the shafting system are installed, is also affected by the overall deflections of the hull. Depending on the loading condition, the foundations of shafting system bearings will undergo different vertical deflections leading to an a priori unknown equilibrium state of the shafting system.

It is common practice to perform the shafting system alignment on a dock, with or without accommodation block attached to the rest of the vessel, or afloat in light ballast condition with the propeller area raised above the water plane. Therefore, it is of paramount importance to achieve a shafting alignment that will keep all bearings loaded within rules' limits for all loading conditions. Such project requires knowledge of hull deflections in the aft end area for each and every loading condition, which can be accurately obtained utilizing a finite element model of the vessel.

2.1. Geometry

2.1.1. Obtain Offset Data Tables

Generation of a vessel's model begins with the geometric representation of the hull. The first step in the whole process is to input offset data in a CAD software. Offset data can be obtained directly through lines plan and offset data tables, although it is not common for yards to provide such detailed drawings to ship owners.

Offset tables provide half breadth location for discrete stations and waterline levels and height above base line for the same discrete stations and respective half breadth positions. These tables offer information about vessel's profile and boundary curves (flat of bottom, flat of side, etc). In such a way, one is able to obtain a list of x, y, z coordinates which, when given as an input to a CAD software, will yield cloud of points in 3D space. A typical offset data table is presented in **Table 2.1**.

TABLE 2.1: Offset data table.

	HALF BREADTH					
STATION	**BASELINE**	**500WL**	**1000WL**	**2000WL**	**3000WL**	**4000WL**
4	1,905	6,205	7,859	9,845	11,743	14,044
5	3,462	8,640	10,714	13,559	15,864	17,990
6	5,180	11,505	14,218	16,890	18,928	20,313
7	6,885	15,047	17,123	19,317	20,721	21,458
8	8,428	17,673	19,065	20,746	21,552	21,928
9	9,789	19,003	20,115	21,372	21,892	22,000
10	16,441	19,353	20,400	21,530	21,967	22,000
11	16,441	19,353	20,400	21,529	21,966	22,000
12	16,441	19,353	20,400	21,529	21,966	22,000
13	14,778	18,475	19,734	21,097	21,712	21,882
14	11,434	15,958	17,631	19,538	20,557	21,019

In case such detailed drawings are not available, construction drawings are to be used. Upon digitization, construction drawings will produce the same, more or less, offset data table. This process is laborious, and accuracy is extremely important to extract as credible results as offset data tables would.

To achieve the aforementioned goal, a digitizer software tool is to be used. One of the best and free to access software is Engauge Digitizer. Each section needs to be extracted to a separate picture format file and then imported to the software. Due to the fact that drawings' scaling differs from one another, a calibration process is required for each section to obtain accurate coordinates. The calibration process requires the user to input three reference points to scale the to be exported data correctly. The bottom of the centerline was chosen as the section plane origin. Thereinafter user adds points to the section curve by picking points along the

drawing. At the end of the process, software exports a comma delimited file (.csv), easily manipulated by the user. Combining all these files, the user ends up creating an offset data table as previously.

2.1.2. Hull Generation

Rhinoceros 3D is a commercial 3D software package developed by Robert McNeel & Associates. Rhinoceros 3D utilises non-uniform rational b-splines (NURBS), which are mathematical representations of 3D geometry to accurately describe any shape (e.g. a vessel's hull).

After having imported offset data tables into Rhinoceros 3D, we end up with a cloud of points in 3D space. Firstly, we develop the ship profile and the boundary curves of the ship by interpolating the respective points. A fairing process of few millimeters is needed before we keep on with hull generation. At this point we interpolate each section's point keeping in mind that tangencies are to be imposed (starting, ending and points through boundary curves).

Afterwards, we need to fair the sections considering we obtained the offsets via a limited accuracy method (digitization). To avoid discrepancies between two faired real section, the fair process is to be conducted with a limiting tolerance of a few millimeters. In an attempt to represent the ship's hull, as faithfully as possible, we need to generate and fair waterline-like curves (e.g. at 0.5m, at 1.0m, at 1.5m and so on). Finally we should refit the sections to incorporate deviations that occurred via the fairing process of the waterline-like curves.

Once the fairing process is over, it is time to create patches (surfaces) representing the ship's hull. In the region of parallel mid-body of the ship, information provided by sections and boundary curves is adequate for surface generation. The aft and fore end areas of the ship require utilization of waterline-like curves to produce surface of G1 continuity. At the end of the whole process, we have several small surfaces of G1 continuity that will reproduce the actual ship's hull.

The most accurate way to compare the surface produced with the actual hull is to examine their hydrostatic properties for a number of drafts. The most important hydrostatic properties are: volume displacement (m^3), wetted surface area (m^2), waterplane area (m^2), longitudinal center of buoyancy (m) and longitudinal center of flotation (m). In general, the developed surface is considered acceptable if relative errors are of the order or below 1%.

2.2. Compartmentation

Every construction drawing is divided into four major sections; shell expansion, decks, buttocks and frames. Working with layers in Rhinoceros 3D is time saving and introduces safeguards to the development of the steel structure. Each layer represents a major section (e.g. hull, deck, buttock, frame) and sublayers reflect subelements (upper deck, main deck, 1st platform, etc).

Overall, the steel structure of a containership consists of numerous vital substructures, the most important of which are presented in the next paragraphs.

2.2.1. Double Bottom

Traditionally, shipbuilding process starts with the bottom part of the vessel and in particular the keel. In small constructions, the keel is an important part of the construction because it contributes to a great extent to the overall strength of the vessel. In large vessels, though, the keel is only a plate of the bottom with increased thickness in comparison to the other plating of the bottom area.

In ships with double bottom (**Figure 2.1**), an additional, continuous plate is used to ensure the tightness of the space enclosed between this plate and the outer bottom. This plate is called “inner bottom”, and is placed at a minimum height from the outer bottom, defined by the Classification Societies. The purpose of this provision is to provide additional safety for the cargo and the ship as a whole, because in case of collision, both plates must be penetrated to cause damage to the cargo due to flooding of the hold.

FIGURE 2.1: Double bottom of a vessel.

2.2.2. Cargo Holds

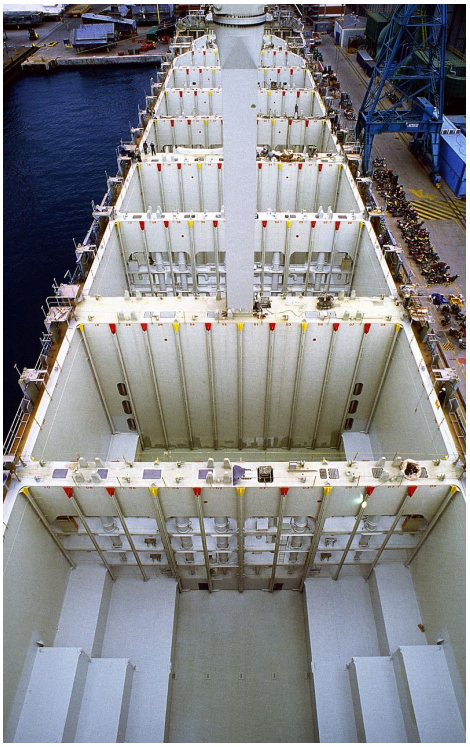

Efficiency has always been a key factor in the design of container ships. A key aspect of container ship specialization is the design of the hatches, the openings from the main deck to the cargo holds. The hatch openings span the entire breadth of the cargo holds, and are surrounded by a raised steel structure known as the hatch coaming. On top of the hatch coamings, the hatch covers are assembled. (**Figure 2.3**).

Another key component of dedicated container-ship design is the use of cell guides (**Figure 2.2**). Cell guides are strong vertical structures constructed of metal installed into a ship's cargo holds. These structures guide containers into well-defined rows and columns during the loading process and provide some support for containers against the ship's rolling at sea.

FIGURE 2.2: A view into the holds of a container vessel; vertical cell guides and bulkheads.

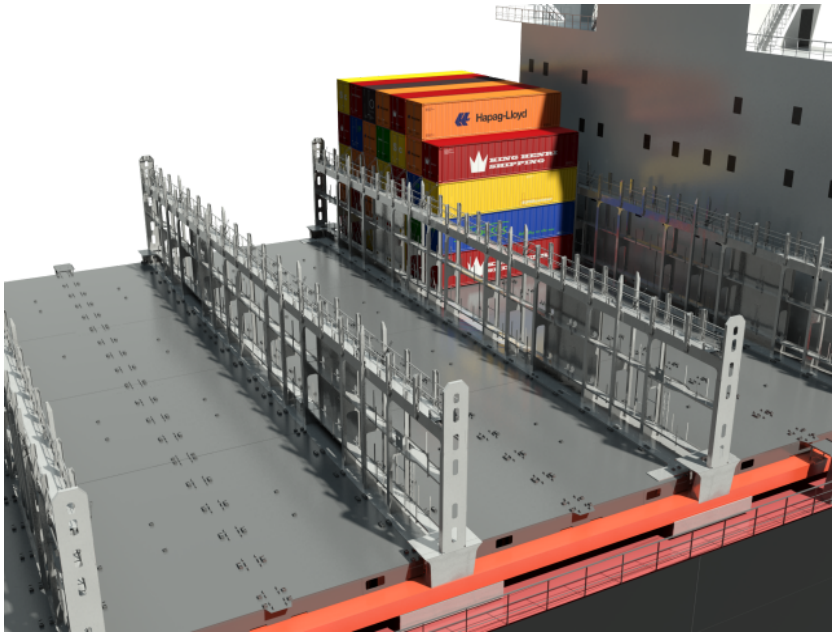

FIGURE 2.3: A view of the upper cargo area of a container vessel; cell guides, hatch coamings and hatch covers.

2.2.3. Bulkheads

Cargo holds are separated by watertight bulkheads (**Figure 2.2**). Watertight bulkheads are vertically designed watertight divisions/walls within the ship's structure to avoid ingress of water in the compartment if the adjacent compartment is flooded due to damage in ship's hull. In small ships, a transverse bulkhead may be constructed from a single plate. However, for larger ships, the plating of a transverse bulkhead usually consists of a series of horizontal strakes welded together. The thickness of these strakes increase with depth, in order to strengthen the bulkhead against the maximum hydrostatic pressure in case the compartment is fully flooded.

The bulkhead plate itself is not resistant enough against large scale transverse forces like shear forces. So they are stiffened, either vertically or horizontally. The sections used for stiffening the bulkheads are usually flat bars, angles or bulb bars, depending upon the required section modulus.

2.2.4. Superstructure

The construction elements located above the main deck are called superstructures. Superstructures contain spaces available for accommodation of the crew and passengers. Part of superstructures is also the bridge of the ship, and the upper deck is the web, which carries navigation and telecommunication instruments. SOLAS regulation concerning visibility onboard containerships has led to a shift of the longitudinal position of the superstructures to accommodate both the needs for visibility and maximum loading capacity (**Figure 2.4**).

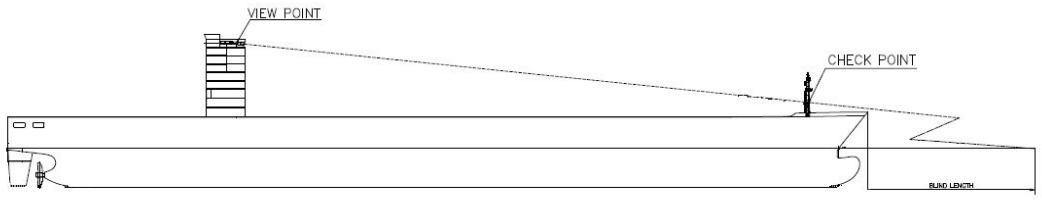

FIGURE 2.4: Visibility line check of a container vessel.

2.2.5. Engine Bedplate

The main engine of the vessel (**Figure 2.5**) is seated on top of the engine bedplate. The engine bedplate is a solid foundation for the engine, characterised by stiffness and strength capable of enduring the engine weights, as well as gas pressure and inertia forces generated during engine operation. Further, it minimizes deflections of the crankshaft due to hull deflections, which may lead lead to crankshaft fatigue failure.

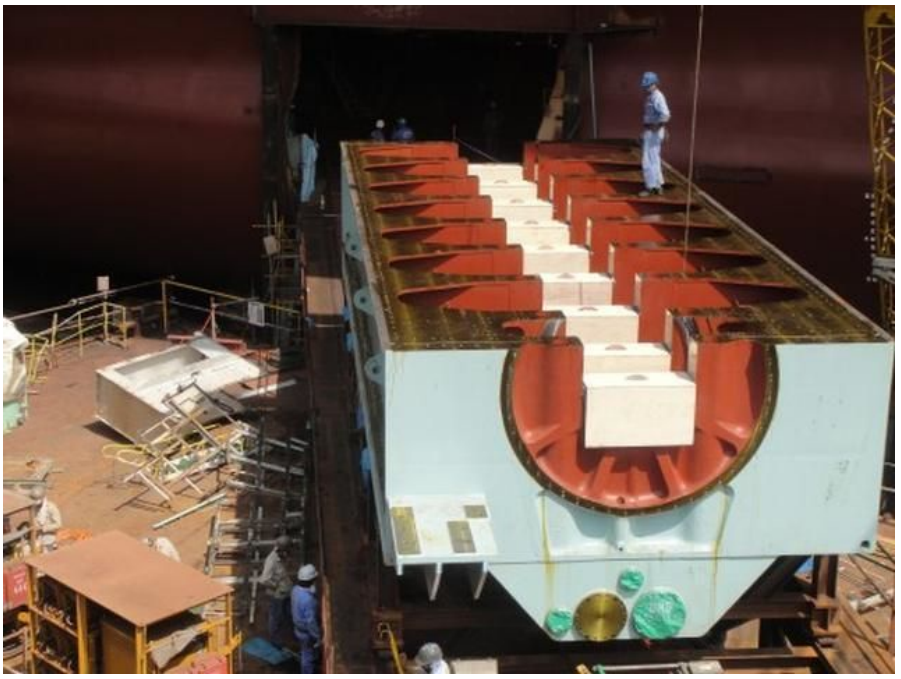

FIGURE 2.5: Engine bedplate of a marine diesel engine.

2.2.6. Stern Tube

The stern tube (**Figure 2.6**) is a hollow tube at the lower aft part of the ship. It is usually equipped with two journal bearings which support the weight of the shaft passing through the tube and that of the overhanged propeller. The main requirements of the stern tube are (a) the proper lubrication of the bearings for optimum tribological performance, and (b) the sealing of the tube so that sea water cannot enter the stern tube volume and the engine room interior. Regarding the finite element modelling of the stern tube, solid elements are used for the representation of the supporting construction.

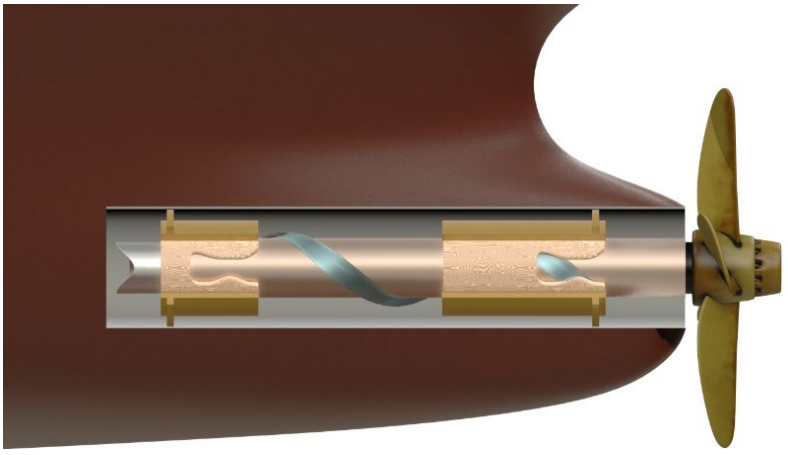

FIGURE 2.6: Stern tube of a vessel.

2.3. Reinforcement

There are several types of stiffeners used for every vessel (**Figure 2.7**); tee profile, flat bars, L profile, bulb flats, etc. All tee profile stiffeners are modelled as shells. Flat bars whose web is 150 millimeters or more are modelled as shells, while smaller ones are modelled as beam elements pasted onto shells (plating). Stiffeners whose profile is L shaped are modelled in a specific way; their web is modelled as shell, while their flange is modelled as beam element pasted onto the shell (flange). In a similar way, bulb flats are modelled as equivalent L profile stiffeners. Cross section and weight calculations are required to transform bulb flats to L profile stiffeners.

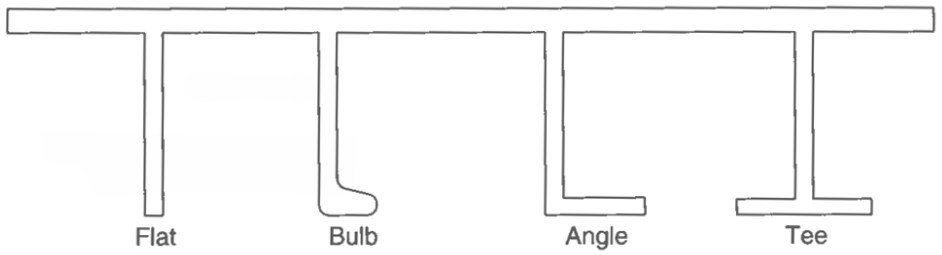

FIGURE 2.7: Various types of beam stiffeners. [18]

2.4. Mesh

BV [9], in their rule note, instruct that the standard size of the finite elements used is to be based on the secondary stiffener spacing. In particular,

- Webs of primary members are to be modeled with at least three elements along their height,
- Plating between two primary supporting members is to be modeled with at least two element stripes,
- The ratio between the longer side and the shorter side of the elements is to be less than 3 in the areas expected to be highly stressed,
- Holes for the passage of ordinary stiffeners may be disregarded.

Moreover, cast part of bossing as well as forward stern tube bush steelwork should be modeled with solid elements. Finally, obvious as it is, longitudinal position of the equivalent supporting points is to be exactly the same on the line shafting and on the structure.

2.5. Boundary Conditions

One of the most serious tasks associated with the proper modelling of ship structures using finite elements is the definition of the boundary conditions. Incorrect boundary conditions may introduce considerable errors by suppressing the deformation of the cross sections at which they are applied or by giving rise to deformation modes that are not realistic. A realistic solution based on engineering principles was introduced by Servis et al. (2004) [12] in their work.

In the work of Servis et. al., only cargo hold no.1 was modelled, and in order to predict primary stresses using the finite element model, the boundary conditions should be such as to induce nodal forces and moments that, when summed, correspond to the hull girder shearing forces and bending moments. For this reason, shear forces and bending moments diagrams were utilized. In particular, locations where shearing force was zero (therefore bending moment recorded a local maximum) and bending moment was zero were identified. These forces and moments are induced to a beam using the boundary conditions presented in **Figure 2.8**.

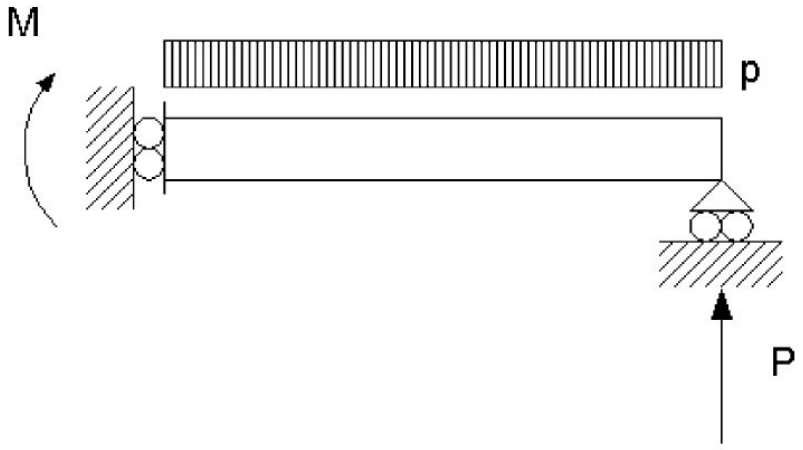

FIGURE 2.8: Beam representing the loading condition and boundary conditions. [12]

The beam in **Figure 2.8** is isostatic. The aftmost boundary condition allows the section to translate vertically but not to translate horizontally or rotate; thus, a bending moment is the reaction at this end. The foremost boundary condition allows the section to translate horizontally and to rotate but not to translate vertically; thus, the reaction is a shearing force. These reactions correspond directly to the bending moment and shearing force as mentioned above.

Correspondingly, modelling of the aft end structure of a ship is equivalent to a cantilever beam as shown in **Figure 2.9**. To clarify, the aftmost end of the ship is a free edge (as shearing force and bending moment is zero), therefore no boundary conditions should be introduced. On the other hand, the foremost end of the substructure is generally exhibiting non-zero shearing force and bending moments. Therefore, the boundary condition at the foremost end should not allow the section

to translate vertically nor rotate in the vertical plane. The chosen boundary conditions will induce the actual shearing forces and bending moments, thus enabling our analysis to capture primary stresses and displacements.

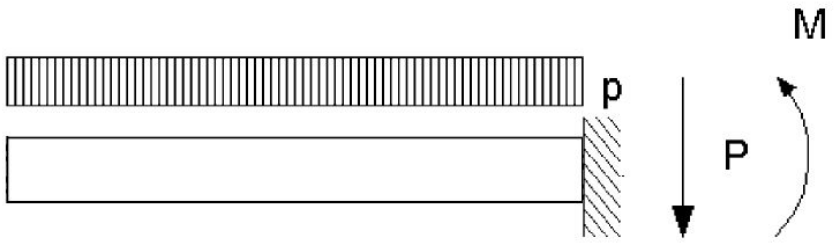

FIGURE 2.9: Beam representing the loading condition and boundary conditions of the present work.

2.6. Loads

As discussed at the beginning of this chapter, a ship is subjected to numerous loads, which can be divided into three major categories: (a) lightship weight, (b) deadweight and (c) buoyancy.

First, lightship weight accounts for all structures modelled in our FEM and is enabled when gravitational field is applied to our analysis. Machinery, auxiliary structures and small constructions that do not contribute to ship strength may or may not be modelled in the FEM. In the latter case, their mass should be applied to the model as non-structural mass. This mass should be appropriately distributed over the FEM, so as to reach the prescribed lightship weight and the corresponding centre of gravity. The engine mass should represented by a lumped mass of corresponding magnitude distributed to the engine foundation positions by MPC elements.

Second, deadweight comprises all consumables as well as payload weight. The contents of the tanks could be represented by lumped mass connected to each hold bottom with RBE3 elements. This approach is an assumption that in general does not simulate the real problem precisely. However, in case our area of interest is not near these tanks, our calculations will not contain any numerical errors.

Last, buoyancy should be applied as pressure at the hull underneath the waterline using appropriate entities. In our analysis, a C++ algorithm was developed to apply hydrostatic pressure for each loading condition. Length between perpendiculars, draft at aft peak and draft at fore peak were used as inputs (along with all the elements and their nodes as exported by the mesher).

3. Shaft Alignment

3.1. Definition

The ship propulsion system typically comprises a two-stroke diesel engine and a shafting system transmitting power to the propeller. In ships with a four-stroke diesel engine installed, a reduction gearbox is required to transmit the generated power to the propeller in the most efficient rotational speed range. The shafting system comprises three individual parts: (a) the crankshaft, (b) the intermediate shaft and (c) the propeller shaft. Each shaft is supported by different (amount and type) journal bearings according to the weights to be supported. (pistons, connecting rod, crosshead, flywheel, flanges, propeller, etc.).

To begin with, the crankshaft is supported by the crankshaft bearings, whose number depends on the number of cylinders of the main engine. In cases where the crankshaft comes as a single piece, the number of crankshaft bearings is the number of cylinders increased by one. On the contrary, in cases where the crankshaft is divided into two parts (i.e. large marine diesel engines) the number of crankshaft bearings is the number of cylinders increased by two. Next, the intermediate shaft is supported by at least one intermediate bearing. Vessels with lengthy shafting systems display more intermediate bearings (up to three for large container vessels). Finally, the propeller shaft is usually supported in the stern tube by two stern tube bearings. Recently, ABS approved shaft alignment plans with just one stern tube bearing; such installation requires detailed calculations and is offered to vessels with short shafting systems.

The propulsion shafting alignment is a process involving the calculation and selection of proper support points to achieve the optimal operation of the shafting system for the service conditions of the vessel. Specifically, shaft alignment consists of two parts:

a. The analysis of the shafting system and the determination of the shaft alignment plan, and
b. The application of the alignment procedure and the subsequent validation through measurements.

According to ABS (2014) [4], shaft alignment calculations and a shaft alignment procedure are to be submitted for the following alignment-sensitive type of installations:

i. Propulsion shafting of diameter larger than 400 mm,
ii. Propulsion shafting with reduction gears where the bull gear is driven by two or more ahead pinions,
iii. Propulsion shafting with power takeoff or with booster power arrangements, and
iv. Propulsion shafting for which the tail shaft bearings are to be bored sloped.

In general, propulsion shafting alignment aims to:

- minimize uneven loading of the bearings,
- avoid negatively loaded bearings,
- minimize shaft deflections and tensile stresses due to bending,
- minimize the number of bending points of the shaft,
- minimize load difference between aft and fore bearing of the reduction gear (if applicable),
- reduce loading of the crankshaft bearings,
- minimize number of system bearings,
- provide reliable operation for both hot and cold M/E condition, and
- provide reliable operation in different loading conditions and weather scenaria.

3.1.1. Importance of Proper Alignment

Failing to design or implement an optimal shaft alignment plan may lead to:

- unloaded or negatively loaded bearings; other bearings have to support extra loads,
- overloaded bearings (beyond their design load capabilities) which in return increases bearing and shaft wear deteriorating system's robustness and shorten its lifespan,
- increased power loss, due to extreme friction at the shafting system,
- excessive wear of M/E bearings and reduction gear (if applicable),
- increased amplitudes of lateral and torsional vibration leading to imminent shaft and bearings failure, and
- shaft bending moments greater than the allowed limit prompting shaft failure due to fatigue.

Most compelling evidence of proper shaft alignment importance is the following case of malfunction [2, 13]. Suppose a serious bearing failure that leads to loss of propulsion and vessel immobilization. A series of events would follow, should the vessel be salvaged and repaired, such as:

- vessel towing to the nearest berth,
- shaft disassembly,
- bearing repairs (order spare parts with urgent priority of delivery),
- shaft reassembly, and
- conduct and implement new shaft alignment plan.

Further, one must keep in mind the possible cargo degradation and delay costs that the shipowner will have to pay. The associated total cost may substantially surpass 1M $, however, most importantly, human lives and property are put at risk possibly at harsh environmental conditions.

3.1.2. “Static” vs “running” condition

All expected conditions of a shafting system can be divided into two categories: static and running. In static conditions:

- The main engine is not running, also known as cold condition,
- The shaft is stationary, therefore hydrodynamic lubrication is not present,
- Propeller induced loads are not considered, because propeller does not produce any thrust. The only propeller load considered is its own weight and buoyancy.

On the other hand, in running conditions the following should be considered:

- The main engine is running, also known as hot condition. In this state, the main engine is subjected to non-uniform thermal expansion, which affects all crankshaft bearings,
- Hydrodynamic lubrication is active, thus oil film is produced in between the shaft and each supporting bearing.
- The propeller produces eccentric thrust, which should be applied as a bending moment.

In the present study, the following assumptions have been made, regarding running conditions of the vessel:

1. A uniform vertical offset of the crankshaft bearings due to thermal expansion,
2. Hydrodynamic lubrication governs the vertical motion of the shaft within each bearing, and
3. Shaft bending moments due to propeller eccentric thrust have not been considered.

3.1.3. Influence Factors

For a given number of support points and a given set of longitudinal positions of those support points, a change in the vertical offset of a single bearing will affect the distribution of reaction forces amongst all bearings. The calculation of the reaction forces of the bearings for any set of vertical offsets is greatly facilitated by the introduction and use of influence factors, defined as follows:

The influence factor of bearing i on bearing j is a measure of the change in reaction force of bearing j, caused by a unit vertical offset of bearing i.

As such, it can be calculated as:

$$\sigma_{ij} = \frac{R_{ij} - R_j^0}{y_i} \tag{3.1}$$

where:

- σ_{ij} is the influence factor of bearing i on bearing j,

- R_{ij} is the reaction force of bearing j when bearing i has moved vertically by an amount of y_i,
- R_j^0 is the reaction force of bearing j, while all bearings have zero vertical offsets, and
- y_i is the vertical offset of bearing i.

Solving **EQ. 2.1** for R_{ij}, every bearing reaction force can be calculated for a set of vertical offsets given the fact that we know the influence factors of the system:

$$R_{ij} = R_j^0 + \sigma_{ij} \cdot y_i \tag{3.2}$$

It should be noted that superposition is valid in our case because the vertical offsets imposed on the bearings (of the order of millimeters) are much smaller than the distance between each bearing (of the order of meters). Therefore, the reaction force of bearing j for any given condition is:

$$R_j = R_j^0 + \sum_{i=1}^{N} \sigma_{ij} \cdot y_i \tag{3.3}$$

Finally, influence factors constitute a criterion of shafting plan sensitivity to external disturbances. The smaller the influence factors are, the less sensitive the system is to such disturbances. On the other hand, if the system's influence factors are large, there is high possibility of unexpected and undesired performance of the system.

3.2. Regulations

3.2.1. Overview

Classification Societies have dealt with the problem of propulsion shaft alignment over the past decade issuing new regulations and guidance notes. Notably, BV (2015) [9] and ABS (2015) [10] released rule notation concerning the shaft alignment procedure onboard large vessels.

Class regulations regarding shaft alignment of rotating machinery, in general, are more or less homogeneous between all major classes. First, the shaft alignment calculations are to be carried out for a set of series of conditions:

- Alignment conditions during the shafting installation,
- Cold, static, afloat conditions,
- Hot, static, afloat conditions, and
- Hot, running conditions.

Basic parameters, information and results of the process are to be submitted to the class:

- Detailed description of the shaftline model
    - Shaft characteristics: material, length, diameter
    - Definition of the reference line,
    - Longitudinal and vertical position of each bearing with respect to the reference line,
    - Bearing characteristics: material, length, clearance, stiffness
- Input parameters
    - Bearing offsets due to hull deflections for various loading conditions
    - Hydrodynamic propeller loads
    - Weight and buoyancy effect of the propeller
    - Engine power and rotational speed
    - Thermal expansion of the main engine
    - Jack-up locations
- Limitations (allowable bearings loads, etc)
- Results
    - Bearing influence factors
    - Expected bearing reactions for a set of series of loading conditions
    - Expected shaft deflections, shear forces and bending moments of the shaftline for a set of series of loading conditions
    - SAG-GAP values
    - Jack-up correction factors

The acceptance criteria for the calculations are also similar between all major classes. The most common criteria according to BV and ABS are presented below.

In particular, BV (2017) [14] states that the results of the shaft alignment calculations are to comply with the following acceptability criteria:

- All bearings are to remain loaded (positive load means supporting the shaft)
- Loads on intermediate shaft bearings are not to exceed 80% of the maximum permissible load specified by the manufacturer
- Relative slope between propeller shaft and aftmost boring axis is not to exceed 0.3 mm/m
- The length of bearings lined with white metal or other antifriction metal is to be not less than twice the rule diameter of the shaft in way of the bearing. The length of the bearing may be less than that given above, provided the nominal bearing pressure is not more than 0.8 N/mm^2 for metallic and 0.6 N/mm^2 for oil-lubricated synthetic bearing materials.
- For the shafts, materials having a specified minimum ultimate tensile strength R_m of 400 N/mm^2 may be used.

Strangely enough, the verification of reaction forces through testing contains a significant amount of uncertainty as BV allows for deviations between prescribed calculations and measured reactions as high as ±20%.

In the same path, ABS (2018) [4,15] sets exactly the same criteria, the only exception being the following:

- For practical reasons, at least 10% of the allowable load would be desired on the bearing in to prevent unloading due to unaccounted-for disturbances.

3.2.2. Elastic/Enhanced Shaft Alignment

To further analyse the scope of Elastic or Enhanced Shaft Alignment, BV and ABS require more detailed calculations to grant ships with respective additional notation ESA.

To specify, BV requires the utilisation of FE model of the vessel, extending from the aft end up to the forward watertight bulkhead of the engine room, to obtain additional bearing offsets due to hull deformations for various loading conditions. The standard size of the finite elements used is to be based on the secondary stiffener spacing. Moreover, cast part of bossing as well as forward stern tube bush steelwork should be modeled with solid elements.

Another key point of the regulation is the requirements concerning the bearings of the shafting system. Firstly, for elastic shaft alignment calculation, line shafting model should include the following bearing particulars:

- effective contact length
- oil groove angular location
- clearances
- mechanical properties of sleeve and anti-friction materials
- machining of slope and partial slope, if any.

Additionally, the aft bush bearing is to be modelled with at least five supporting points in order to have detailed results at each section of the bearing.

Another part of the BV guidance note concern the hull deflections due to sea swell. In detail, BV states that wave parameters (direction, height H and wave length λ) are to be chosen as follows:

- Couple (H, λ) is to be physically realistic (i.e: the wave should not break with the chosen values), and
- Only head sea condition should be investigated.

BV also gives general guidelines on an acceptable method for elastic alignment calculations in static and running conditions. In the first case (static condition), when the shaft line is is laying on bearings without rotation, the Hertz contact theory is applicable to describe the characteristics of the contact: stiffness, reaction, length of contact, maximum pressure, squeezing. On the other hand (running condition), When the shaft rotates at a sufficient speed, a flow of oil is induced by its viscosity and the shaft speed creates a lift of the shaft. There is no more contact between the shaft and the bearing: the oil film is built-up. The calculation of this oil film is to be carried-out on the basis of a hydrodynamic differential equation which determines the behaviour of a thin and viscous fluid (Reynolds equation).

Finally, BV's regulation sets acceptance criteria for alignment calculations in running conditions in terms of minimum oil film thickness (h_{min}) which shouldn't be lower than 30μm.

3.3. Shaft alignment plan implementation

3.3.1. Design - Calculations

Choosing the number and longitudinal position of support points is the first step taken in our seek to achieve proper alignment. After that and with all bearing being in the same vertical position (zero vertical offsets), we calculate the reaction forces of each bearing. At the same time, we determine the elastic shaft line enabling us to calculate shaft deflections, tensile stresses due to bending, etc. At this point, the system's influence factors are also calculated. Thereinafter and taking into consideration all objectives of proper shaft alignment, we determine appropriate vertical offsets for each bearing. This is an iterative process **(Figure 3.1)** facilitated by the use of influence factors. At the end of the above procedure, we calculate the needed slope boring that will be applied to the aft stern tube bearing. Finally, we calculate SAG-GAP values for all shafts in decoupled state; provisions should be made in case temporary support points are needed.

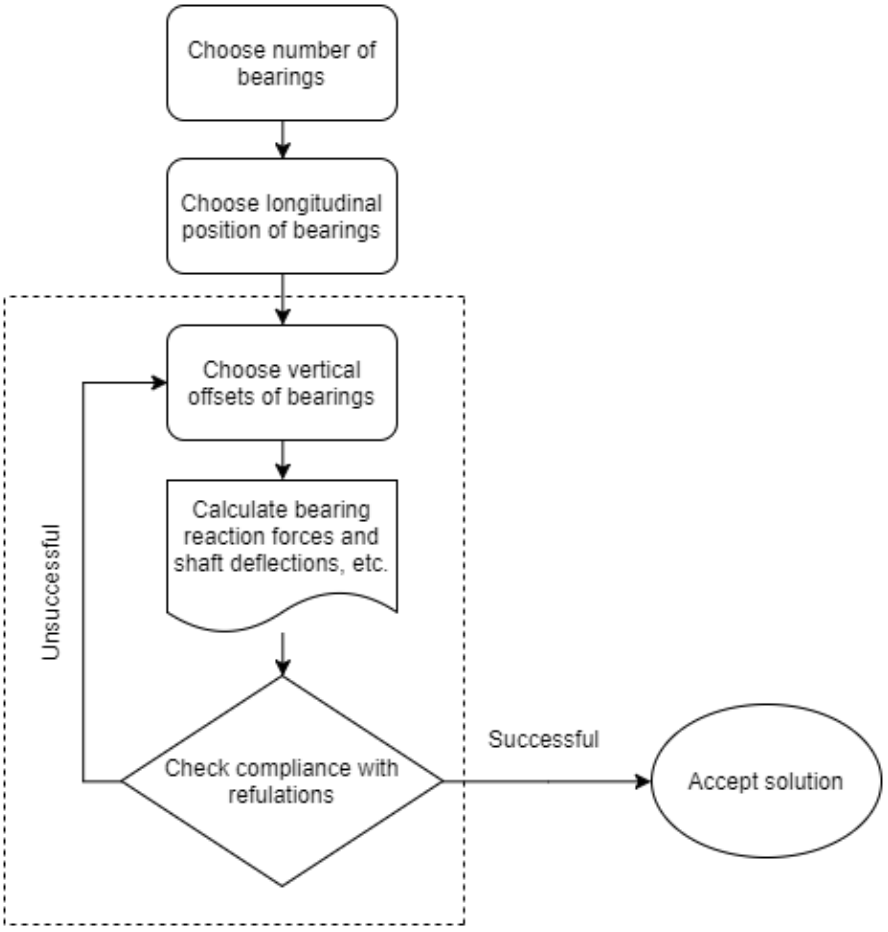

FIGURE 3.1: Iterative process of deciding number and position of bearings.

3.3.2. Application

The next stage of the whole process is the installation of the shafting system. The shaft alignment procedure should start only after heavy stern structure is put in place.

First, a reference line (**Figure 3.2**) is established between the M/E and the aft end of the stern tube. The procedure is implemented by piano wire method, optical or laser means (**Figure 3.3**).

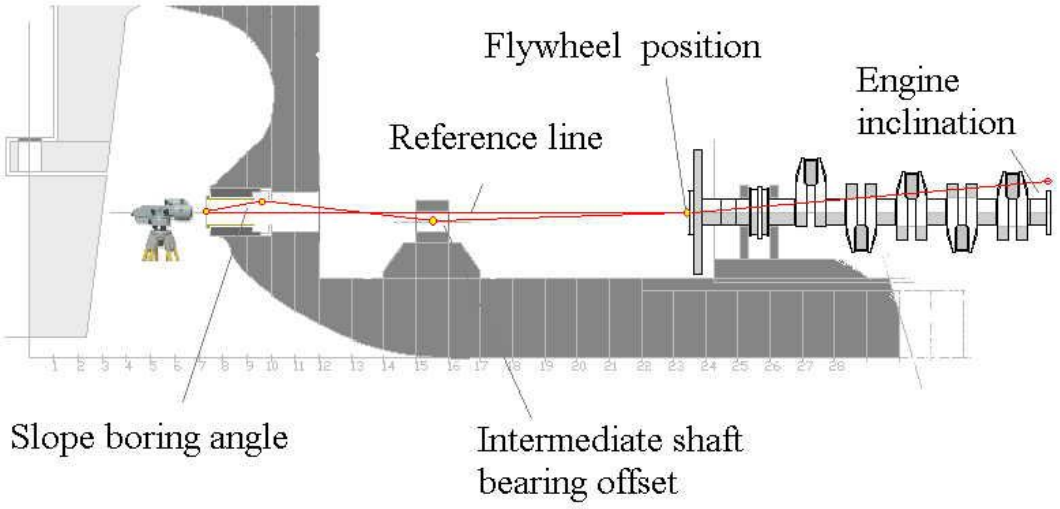

FIGURE 3.2: Shaft alignment procedure. Definition of reference line. [4]

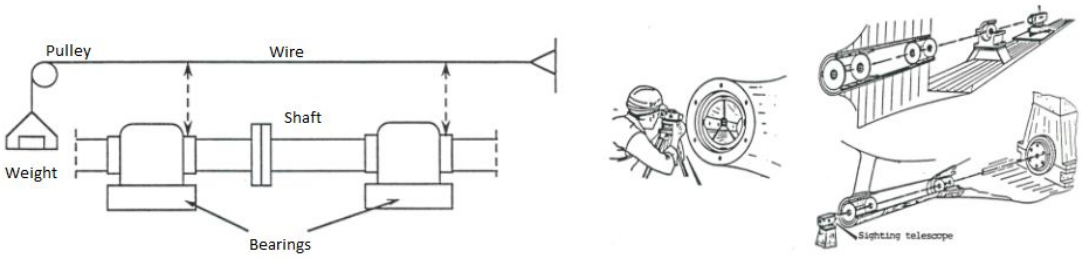

FIGURE 3.3: Piano wire method and optical/laser system. [17]

Further, the established shafting reference line is rectified by a slope boring of the stern tube bearing. This procedure can be done in two ways: (a) machining of the aft stern tube bearing, and (b) rotation of the bearing. In the first case, the bearing is placed with an initial diameter smaller than the final. A special bore is used (**Figure 3.4**), for generating the required slope. Machining of the slope is performed with several passes so as to reach the required clearance without excessive thermal stresses to the bearing anti-friction material. In case of a prefabricated bearing, the bearing is loosely installed allowing rotation along the bearing center axis. The final slope is determined and the bearing is fastened to its final position with the use of epoxy resins (**Figure 3.5**).

FIGURE 3.4: Slope boring machine. [4]

Before, shaft segments are placed upon the supporting points, a pre-sagging procedure of the M/E bedplate takes place. Large two-stroke low-speed cross-head diesel engines have a relatively flexible structure, which is therefore susceptible to disturbances which can result from ship's hull deflections and temperature change. Engine is installed when the vessel is in dry dock or afloat at very light ballast condition. It is expected that the effect of the bedplate pre-sagging will be annihilated due to the deflection of the hull structure of the vessel and thermal rise of the engine's bedplate.

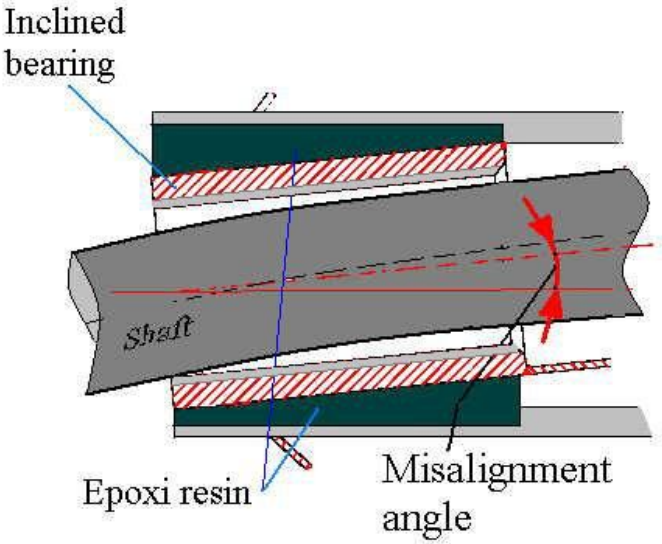

FIGURE 3.5: Bearing inclination. [4]

Then, all shaft segments are being put in place, and if necessary, upon additional temporary support points. The additional (temporary) bearings are used to assist the assembly. At this stage, it is normal practice for the yard to verify pre-assembly alignment condition of the shafting by conducting SAG-GAP procedure. SAG-GAP and deflection values are gauged using filler gauges. SAG and GAP values should be verified between mating flanges and have to be in accordance to the pre-calculated values. Until SAG and GAP values are in accordance with (or match) the design values, height adjustments are made to achieve the desired condition. The working crew usually starts by laying down the propeller shaft first and letting it hang freely. With the flange of the propeller shaft as a reference point, all temporary supports are placed and forces are applied to ensure that correct SAG and GAP values between that and the next segment, which is the intermediate shaft, are achieved. The same process is repeated between the I/M shaft and the crankshaft.

After all shafts have been coupled, extensive testing and measurement of shafting plan parameters is performed. The key objective is to obtain bearing reactions forces equal to the pre-calculated ones. Should they be found to differ from the calculated values, corrective actions are taken to rectify any inequalities.

3.4. Measurements

3.4.1. Reference Line

Broadly, the shaft alignment plan is defined as a set of vertical offsets (of the bearings) from a pre-defined reference line. Accurate implementation of a shaft alignment plan requires a well defined reference line, as well as reliable means of measuring the vertical offsets. Industry relies on the following two methods to establish and evaluate the reference line: (a) piano wire method, and (b) optical methods.

The piano wire method

The piano wire method utilises a thin metal wire, whose one end is bound the aft part of the M/E, and on the other end a weight is suspended via a pulley so that the wire is always tense (**Figure 3.6**).

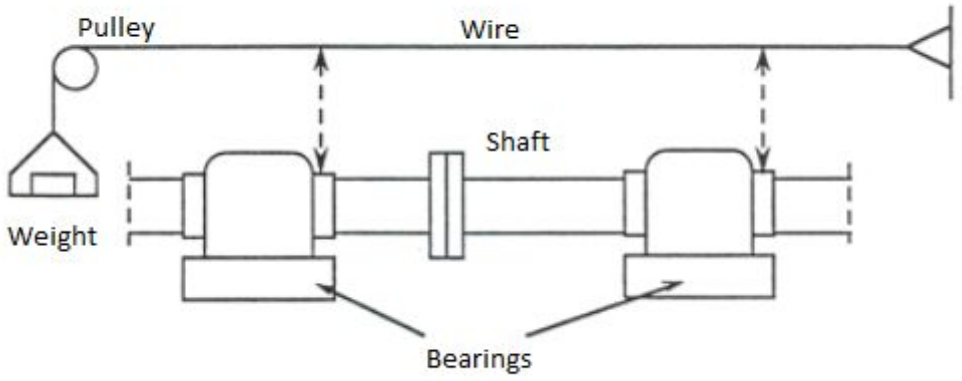

FIGURE 3.6: Piano wire method.

A micrometer is used to calculate the distances of the shafts and the bearings from the wire. Special attention should be given to the fact that the wire is not straight by itself, but has its own catenary. Therefore, deflections of the wire along the its length need to be evaluated, and then added to the distances calculated with the micrometer. This method is not very accurate and this can be attributed to the following reasons:

- The catenary deflections of the wire are based on the fact that the material is homogenous,
- The wire can never perfectly rest and will always vibrate at small amplitudes. It should be noted that the shaft alignment procedure is conducted along with other works, which will surely affect the piano wire, and
- It is hard to attach the micrometer to the wire without altering the vertical position of the wire.

Relative measurements [19] have shown that the deflections of the wire are calculated with satisfactory accuracy, if we assume the elastic line of the wire to be a parabola:

$$z = \frac{w}{2T} \cdot x^2 \tag{3.4}$$

then,

$$y = \frac{w}{2T} \left[\left(\frac{l}{2} \right)^2 - x^2 \right] \tag{3.5}$$

Where,

- x distance of the point from the middle of the wire
- y deflection of the wire at position x
- T tension force of the wire (equal to the suspended weight, if friction is neglected)
- w weight of the wire per running meter
- l wire length (distance between the pulley and the boundary point to the M/E)

Optical Methods

The key components of an optical system are: (a) the telescope (**Figure 3.7**), (b) the telescope base, (c) the reference targets, and (d) the mounts of the reference targets.

The telescope can be adjusted through a set of three graded dials; One is used to focus at a specific distance, and the other two are used to adjust the telescope's vertical and lateral offset. The special telescope base has a spherical bearing enabling the telescope to rotate, while the other support point is adjustable in means of transverse plane.

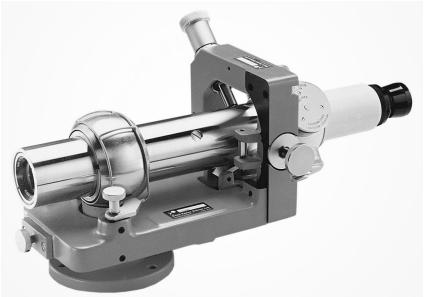

FIGURE 3.7: A telescope used for shaft alignment. [17]

The reference targets are glass disks with a diameter of 35-60 mm and a thickness of 9-13 mm. Moreover, the targets are inscribed with concentric circles various diameters and mounted on metal bases. Finally, the optical reference line, is defined as follows:

1. The telescope is positioned on one end of the shafting system (usually right outside of the stern tube), and the reference target is positioned on the other end of the shafting system,
2. The two micrometer screws of horizontal and vertical deflection are rotated until they come to the zero position,
3. The telescope is focused on the reference target, and
4. The adjusting screws, at the base of the telescope, are rotated so that the center of the crosshairs coincides with the center of the reference target.

The rest of the targets are positioned in the exact vertical and longitudinal positions that the shafting plan dictates support bearings should be. The position of a point with respect to the optical reference line is determined as follows:

1. The telescope is focused on the corresponding reference target,
2. The adjusting screws, at the base of the telescope, are rotated so that the center of the crosshairs coincides with the center of the reference target, and
3. The read-out from the dials combined with the reference values produces the actual offset of each target. In case the resolution of scale on the graded dials is not sufficient, the value is determined with the aid of the nearest concentric circle.

Although the optical alignment systems are more expensive than the wire method, they have extreme accuracy, credibility and repeatability of the measurements. Nowadays, industry utilises laser systems to facilitate the alignment procedure.

3.4.2. SAG and GAP

Following the positioning of the bearings in their final position, all shaft segments are placed onto their respective support bearings in an uncoupled state. Each segment is supported by one or two bearings (one of which is a temporary support). In this state, each shaft segment has its own elastic line, thus the flanges of two adjacent segments have a specific distance. A way of measuring flange distance employs two variables: SAG and GAP (**Figure 3.8**). SAG is the vertical distance between the top edges of each flange. Respectively GAP is the minimum horizontal distance between facing flange edges, or sometimes the horizontal distance between a flange's upper and lower edge.

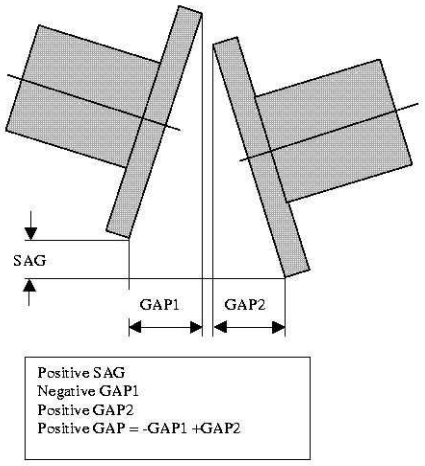

FIGURE 3.8: SAG and GAP value measurement.

The ultimate goal of this procedure is to properly position the shaft segment before assembly to produce the prescribed alignment state.

3.4.3. Bearing Reaction Forces

Once the shafting system has been assembled, all shafts have been coupled and all temporary support points have been removed, it is necessary to measure the reaction forces of the support points. This is a key step to the alignment procedure, because we can verify that all preliminary calculations of the designed shafting plan were accurate. The bearing reaction forces can be evaluated directly or indirectly. The most common ways to measure the alignment status are: (a) hydraulic jack testing, and (b) strain gauge testing.

Hydraulic Jack Testing

The most commonly used method used to measure the bearing reaction forces is hydraulic jack testing. This method method is performed while the M/E is not running. A jack is positioned as close to the bearing as possible while still being beneath the shaft along its centreline. A micrometer is placed right on top of the shaft and a load cell is placed between the jack and the shaft (**Figure 3.9**).

Firstly the shaft is lifted for at least 0.5 mm to ensure that there is enough tolerance for the testing to actually take place. Afterwards, the shaft is lifted all the way upwards until it comes in contact with the upper shell of the bearing. Then the shaft is jacked down. This process is done iteratively while taking measurements of the vertical offset of the shaft and the reaction force of the load cell.

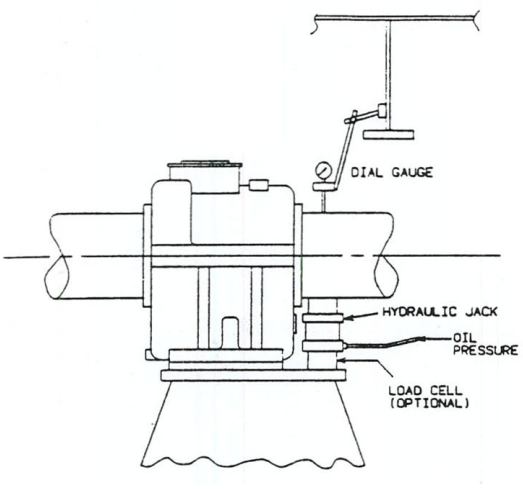

FIGURE 3.9: Hydraulic jack and micrometer gauge placement. [11]

Figure 3.10 illustrates a typical curve of jack load against shaft displacement, obtained from the above mentioned process. The first part of the curve resembles a milder slope, which is attributed to the fact that the shaft load is supported by both the bearing and the jack. At this point, the stiffness of the system (which is the inverse of the slope) is the summation of the stiffness of the bearing and the jack. The next part of the diagram features a steeper slope, which corresponds to the fact the shaft load is barely supported only by the jack. At this instant, the stiffness of the system is the stiffness of the jack. Moreover, the slope corresponds to the influence factor of a support point placed at the exact location of the jack upon itself. The closer the jack is to the bearing, the closer this influence factor's value is to the bearing's actual influence factor. For this reason the jack needs to be as close to the bearing as possible. Last but not least, one can notice the differentiation of the measurements depending on whether they were taken while the shaft was being lifted upwards by the jack or on the way down. This phenomenon is called hysteris and is attributed to friction.

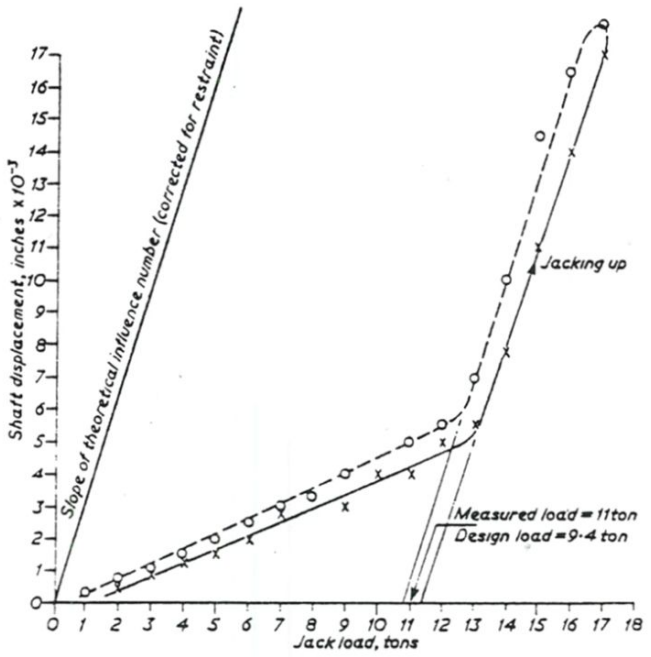

FIGURE 3.10: Jack-up testing measurement curves. [11]

In order to obtain the load of the bearing, using the above diagram, we need to extend the steeper part of the curve downwards until in intersects with the load (horizontal) axis. The load value at the intersection is actual load of the bearing.

This method can also be used to inspect the shaft and determine whether it has suffered permanent deformations in the form of bending. Simply by taking four measurements (shaft position at 0º, 90º, 180º and 270º), we can compare the reactions obtained and if they do not much within some tolerance, we can state with certainty that the shaft is skewed.

The downsides of the hydraulic jack method is the overall error of the method, which is approximately 10-15% and the fact that a cold condition is only validated. The error of this method is due to the inaccuracy of the manometer measuring the oil pressure and the friction between the cylinder and the piston of the jack.

Strain Gauge Testing

Another method of validating a shafting plan is through the use of strain gauges. Bending stress can be measured at any point of the shaft by applying a strain gauge (**Figure 3.11**) during alignment. Further, stains of the shaft surface can be measured, thus enabling calculation of reaction forces.

The advantages of this method can be seen below:

- Quick and straightforward measurement,
- Lateral deformations can also be measured,
- Reaction forces can be measured in inaccessible places, and

- Both static and dynamic loads can be measured.

The major drawback of this method is the meticulous modelling of the shafting system needed to produce accurate reaction forces from the measured deformations.

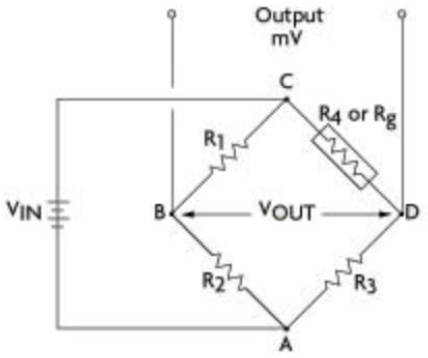

FIGURE 3.11: Typical Wheatstone bridge for bending moments measurement.

3.4.4. Crankshaft Deflections

Crankshaft deflections are an indirect measurement of the stress level in the crankshaft, as well as an indication of the crankshaft bearing loading. The crankshaft deflections must be verified after the alignment process is over and need to be within the engine manufacturer-required limits.

Crankshaft deflection measurement is conducted with a dial indicator (**Figure 3.12**) being placed at a predefined location between crank webs. The crankshaft is then rotated and the readings are taken at the prescribed angular locations. It must be noted that web deflections are measured between each cylinder.

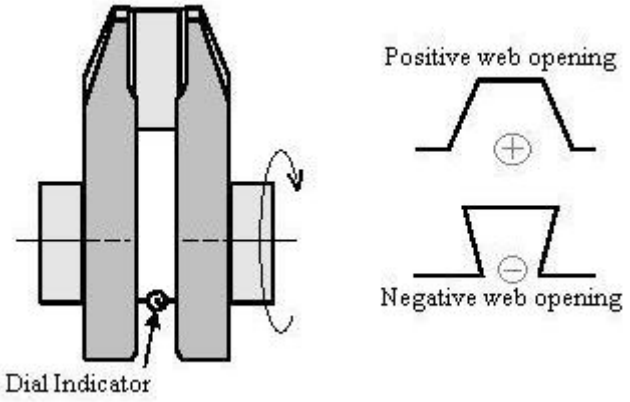

FIGURE 3.12: Crankshaft deflection measurements. [4]

4. Journal Bearings

4.1. Introduction

Journal bearings are the simplest type of radial bearings. In these bearings, the stator is a plain hollow cylinder, while the rotor (shaft) sits on the inner bearing surface. Between the stator and the rotor, there is a small clearance; usually filled with lubricant. **Figure 4.1** illustrates a cross section of a typical journal bearing. The principle behind hydrodynamic lubrication of journal bearings is as follows:

1. The rotor begins to rotorate within the stator, therefore lubricant is dragged along the perimeter of the shaft,
2. Lubricant is forced to enter a converging (wedge-like) geometry between the stator and the rotor,
3. Given the fact that the lubricant is incompressible, it develops pressure, thus lifts the shaft over the bearing, preventing a “dry-friction” situation caused by metal to metal contact.

The main advantages of journal bearings are summarised below:

- Simple construction,
- Can be constructed with small tolerances, thus can be used in projects with requirements of high precision,
- Increased lifespan and reliability due to beneficiary hydrodynamic lubrication,
- High load capacity, as well as absorption and damping characteristics.

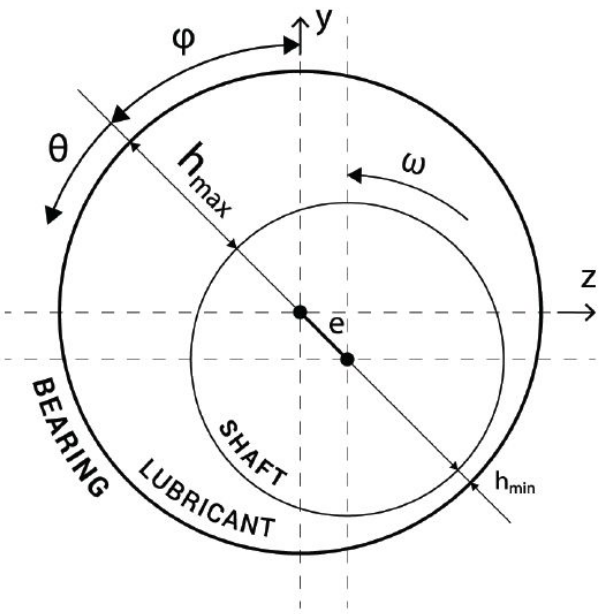

FIGURE 4.1: Bearing geometry.

4.2. Hydrodynamic Lubrication Principles

In order to discuss the hydrodynamic lubrication principles, we should firstly define a problem similar to that of a shaft within a journal bearing. To begin with, suppose we have a **shaft of diameter (d)** rotating inside the inner surface of a **hollow cylinder of diameter (D)**, where D > d. We call **bearing clearance (c)** the quantity D - d. Furthermore, the space between the two surfaces is filled with sufficient amount of lubricant. As illustrated in **Figure 4.1**, during steady state operation (rotational speed constant), the shaft rests slightly off center in comparison to the bearing. One notices that there is a point along the periphery where the distance between the two surfaces is minimal. This offset is interpreted using three variables:

- **Attitude angle (ϕ)**: The angle where minimal distance between the two surfaces occurs,
- **Eccentricity (e):** The off-center distance along the radius at attitude angle.
- **Eccentricity ratio (κ):** The ratio of eccentricity over the radial clearance. Eccentricity ratio equal to zero means that the journal and the bearing are concentric and eccentricity ratio equal unity means that the journal is in contact with the bearing metal.

To further simplify the analysis of the problem, we may picture the inner bearing surface as if it had been cut along its length and upwarped on a flat surface as pictured in **Figure 4.2**. In the same fashion, we can make the same mental abstraction for the shaft, preserving the distance between stator and rotor. Finally, we end up having two surfaces facing each other and forming a converging geometry (**Figure 4.3**). In this converging region, the shaft and bearing distance grows smaller as the circumferential coordinate grows bigger, until it reaches its minimum at the **attitude angle (ϕ)**. Beyond this point, a diverging region is formed where the exact opposite takes place. Since the gap between the two surfaces is filled with lubricant, the minimum distance point corresponds to the minimum oil film thickness.

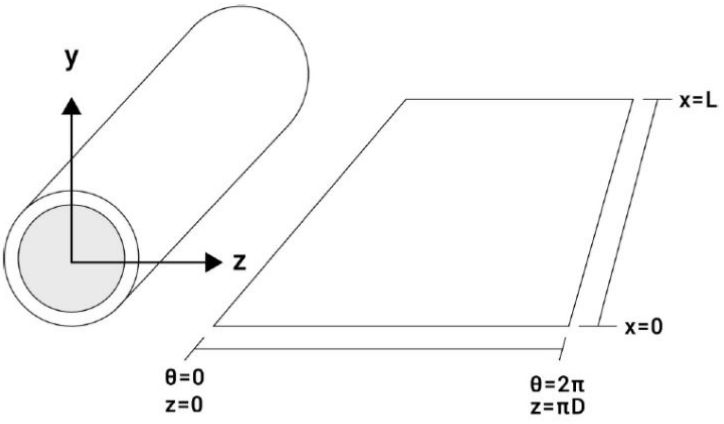

FIGURE 4.2: Unwarped bearing geometry.

In journal bearings, pressure is developed by means of hydrodynamic lubrication. The buildup pressure of the lubricant, initially separates and then, keeps the two surfaces apart. Reynolds was interested in the phenomena related to lubrication and made some basic assumptions [16] related to this analysis:

- Gravitational forces can be ignored in comparison with the viscous forces,
- The pressure is constant through the thickness of the film,
- The curvature of the surfaces is large compared with film thickness,
- There is no slip between the fluid and the solid surface,
- The lubricant is a Newtonian viscous fluid,
- Lubricant flow is laminar (steady-state condition is assumed),
- Inertia induced forces can be neglected compared to viscous forces,
- Lubricant viscosity remains spatially constant (iso-viscous condition).

Ultimately, the mathematical expression governing hydrodynamic lubrication is called the Reynolds equation:

$$\frac{U}{2} \cdot \frac{\vartheta h}{\vartheta z} = \frac{1}{\mu} \left[\frac{\vartheta}{\vartheta z} \left(\frac{h^3}{12} \cdot \frac{\vartheta p}{\vartheta z} \right) + \frac{\vartheta}{\vartheta x} \left(\frac{h^3}{12} \cdot \frac{\vartheta p}{\vartheta x} \right) \right] \tag{4.1}$$

Where,

- U is the tangential velocity of the shaft,
- μ is the lubricant dynamic viscosity,
- h is a function that describes the oil film thickness in 3D space, and
- p is the pressure distribution in 3D space

Reynolds equation is derived from the Navier-Stokes equations with the application of the aforementioned assumptions. It is obvious that in order for hydrodynamic lubrication to come into effect, we need a non-zero relative angular velocity term. Reynolds equation also describes the geometry's influence on the spatial gradient of the pressure. The reason why oil builds pressure is the converging (wedge-like) geometry.

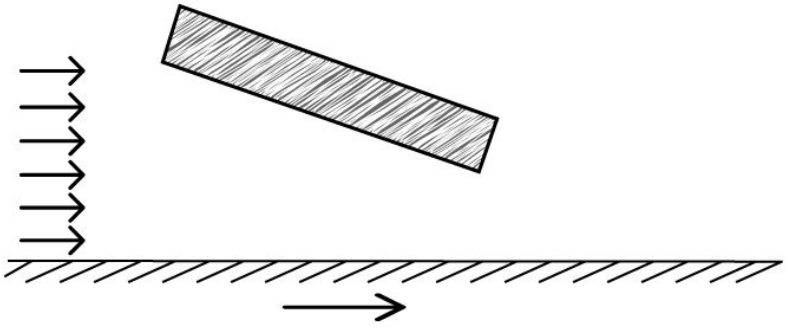

FIGURE 4.3: Converging geometry of journal bearing.

As discussed above, as the shaft rotates, oil is dragged into the wedge volume. In order for mass to be conserved along the flow direction, a gradient of pressure is generated as the wedge converges. Pressure increases at the beginning of the wedge, restricting flow. On other hand, pressure decreases near the end of the wedge, thus boosting outflow. The existence of a pressure gradient causes the fluid velocity profile to bend inwards at the entrance and to bend outwards at the exit.

Boundary conditions are required to solve Reynolds' equation, **EQ. 4.1**. In the case of a journal bearing, the boundary condition at an end of the bearing is simply that the oil film pressure is equal to ambient air pressure, because the boundary of the oil film at the end of the bearing is clear-cut. Of all the boundary conditions proposed, the most notable are:

- *Sommerfeld's boundary condition* assumes that pressure is equal to zero at the edges of the unwarped bearing geometry. The converging section of the geometry develops positive pressure distribution, while the diverging section develops a similar negative pressure distribution. The above analysis concludes that total pressure is equal to zero, thus the lubricant is not capable of supporting any weight. This conditions is, obviously, unrealistic.
- For *Gümbel's boundary condition* pressure distribution at the converging section is identical to the one given by Sommerfeld condition. In contrast, pressure distribution at the diverging section is equal to zero. This boundary condition leads to inaccurate results, because it is violating mass conservation in the diverging part of the bearing. Gümbel's boundary condition is also known as half Sommerfeld's condition.
- In *Reynolds' boundary condition*, the oil film is assumed to terminate at a certain position ($\phi = \pi + \delta$) at which both the pressure and pressure gradient are zero, simultaneously. This condition eliminates a discontinuity of oil flow at $\phi = \pi$, a physical contradiction involved in Gümbel's condition. This is also known as Swift–Stieber's condition. Reynolds' boundary condition gives more accurate results than the two other boundary conditions.

Figure 4.4 depicts the pressure distribution along the flow direction for the three mentioned boundary conditions.

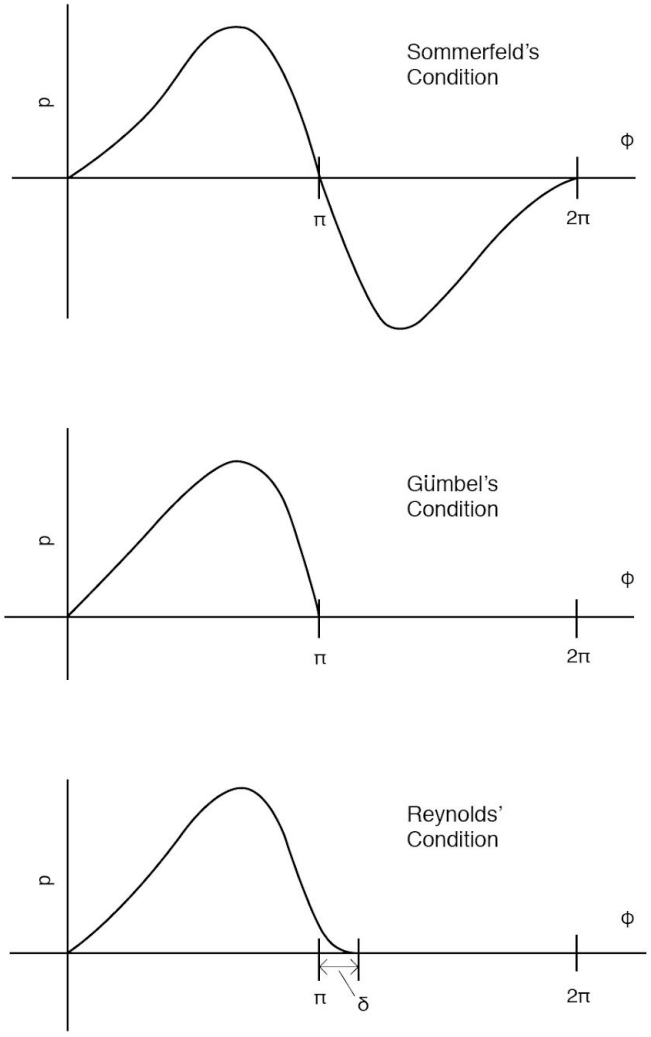

FIGURE 4.4: Boundary conditions for the oil film.

4.3. Operational and Performance Parameters

4.3.1. Load Capacity

The hydrodynamic load carried by the oil film can be calculated by integration of the lubricant pressure along the circumference and length of the outer shaft surface. This load may be further broken down into a pair of perpendicular forces acting along the main system coordinate axes y-z (**Figure 4.1**), whose resultant force is equal to the total bearing load.

$$W_y = \int_0^{2\pi} \int_0^L p \cdot sin\left(\phi + \theta - \frac{\pi}{2}\right) \cdot R \cdot dx \cdot d\theta \tag{4.2}$$

$$W_z = \int_0^{2\pi} \int_0^L p \cdot cos\left(\phi + \theta - \frac{\pi}{2}\right) \cdot R \cdot dx \cdot d\theta \tag{4.3}$$

$$W = \sqrt{W_y^2 + W_z^2} \tag{4.4}$$

4.3.2. Sommerfeld Number

The Sommerfeld number is a non-dimensional characteristic bearing parameter. It comprises both design (R, c, L, D) and operating (μ, ω, W) parameters. All bearings operating at the same Sommerfeld number have same operational characteristics and equal non-dimensional parameter values. Sommerfeld number is given by the following formula:

$$S = \left(\frac{R}{c}\right)^2 \cdot \frac{\mu \cdot \omega \cdot L \cdot D}{W} \tag{4.5}$$

Where,

R is the shaft radius,

c is the radial bearing clearance,

μ is the dynamic viscosity of the lubricant,

ω is the rotational speed of the shaft,

L is the bearing length,

D is the bearing diameter, and

W is the total, externally applied, load.

It is profound that the Sommerfeld number is a dimensionless quantity, as long as consistent units are used (i.e. S.I.). The Sommerfeld number is a key parameter because combines all the variables involved in the design and operation of a bearing. For a given bearing, the larger the value of the Sommerfeld number, the less severe the loading of the bearing is, and vice versa.

4.3.3. Friction Force and Friction Coefficient

In the first place, Reynolds' assumptions demanded that the lubricant is a Newtonian viscous fluid, whose viscosity cannot be neglected. An implication of this assumption is that shear stresses are present at the shaft-lubricant interface. The integral of these shear stresses gives the total friction force.

$$F = \int_0^L \int_0^{\pi D} \left(\frac{2y - h}{2} \cdot \frac{\vartheta p}{\vartheta z} + \frac{U}{h} \right) \cdot dz \cdot dx \tag{4.6}$$

Friction coefficient (f*) can be defined as a ratio of friction force over total bearing load.

$$f^* = \frac{F}{W} \tag{4.7}$$

4.3.4 Power Loss

As a consequence, friction forces produce power losses. If the shaft was able to transmit the full amount of power available to the propeller, there wouldn't be any power losses. That is not the case though. Some of the transmitted power is taken away by friction in each support bearing. Friction power loss of a bearing can be calculated using the following formula:

$$P_{loss} = F \cdot U = W \cdot f^* \cdot \omega \cdot R \tag{4.8}$$

5. Case Study

5.1. General Particular of the Studied Vessel

In the present study, a typical 10,000 TEU containership is considered. The vessel under consideration, whose main particulars are listed in table 5.1, is shaft alignment sensitive taking into consideration the following facts:

- Power output: 51,000 kW x 84 RPM
- Shafting system length: Over 50 meters
- Number of intermediate bearings: Three (3)
- Propeller shaft diameter: 990 mm

TABLE 5.1: Main characteristics of the studied vessel.

TYPE	10,000 TEU CONTAINERSHIP
LENGTH BETW. PERP.	320.00 M
BREADTH	48.20 M
DEPTH	27.20 M
DESIGN DRAFT	13.00 M
SCANTLING DRAFT	15.20 M
SERVICE SPEED	23.80 KN
MAIN ENGINE	MAN B&W 10S90ME-C9.2-TII
POWER OUTPUT	51,000 kW x 84 RPM
KEEL LAID	2013

5.2. Geometry Generation

5.2.1. Hull

It is common shipyard practise to not provide detailed drawings of a vessel's hull to the future owner. As a consequence, the available construction drawings were utilised to generate the vessel's hull. These drawings had to be digitised to be further used. A series of point coordinates on the Y-Z plane were recorded for each section presented in the drawings. As mentioned in Chapter 2, Engauge Digitizer was used to obtain the point coordinates (**Figure 5.1**).

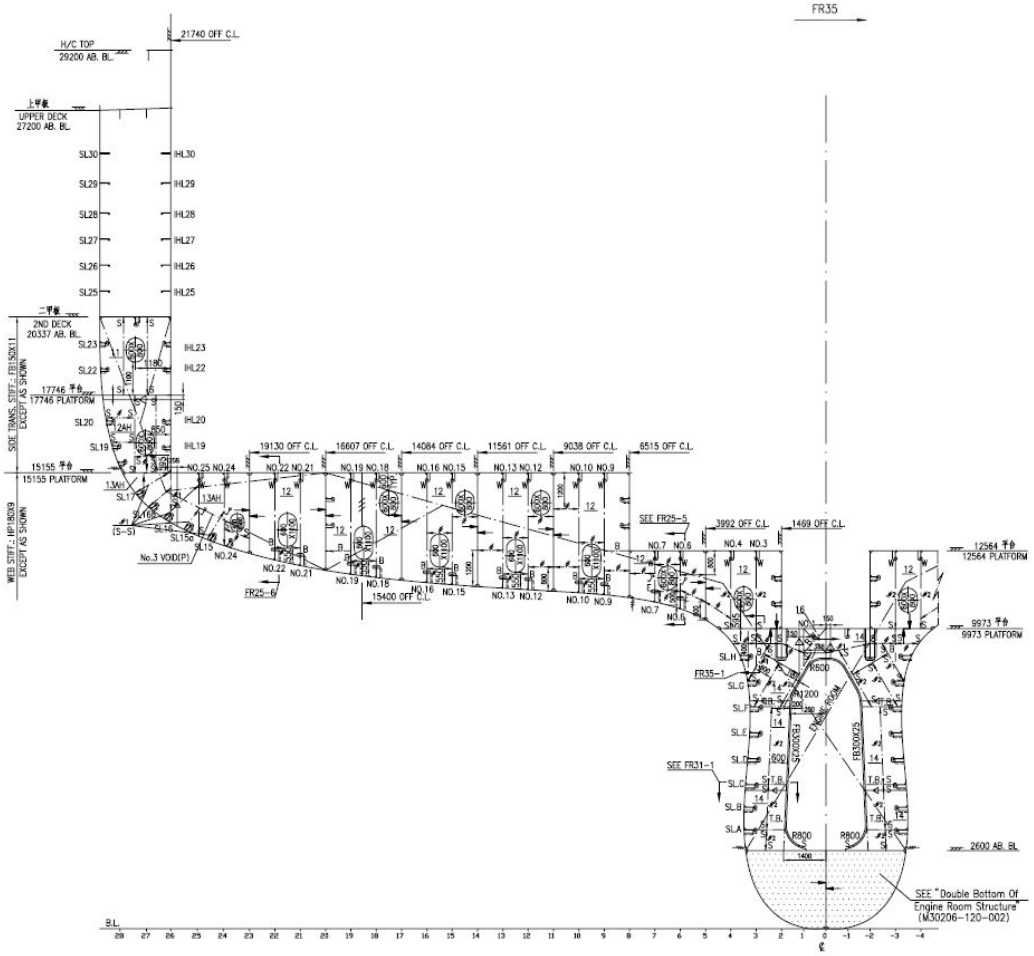

FIGURE 5.1: Construction drawing of Frame 46.

Combining all coordinates exported from the digitizing software for each frame, we end up with a cloud of points in 3D space. Following the procedure described in Chapter 2, we develop the boundary curves and then the stations carefully imposing all tangencies (**Figure 5.2**).

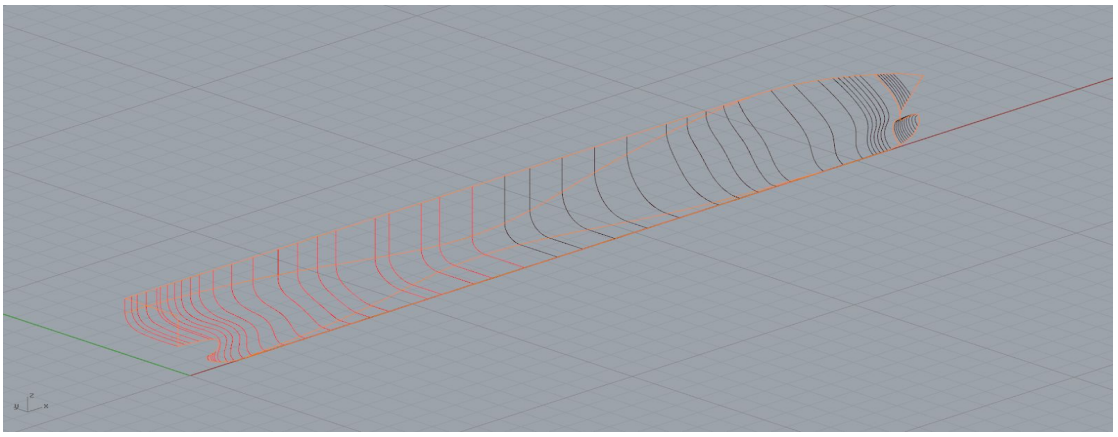

FIGURE 5.2: Boundary curves (orange) and stations (red - aft, black - fore).

Once the fairing process is over (**Figure 5.3**), it is time to fit surfaces that will represent the outer skin of the hull. Our goal is to create a unified surface with at least G1 geometric continuity. To this extent, aft and fore parts of the ship were broken down to smaller surfaces (**Figure 5.4**). Waterline-like curves were fitted from the faired section and then faired to resemble the vessel's hull as accurate as possible.

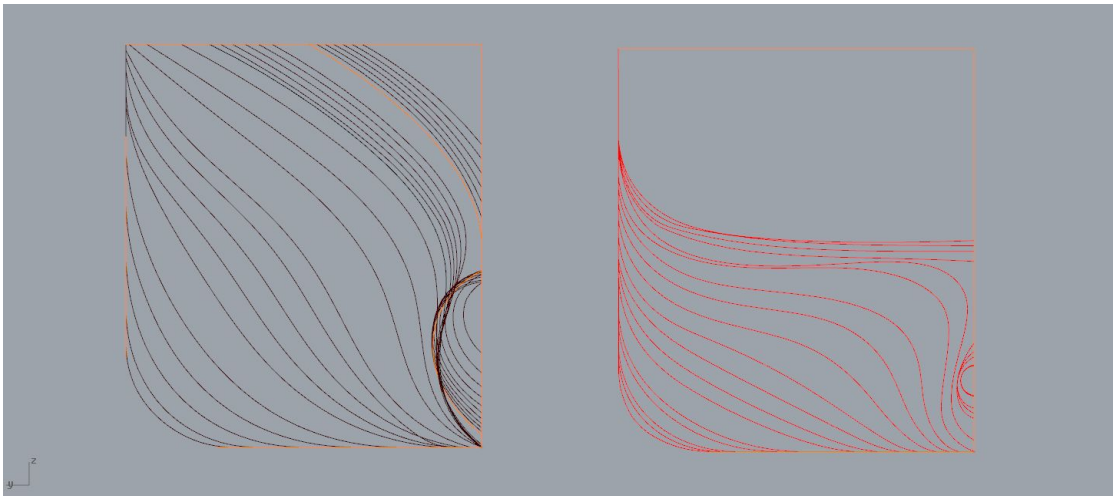

FIGURE 5.3: View of the aft (red) and fore (black) stations after fairing.

Before diving into the modelling of the ship structure, we need to verify that the modelled hull is a faithful representation of the actual vessel's hull. The most accurate way to compare the surface produced to examine the hydrostatic properties for a number of drafts. The most important hydrostatic properties are: volume displacement (m^3), wetted surface area (m^2), waterplane area (m^2), longitudinal center of buoyancy (m) and longitudinal center of flotation (m).

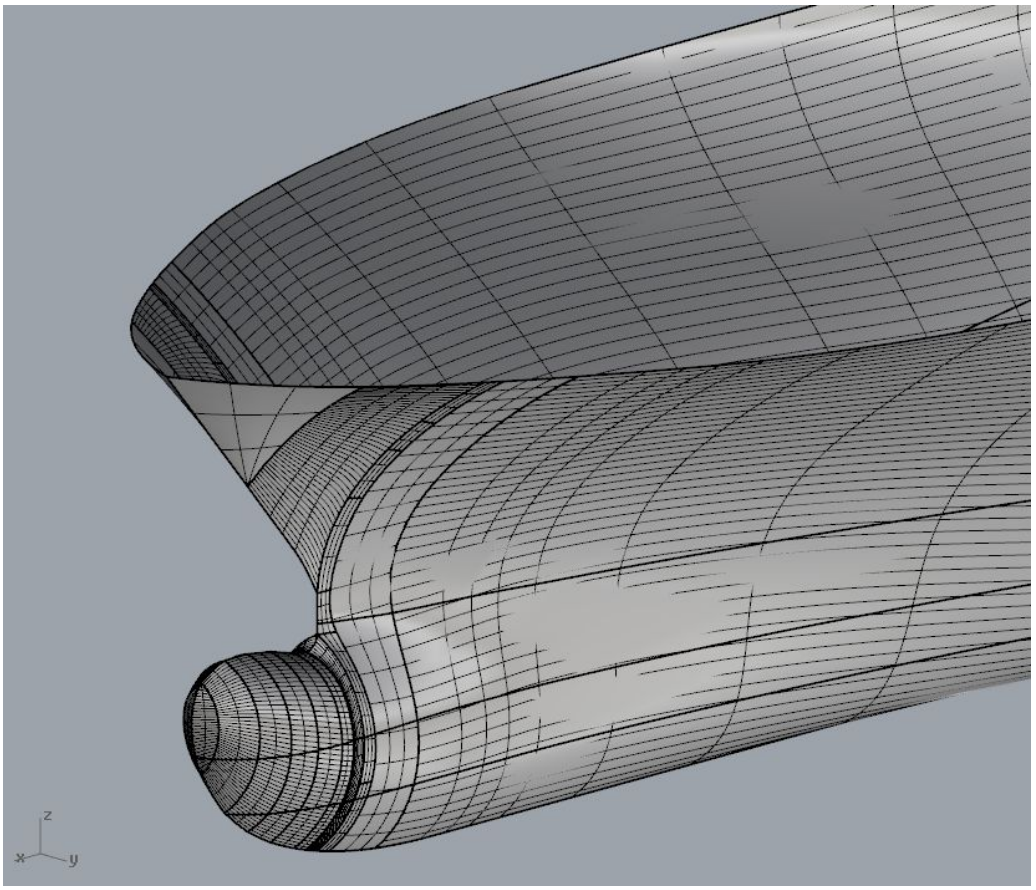

FIGURE 5.4: Surface detail of the fore part of the model.

TABLE 5.2a: Hydrostatics comparison between model and actual vessel for a sets of drafts.

Displacement Volume				Wetter Surface Area			
Draft	**Model**	**Real**	**Difference**	**Draft**	**Model**	**Real**	**Difference**
(m)	**(m3)**	**(m3)**	**%**	**(m)**	**(m2)**	**(m2)**	**%**
4.5	32707.6	32915.0	-0.63%	4.5	9856.1	9965.7	-1.10%
5.0	37144.2	37368.4	-0.60%	5.0	10280.4	10389.5	-1.05%
5.5	41696.9	41927.5	-0.55%	5.5	10707.0	10816.2	-1.01%
6.0	46344.3	46591.2	-0.53%	6.0	11113.8	11218.1	-0.93%
6.5	51077.2	51344.2	-0.52%	6.5	11514.2	11616.4	-0.88%
7.0	55896.0	56182.5	-0.51%	7.0	11922.1	12011.0	-0.74%
8.0	65790.3	66107.6	-0.48%	8.0	12716.2	12799.4	-0.65%
9.0	76005.6	76356.8	-0.46%	9.0	13517.7	13597.9	-0.59%
10.0	86538.9	86930.1	-0.45%	10.0	14359.7	14423.2	-0.44%
11.0	97422.6	97843.3	-0.43%	11.0	15247.4	15297.9	-0.33%
12.0	108674.7	109133.1	-0.42%	12.0	16213.1	16244.0	-0.19%
13.0	120427.2	120910.8	-0.40%	13.0	17258.8	17272.6	-0.08%
14.0	132798.6	133291.8	-0.37%	14.0	18367.7	18369.5	-0.01%
15.0	145753.2	146279.8	-0.36%	15.0	19382.8	19371.2	0.06%
16.0	159056.7	159631.4	-0.36%	16.0	20157.7	20135.6	0.11%

TABLE 5.2b: Hydrostatics comparison between model and actual vessel for a sets of drafts.

Longitudinal Center of Buoyancy				Longitudinal Center of Flotation			
Draft	**Model**	**Real**	**Difference**	**Draft**	**Model**	**Real**	**Difference**
(m)	**(m)**	**(m)**	**%**	**(m)**	**(m)**	**(m)**	**%**
4.5	157.92	157.86	0.04%	4.5	159.90	159.77	0.08%
5.0	158.15	158.10	0.03%	5.0	159.98	159.84	0.09%
5.5	158.33	158.28	0.03%	5.5	159.98	159.82	0.10%
6.0	158.46	158.43	0.02%	6.0	159.84	159.68	0.10%
6.5	158.56	158.53	0.02%	6.5	159.54	159.43	0.07%
7.0	158.62	158.59	0.02%	7.0	159.16	159.03	0.08%
8.0	158.60	158.58	0.01%	8.0	157.99	157.90	0.06%
9.0	158.39	158.39	0.00%	9.0	156.41	156.32	0.06%
10.0	158.01	158.01	0.00%	10.0	154.30	154.25	0.03%
11.0	157.43	157.45	-0.01%	11.0	151.63	151.57	0.04%
12.0	156.65	156.67	-0.01%	12.0	148.25	148.24	0.01%
13.0	155.64	155.67	-0.02%	13.0	144.34	144.37	-0.02%
14.0	154.39	154.42	-0.02%	14.0	140.07	140.11	-0.03%
15.0	152.94	152.99	-0.03%	15.0	137.35	137.36	-0.01%
16.0	151.64	151.69	-0.03%	16.0	137.66	137.67	-0.01%

Based on the above comparison, the end result is satisfying. On average, most of the above hydrostatic properties are off the mark by a maximum absolute value of less than 1%.

5.2.2. Compartmentation

In our study, only the aft end of the vessel is modelled (from the aftmost end to the watertight bulkhead of the engine room). The modelling of the steel structure of the vessel was done in parts for better supervision and resources management (RAM). The construction drawings of the vessel were also divided in discrete parts:

- After End Structure (Transom - Fr. 13)
- Stern Frame (Fr. 11 - Fr. 21)
- After Cargo Hold Area Structure (Fr. 14 - Fr. 82)
- Engine Room Structure (Fr. 83 - Fr. 106)
- Double Bottom of Engine Room (Fr. 22 - Fr. 106)
- Deck House & Funnel Structure

Each of these drawings is further divided into four categories of drawings:

- Shell Expansion
- Decks
- Buttocks
- Sections

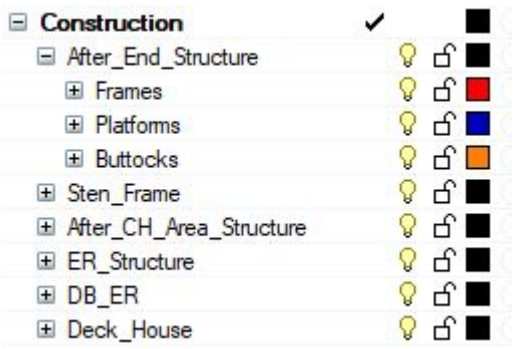

The abovementioned division was used to model the steel structure of the vessel. A color code was established to distinguish different construction entities; red for frames, blue for decks/platforms and orange for buttocks.

FIGURE 5.5: Layer tree in Rhinoceros 3D.

Figure 5.6 illustrates the color code subdivision of the double bottom modelling. This way, structural entities are modelled quickly and efficiently. **Figure 5.7** shows structural details of the double bottom structure such as: longitudinal girders, manholes, stiffeners, etc.

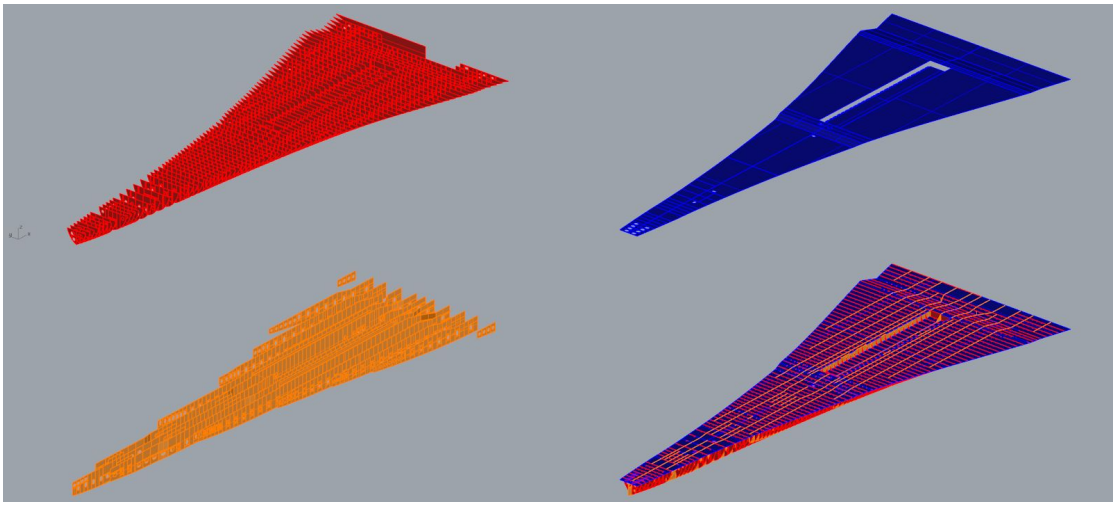

FIGURE 5.6: Color code subdivision of double bottom structure.

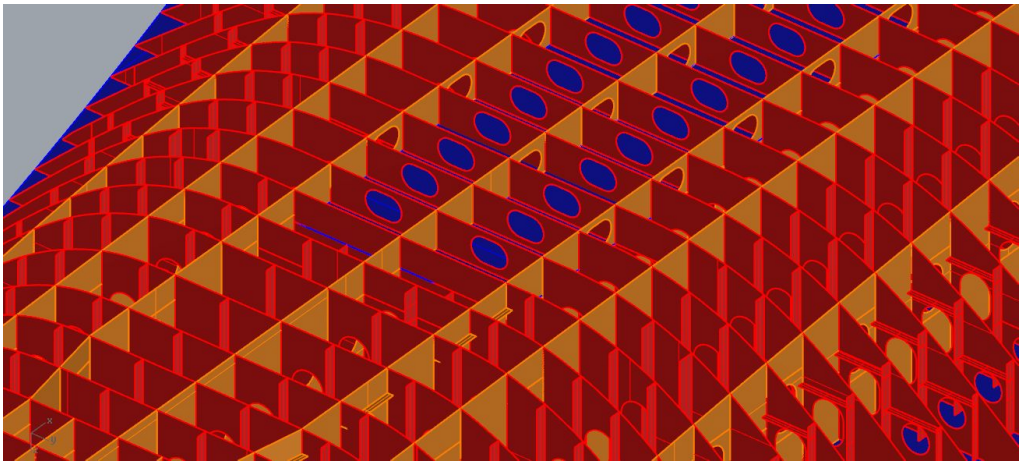

FIGURE 5.7: Structural details in double bottom structure.

In the same fashion, **Figures 5.8 to 5.20** illustrate the color code subdivision and the respective details of the other structure parts of the vessel.

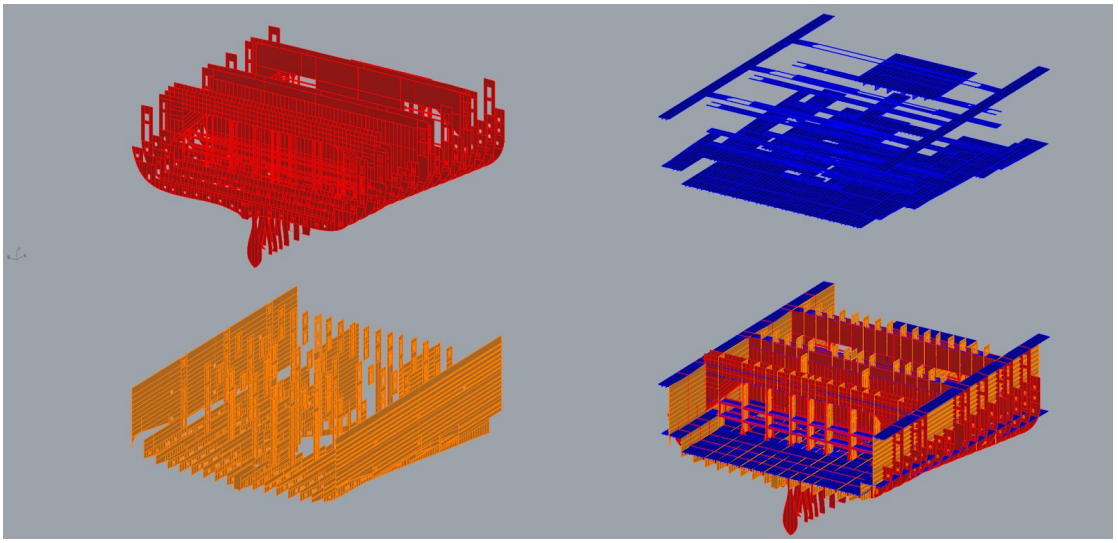

FIGURE 5.8: Color code subdivision of after cargo hold structure.

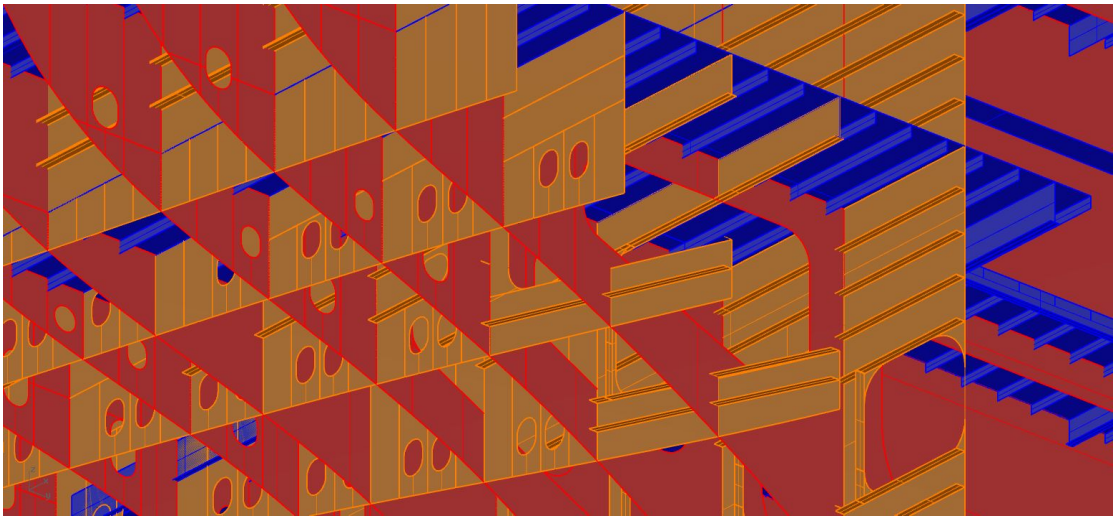

FIGURE 5.9: Structural details in after cargo hold structure.

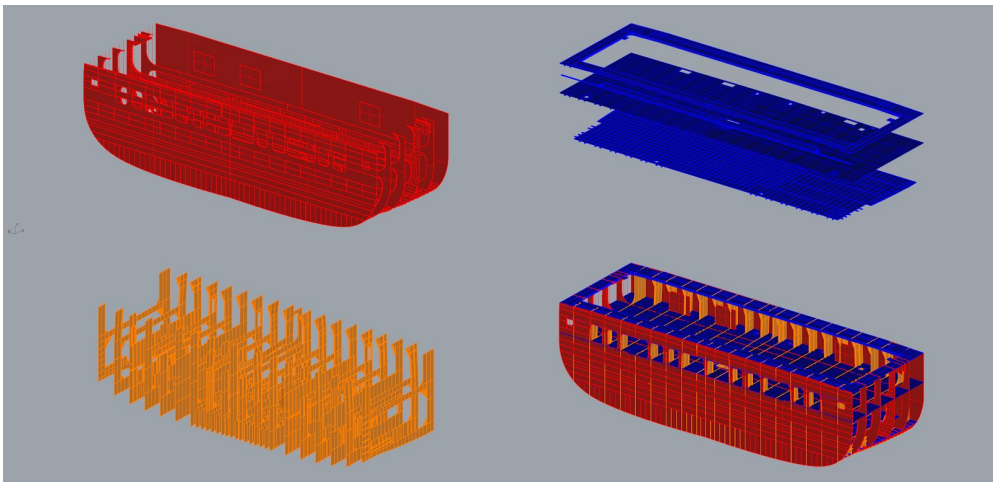

FIGURE 5.10: Color code subdivision of after end structure.

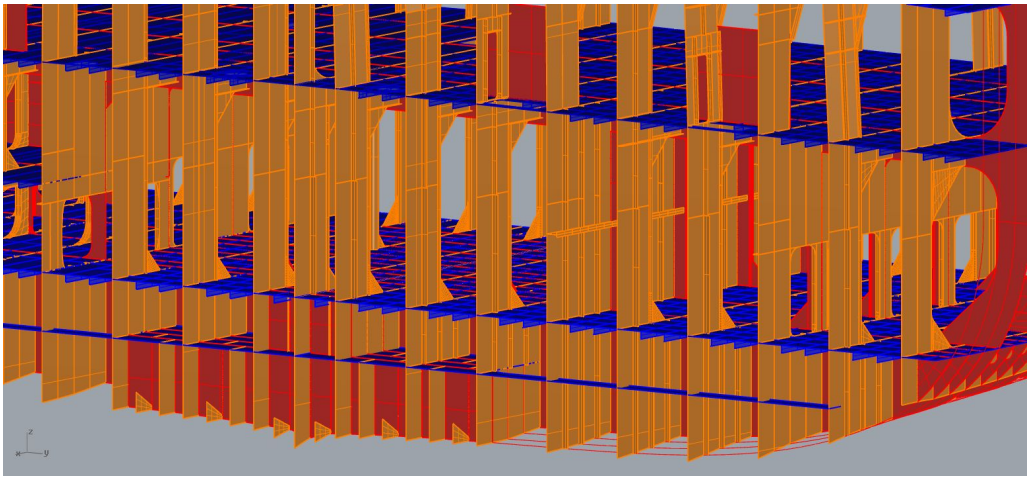

FIGURE 5.11: Structural details in after end structure.

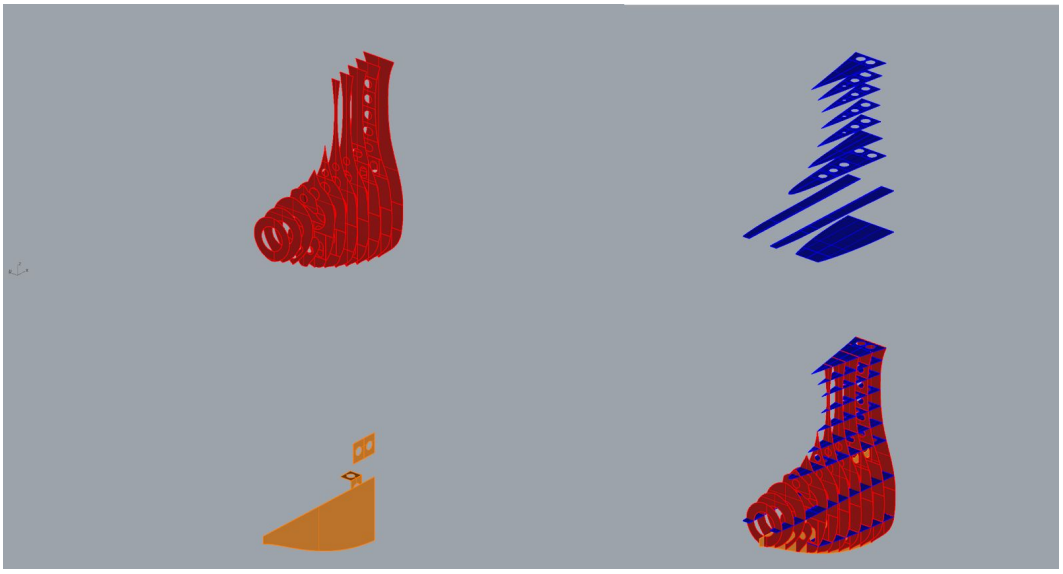

FIGURE 5.12: Color code subdivision of stern frame structure.

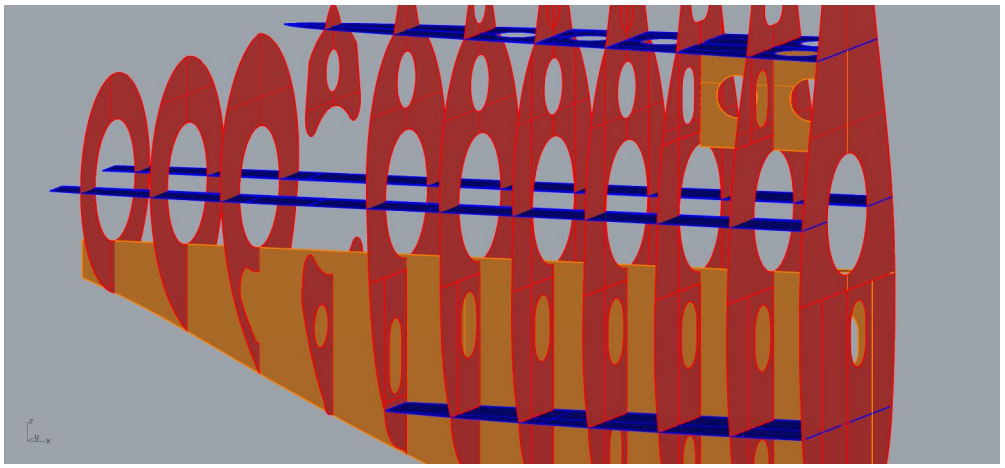

FIGURE 5.13: Structural details in stern frame structure.

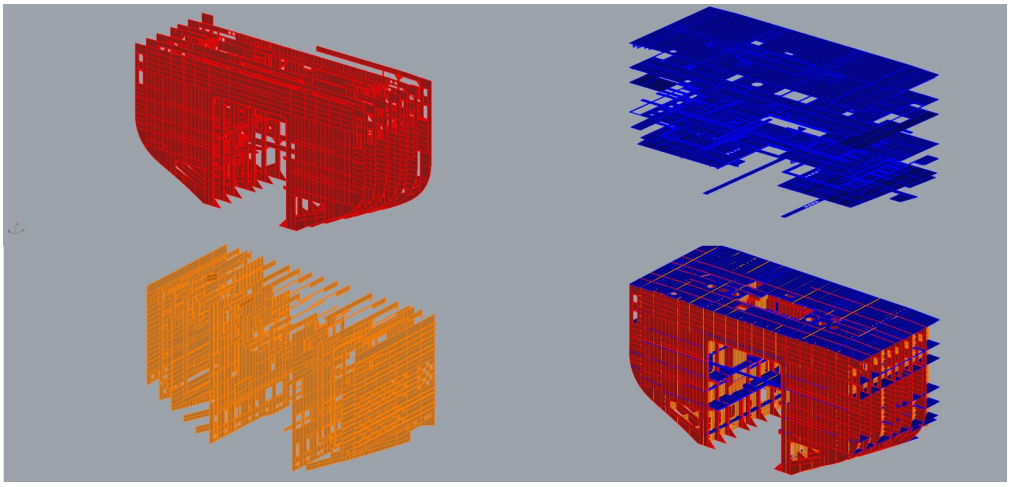

FIGURE 5.14: Color code subdivision of engine room structure.

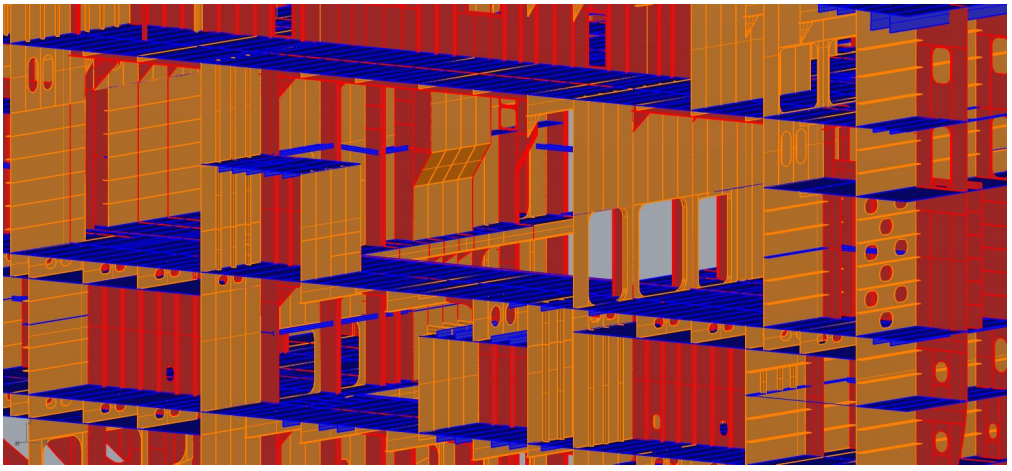

FIGURE 5.15: Structural details in engine room structure.

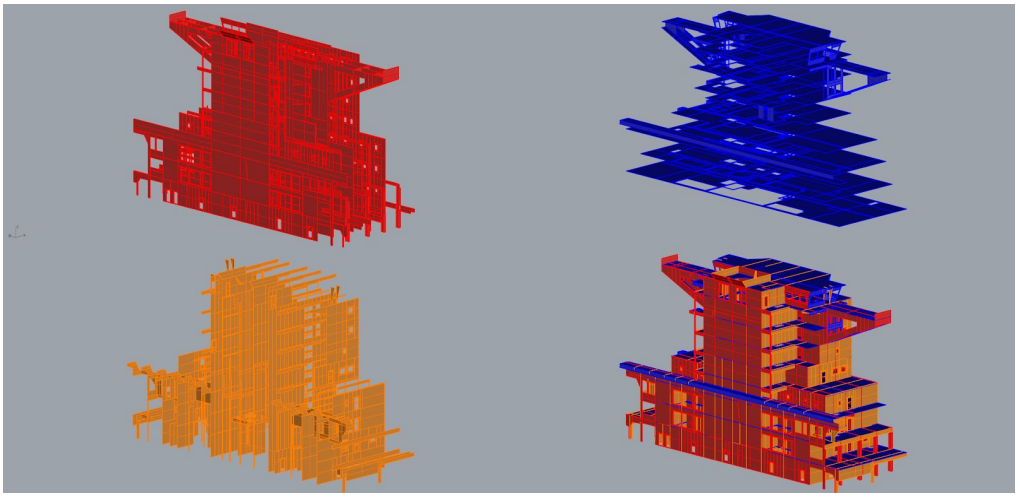

FIGURE 5.16: Color code subdivision of superstructure.

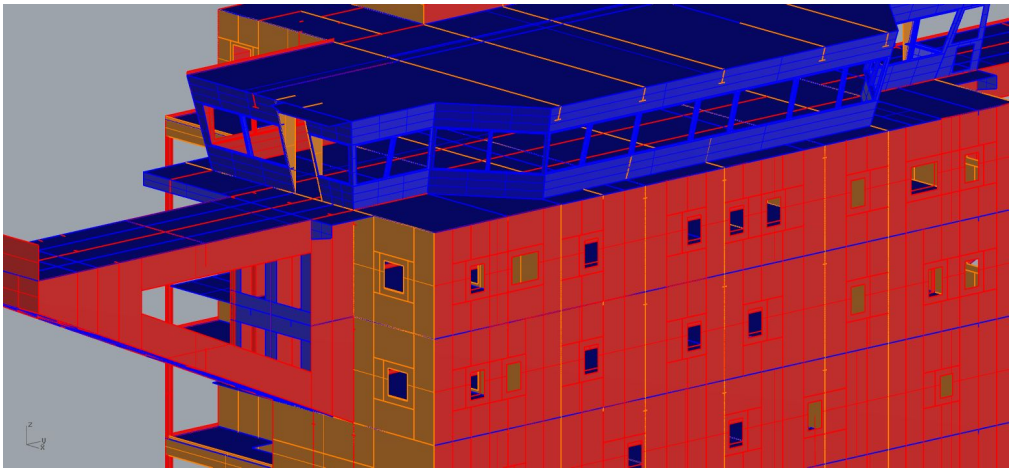

FIGURE 5.17: Structural details in superstructure.

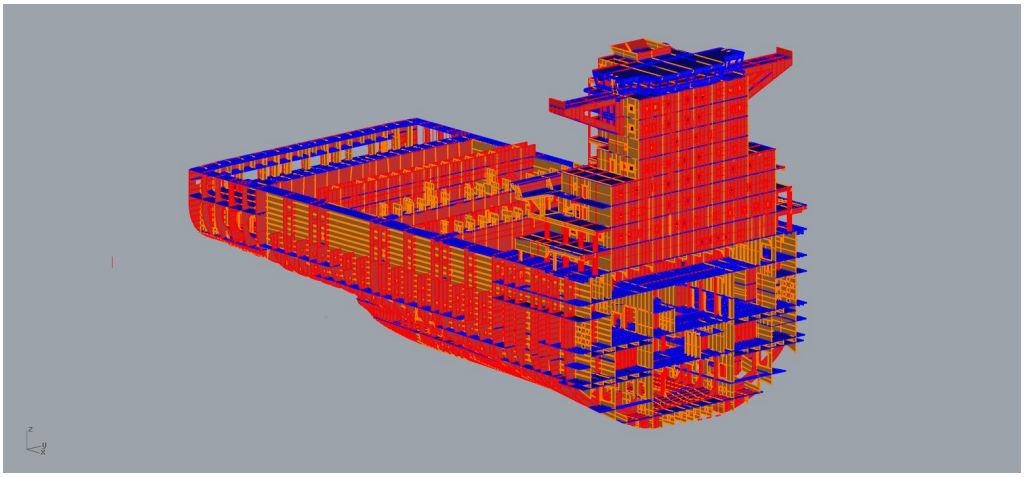

FIGURE 5.18: Structural details of the modelled structure (I).

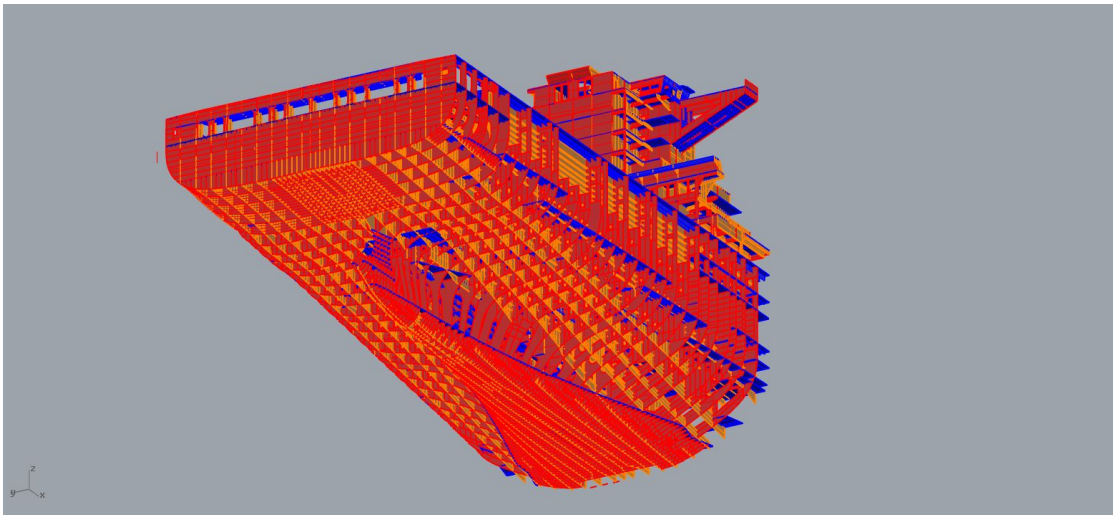

FIGURE 5.19: Structural details of the modelled structure (II).

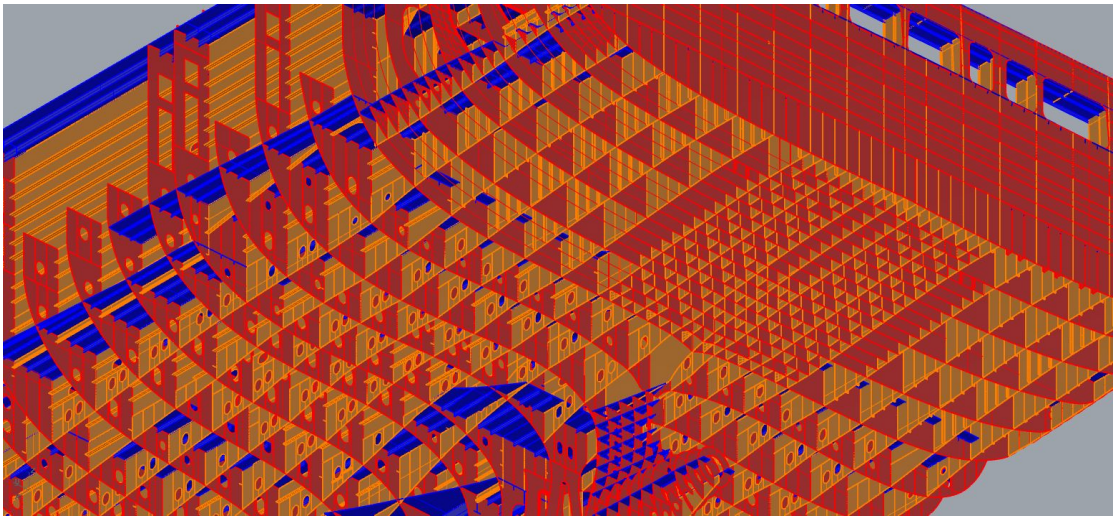

FIGURE 5.20: Structural details of the modelled structure (III).

5.3. Finite Element Analysis of the Vessel

5.3.1. FEM Generation

The main characteristics of the studied containership have been presented in **Table 5.1**. Finite Element Analysis is performed to calculate the hull deformations of the vessel, at different loading conditions. The static analyses are conducted with the aid of the ANSA pre-processor and the ABAQUS solver. Here, thermal loads from the engine or the environment are not taken into consideration. First, a Finite Element Model of the ship structure is generated. The whole structure of the ship is represented by first-order shell elements; at the stern tube region, solid tetrahedral elements are used. Stiffeners are represented as explained in Chapter 2. A coarse mesh is generated for the whole structure (element length of 250 mm), except for the engine room floor, where finer mesh (element length of 100 mm) ensures improved accuracy, **Figures 5.21** through **5.23**.

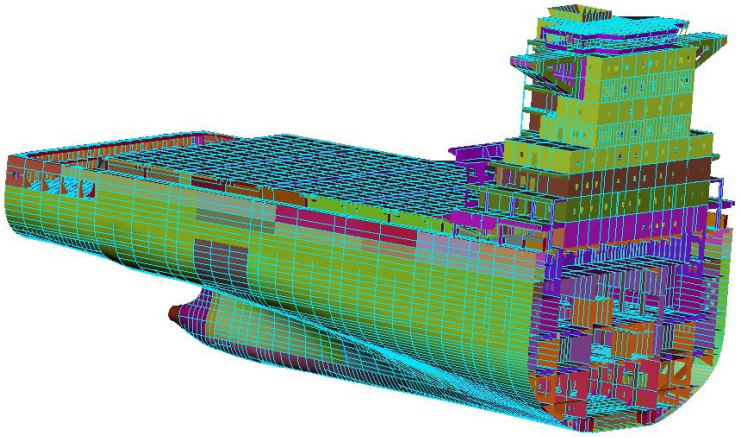

FIGURE 5.21: Global FEM of the studied container vessel.

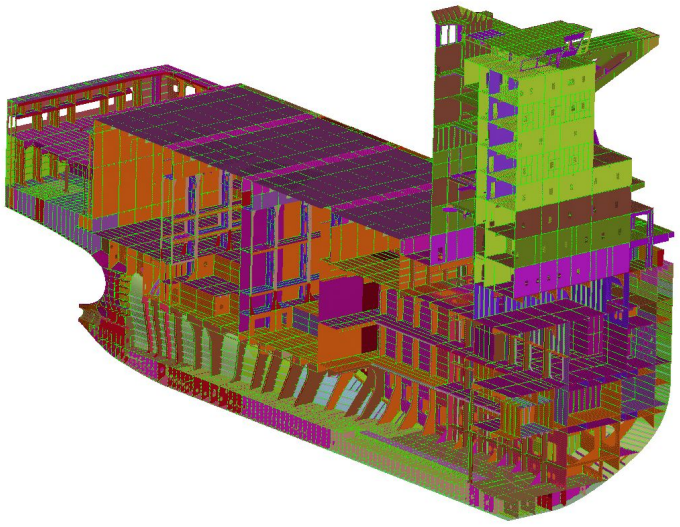

FIGURE 5.22: Details of global FEM of the studied container vessel.

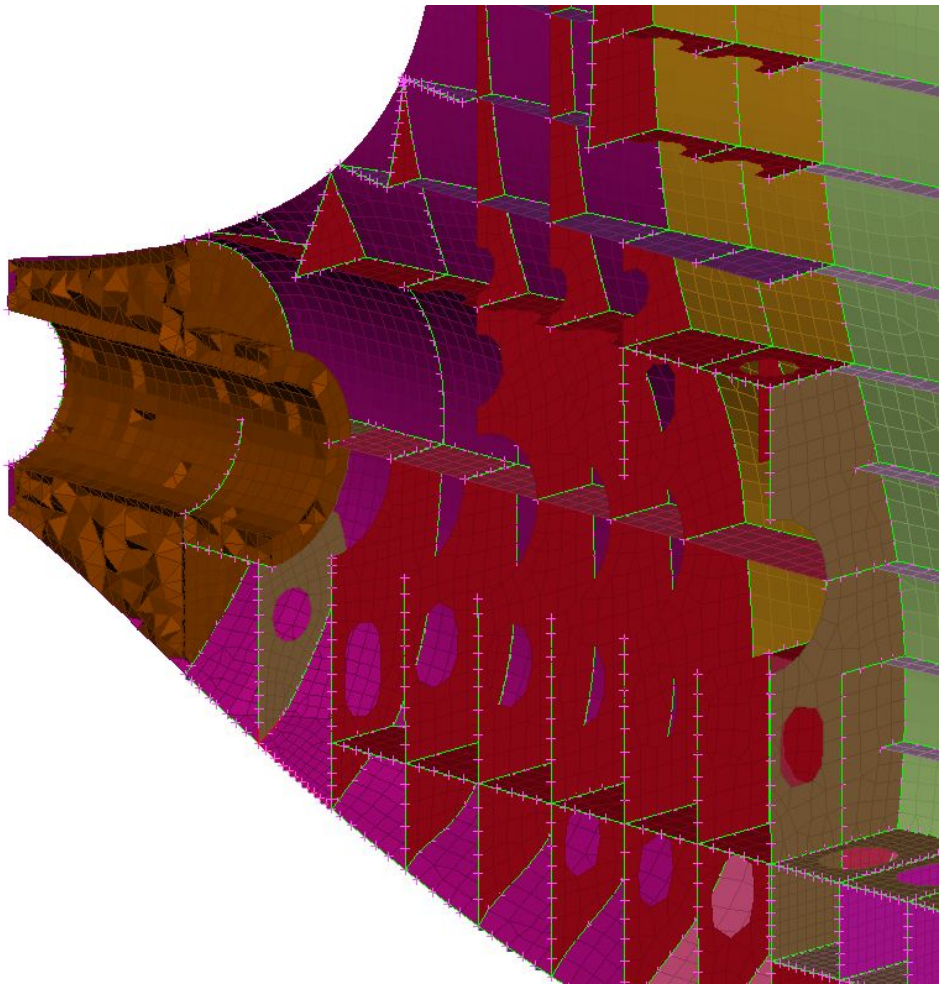

FIGURE 5.23: Detail of the generated FE mesh at the stern tube region of the vessel.

The mesh generation is an automated process performed by the ANSA Batch Meshing Tool. Meshing parameters and quality criteria are defined in two meshing scenarios (fine mesh for the engine room floor and coarse mesh for the rest of the structure, **Table 5.3**). Re-meshing algorithms act on areas with poor mesh quality until the predefined quality criteria are fulfilled. The final model comprises over 2,500,000 shell elements and 21,000 solid tetrahedrals.

The shaft of the vessel comprises 78 beam elements of different properties and cross sections representing the diameter variations of the shaft along its length. The bearings are considered as rigid bodies and they are represented by RBE2 elements connecting the bearing foundation to the shaft centre line, **Figure 5.24**.

Machinery, auxiliary structures and small constructions that do not contribute to ship strength are not modelled in the present FEM model. Their mass is applied to the model as non-structural mass. This mass is appropriately distributed over the FEM model, so as to reach the prescribed lightship and the corresponding centre of gravity. The engine mass is represented by a lumped mass of 1720 t distributed to the engine foundation positions by RBE3 elements.

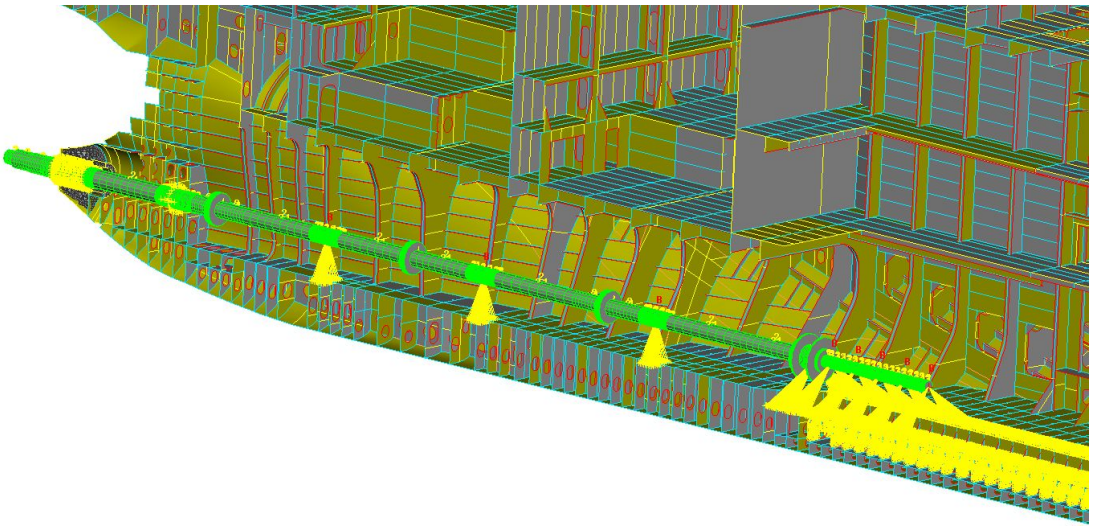

FIGURE 5.24: Engine and bearings representation in the studied FE model.

TABLE 5.3: Meshing parameters and quality criteria.

Global Meshing Parameters	
Element length	250 mm
Engine Room Floor Meshing Parameters	
Element length	100 mm
Mesh Quality Criteria	
Aspect ratio	3
Skewness	30º
Angle (QUADS)	45-135º
Angle (TRIAS)	30-120º

Fifteen loading conditions of the vessel are considered in the present analysis as shown at **Table 5.4**. The contents of the tanks are represented by lumped mass connected to each hold bottom with RBE3 elements. The ship is positioned on still water considering the vessel's total displacement and centre of gravity. Buoyancy is applied as pressure at the hull underneath the waterline using PLOAD4 entities, **Figure 5.25**.

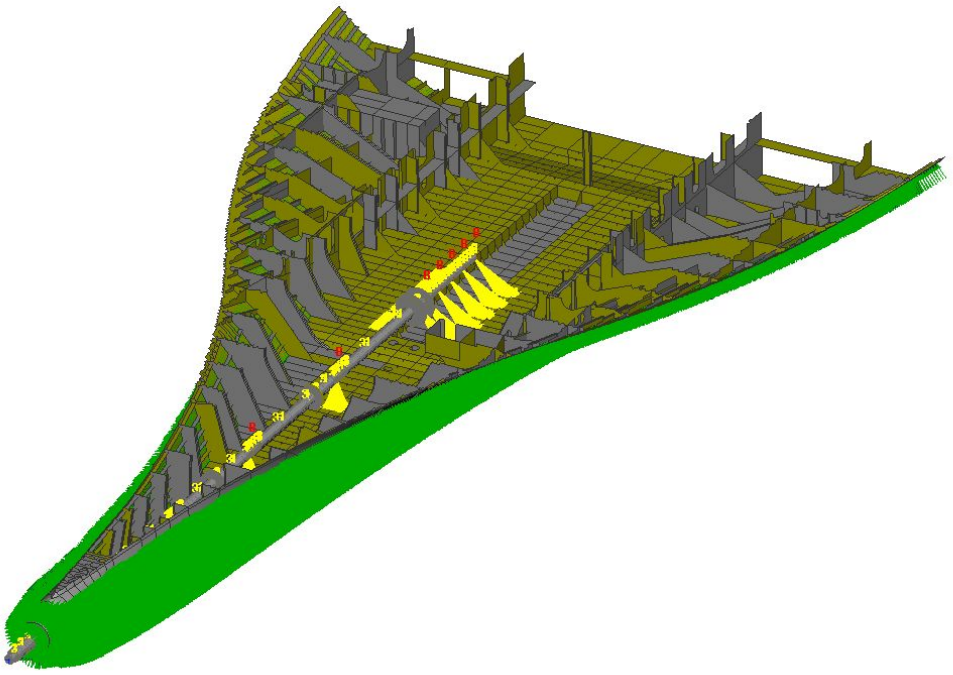

FIGURE 5.25: Application of hydrostatic pressure due to buoyancy in the FE model.

TABLE 5.4: Representative loading conditions of the vessel.

#	Case	Description	Draft Aft	Draft Fore
1	DOCK1	NORMAL DOCKING	6157	6168
2	DOCK2	DOCKING WITH 12000t CARGO (12T x 1000)	6610	6576
3	BLD	BALLAST DEP.	10854	6951
4	BLD-S11.1	BALLAST DEP. (URS11.1)	11186	5575
5	BLD-PANAMA	BALLAST DEP. - PANAMA	9915	8649
6	BLM-PANAMA	BALLAST MID. - PANAMA	9450	8104
7	BLA-PANAMA	BALLAST ARR. - PANAMA	9054	7669
8	16TDD	16T/TEU DEP. AT DESIGN DRAFT (16T x 4676)	13326	12595
9	16TAD	16T/TEU DEP. AT DESIGN DRAFT (16T x 4676)	12803	11454
10	11TDS	11T/TEU DEP. AT SCANTLING DRAFT (11T x 8984)	15431	14886
11	11TAS	11T/TEU ARR. AT SCANTLING DRAFT (11T x 8984)	15495	14511
12	16TDS	16T/TEU DEP. AT SCANTLING DRAFT (16T x 6474)	15409	14916
13	16TAS	16T/TEU ARR. AT SCANTLING DRAFT (16T x 6474)	15122	14185
14	MAX	HOMO. AT 15.2m DRAFT FOR CLASS (14T x 7390)	15203	15194

5.3.2. FEM Validation

In our analysis, the best way to ensure the validity of the results is to compare the reaction forces induced by the used boundary conditions with the reaction forces listed in the loading manual of the vessel. **APPENDIX B** enlists all the studied loading conditions along with the expected shearing forces and bending moments. **Table 5.5** summarises the comparison between the loading manual values and the numerical ones. Shearing forces exhibit a mean absolute deviation of 2.52%, while bending moments resemble a 3.78% mean absolute deviation. Taking these deviation values into consideration, we can conclude that our analysis is valid; hence, hull deflections calculated are also valid.

TABLE 5.5: Reaction forces comparison between loading manual and numerical analysis.

A/A	Case	Reaction Forces at Frame 106 (Engine Room Bulkhead)					
		Loading Manual		Numerical		% Difference	
		SF (N)	BM (N*mm)	SF (N)	BM (N*mm)	SF	BM
1	DOCK1	9.085E+07	3.799E+12	9.09E+07	3.81E+12	0.10%	0.35%
2	DOCK2	8.409E+07	3.648E+12	8.41E+07	3.67E+12	0.03%	0.51%
3	BLD	4.487E+07	2.655E+12	4.45E+07	2.72E+12	-0.89%	2.47%
4	BLD-S11.1	4.464E+07	2.621E+12	4.43E+07	2.68E+12	-0.84%	2.30%
5	BLD-PANAMA	5.477E+07	2.950E+12	5.44E+07	3.02E+12	-0.72%	2.21%
6	BLM-PANAMA	5.886E+07	3.162E+12	5.85E+07	3.22E+12	-0.63%	1.73%
7	BLA-PANAMA	6.191E+07	3.327E+12	6.19E+07	3.38E+12	-0.06%	1.48%
8	16TDD	3.014E+07	3.176E+12	3.13E+07	3.43E+12	3.95%	8.05%
9	16TAD	3.971E+07	3.832E+12	4.09E+07	4.06E+12	3.02%	6.05%
10	11TDS	4.426E+07	5.501E+12	4.56E+07	5.81E+12	3.07%	5.60%
11	11TAS	3.249E+07	5.768E+12	3.39E+07	5.68E+12	4.42%	-1.57%
12	16TDS	1.848E+07	3.741E+12	1.98E+07	4.05E+12	7.19%	8.24%
13	16TAS	2.202E+07	4.304E+12	2.32E+07	4.59E+12	5.60%	6.65%
14	MAX	3.555E+07	4.369E+12	3.79E+07	4.75E+12	6.69%	8.77%

5.4. Shaft Alignment Calculations - Input Data

5.4.1. Shafting System Particulars

Figure 5.26 illustrates the shafting system model of the studied containership. The shafting system model comprises the propeller shaft, the intermediate shaft and part of the crankshaft. Two stern tube bearings support the propeller shaft, while the intermediate shaft is supported by three bearings. In our study, only the first six crankshaft bearings are taken into consideration. Bearing characteristics are presented below:

Aft Stern Tube Bearing (ASB)

- Outer shaft diameter 988 mm
- Effective bearing length 2174 mm
- Length over diameter 2.20
- Radial clearance 0.75 mm
- Max permissible load 0.8 MPa / 1718 kN
- Foundation stiffness 3.5E+10 N/m

Forward Stern Tube Bearings (FSB)

- Outer shaft diameter 990 mm
- Effective bearing length 990 mm
- Length over diameter 1.00
- Radial clearance 0.75 mm
- Max permissible load 0.8 MPa / 784 kN
- Foundation stiffness 2.0E+10 N/m

Intermediate Shaft Bearing (ISB)

- Outer shaft diameter 830 mm
- Effective bearing length 850 mm
- Length over diameter 1.02
- Radial clearance 0.40 mm
- Max permissible load 1.0 MPa / 705 kN
- Foundation stiffness 5.0E+10 N/m

General Considerations

- Shaft density 7850 kg/m^3
- Young's modulus 2.1×10^{11} N/m^2
- Lubricant dynamic viscosity 0.1 Pa S

The shaft consists of 78 beam elements and a total of 79 nodes. The geometry characteristics and various loads of each beam are presented in **APPENDIX A**.

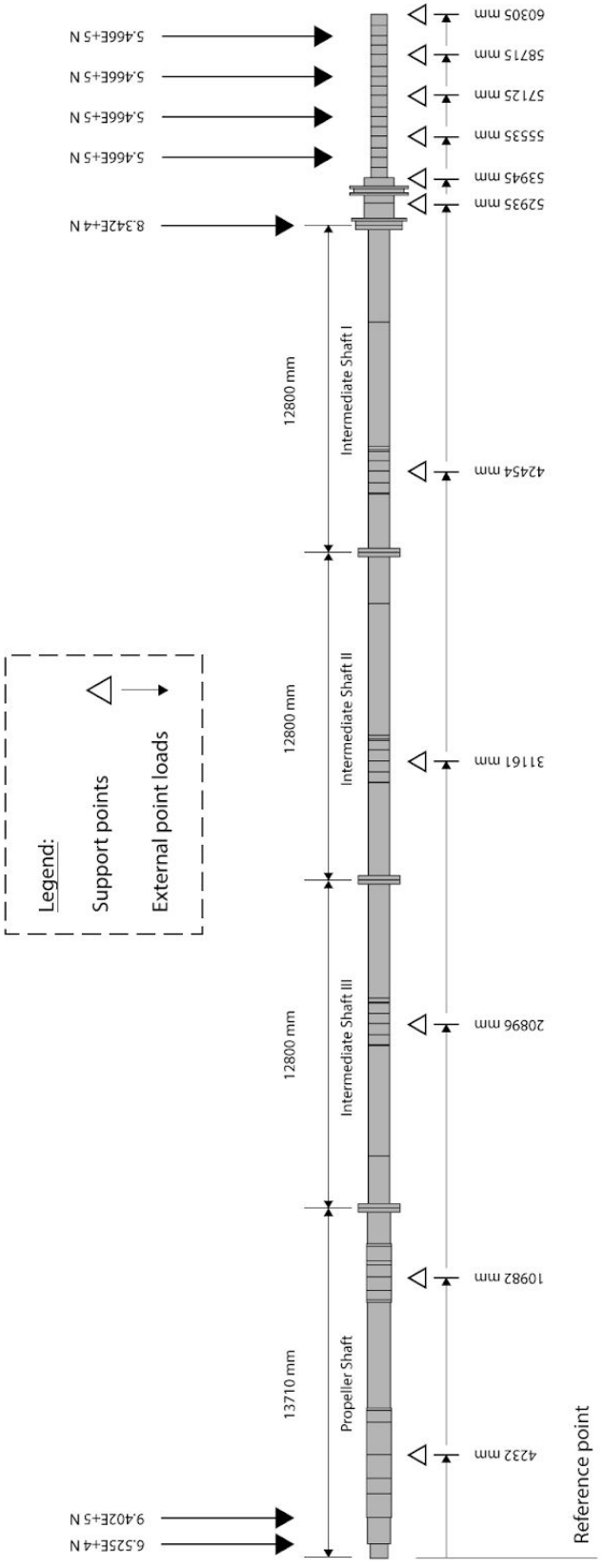

FIGURE 5.26: Detailed model of the shafting system of the present study.

5.4.2. Operation parameters

For hot and running main engine condition, additional considerations have to be made. Such considerations are (a) additional vertical offsets for each crankshaft bearing due to thermal expansion of the M/E, and (b) additional vertical offsets due to hydrodynamic lubrication. Each M/E bearing is elevated by 0.41 mm, as per the manufacturer's instructions when considering the hot M/E condition. Regarding the offsets due to hydrodynamic lubrication, a shaft alignment software, developed by Orestis Vlachos in the course of his diploma thesis [11], is utilised to obtain the reaction forces of the system's bearings for each loading condition.

The ship of the present study is outfitted with a main engine capable of delivering 45,900 kW of power, at 81 RPM at N.C.R. which corresponds to a service speed of 23.8 knots. Each loading condition corresponds to a different displacement, which means that in order to achieve the service speed of 23.8 knots, the propeller rotational speed will be slower, given the decrease in total resistance.

In our quest for estimation of propeller rotational speed, propeller curve and admiralty coefficient were also utilised. Propeller curve provides the power output as a function of propeller rotational speed. In general, propeller curve is different depending on the loading condition; in our study, propeller curve was considered constant for all loading conditions, and equal to:

$$P = 0.08637 \cdot n^3 \tag{5.1}$$

Figure 5.27 depicts the propeller curve along with the two known operating points of the main engine; N.C.R. and M.C.R.

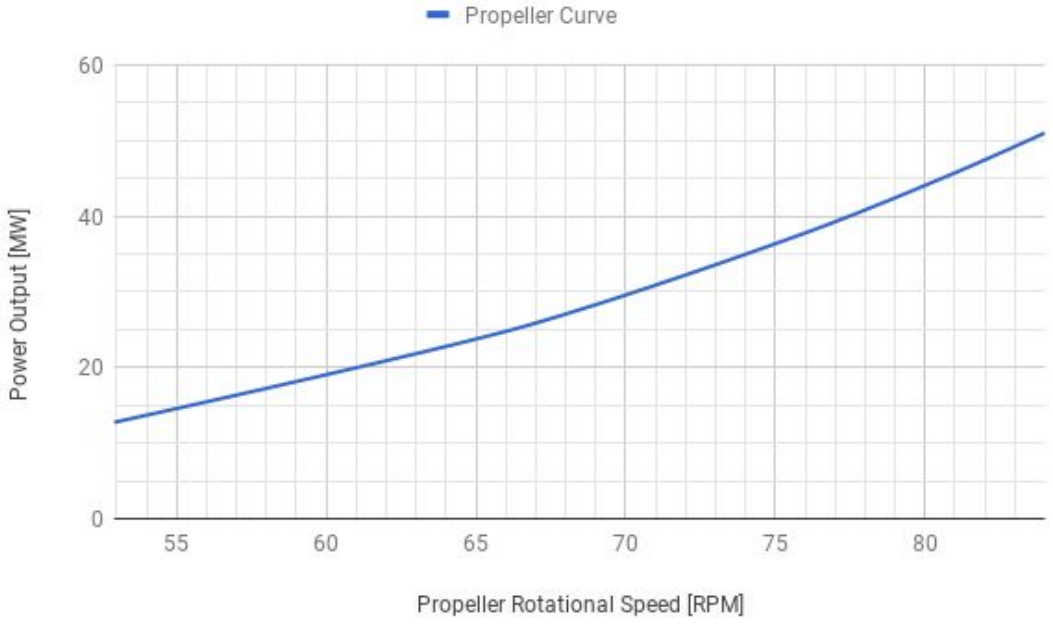

FIGURE 5.27: Propeller curve of the studied vessel.

The Admiralty coefficient **(A)** is a constant valid for a given ship and is useful when simple ship estimations are needed. The Admiralty coefficient **(A)** is constant for a given hull and gives the approximate relationships between the needed propulsion power **(P)**, ship speed **(V)** and displacement **(Δ)**. Thus, the Admiralty coefficient is defined as follows:

$$A = \frac{\Delta^{\frac{2}{3}} \cdot P^3}{V} \tag{5.2}$$

As mentioned above, the installed main engine is capable of delivering 45,900 kW of power, at 81 RPM at N.C.R. corresponding to a service speed of 23.8 knots. After having calculated the Admiralty coefficient and keeping the service speed as constant, we can calculate the required output power for each different displacement (loading condition). Finally, the rotational propeller speed can be calculated using **EQ. 5.1**. **Table 5.6** outlines the final values of rotational propeller speed as calculated above.

TABLE 5.6: Estimated value of propeller rotational speed for the studied loading conditions of the vessel.

L.C.	DOCK1	DOCK2	BLD	BLD-S11.1	BLD-PANAMA	BLM-PANAMA	BLA-PANAMA
RPM	66.2	67.3	73.2	72.1	73.9	72.3	71.8
L.C.	16TDD	16TAD	11TDS	11TAS	16TDS	16TAS	MAX
RPM	81.1	79.6	84.9	84.7	84.9	84.1	84.9

5.4.3. Initial static shaft alignment plan - Reference Condition

The line running through the centre of the stern tube is defined as the reference line. A docking condition, whilst the vessel would be afloat, is considered as the reference condition. In **Table 5.7**, initial vertical offsets of the bearings relative to the reference line, based on the shaft alignment plan of the vessel.

The following considerations have been made for the calculation presented in this section:

- The main engine is cold and not running; thus no vertical offsets due to thermal expansion or hydrodynamic lubrication are incorporated.
- The propeller and parts of the propeller shaft are partially immersed in water. Therefore, buoyancy effect is considered.

TABLE 5.7: Initial shaft alignment plan - Reference condition.

Bearing No.	Bearing	Diametrical Clearance (mm)	Bearing Foundation Stiffness (N/m)	L/D	Offsets (mm)	Reactions (N)	Mean Pressure (Pa)
1	ASB	1.50	3.5E+09	0.988	0.75	1.549E+6	0.72
2	FSB	1.50	3.5E+09	0.990	0.75	2.461E+5	0.25
3	ISB3	0.80	2.0E+09	0.830	-2.0	3.685E+5	0.52
4	ISB2	0.80	2.0E+09	0.830	-3.0	4.842E+5	0.69
5	ISB1	0.80	2.0E+09	0.830	-4.0	5.093E+5	0.72
6	MB13	0.60	5.0E+09	1.180	-6.0	4.425E+5	0.41
7	MB12	0.60	5.0E+09	1.180	-6.0	3.851E+5	0.44
8	MB11	0.60	5.0E+09	0.602	-6.0	4.891E+5	0.97
9	MB10	0.60	5.0E+09	0.602	-6.0	5.697E+5	1.13
10	MB9	0.60	5.0E+09	0.602	-6.0	5.712E+5	1.13
11	MB8	0.60	5.0E+09	0.602	-6.0	2.293E+5	0.45

5.5. Shaft Alignment Calculations - Results

5.5.1. Effect of Hull Deformations on Shaft Alignment

The hull deformations predicted by the FEM are applied to the initial shafting plan corresponding to a docking condition. The resulting vertical position of each bearing relative to the reference line is presented in **Figure 5.28** for every loading condition under consideration. In **APPENDIX C**, screenshots of hull deformation for representative loading conditions of the vessel are presented. Further, in **APPENDIX D**, screenshots of the shaft alignment calculations, performed with the aid of the inhouse software are presented.

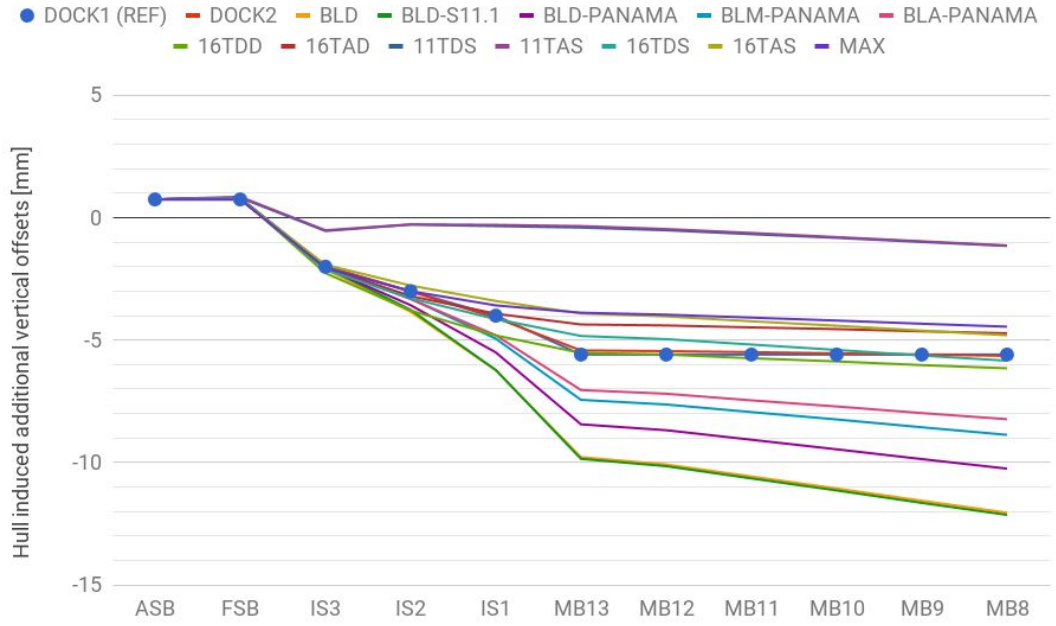

FIGURE 5.28: Hull induced additional vertical bearing offsets for different loading conditions of the studied vessel.

In **Table 5.8** and **Figure 5.29**, the calculated bearing reaction forces are presented for the loading conditions studied in the present work. It is observed that, the overall state of the shafting system is satisfactory; all bearings are loaded, no bearings are overloaded, load equidistribution is evident. In particular, the reaction force of the aft stern tube bearing ranges from 1492 kN to 1549 kN (maximum deviation 3.7%). Similarly, the reaction force of the aft stern tube bearing ranges from 200 kN to 244 kN (maximum deviation 18.0%). MB13 and MB12 exhibit the maximum deviation (34.6% and 47.2% respectively); no concerns arise for the sustainability of the shafting system.

Evidently, the shaft alignment plan for the studied vessel is well conducted. Hull deformations were surely taken into consideration given the fact that the bearing loads in all shaft bearings were found to be within the recommended limits.

TABLE 5.8: Bearing reaction forces and vertical offsets for each studied loading condition.

DOCK2			BLD			BLD-S11.1		
Vertical Offsets (mm)	Reactions (N)	Diff (%)	Vertical Offsets (mm)	Reactions (N)	Diff (%)	Vertical Offsets (mm)	Reactions (N)	Diff (%)
5.862E-4	1.542E+6	-0.45	6.064E-4	1.495E+6	-3.49	6.056E-4	1.494E+6	-3.51
9.324E-4	2.467E+5	0.27	9.402E-4	2.527E+5	2.69	9.706E-4	2.522E+5	2.51
-2.025E-3	3.684E+5	-0.02	-2.155E-3	3.699E+5	0.37	-2.074E-3	3.708E+5	0.62
-3.128E-3	4.847E+5	0.10	-3.955E-3	4.866E+5	0.51	-3.880E-3	4.864E+5	0.46
-4.228E-3	5.072E+5	-0.42	-6.342E-3	4.935E+5	-3.09	-6.337E-3	4.947E+5	-2.86
-5.847E-3	4.590E+5	3.73	-1.020E-2	4.697E+5	6.15	-1.026E-2	4.637E+5	4.79
-5.855E-3	3.698E+5	-3.97	-1.049E-2	4.873E+5	26.53	-1.056E-2	4.751E+5	23.37
-5.913E-3	4.936E+5	0.93	-1.096E-2	3.873E+5	-20.81	-1.103E-2	4.291E+5	-12.26
-5.979E-3	5.672E+5	-0.43	-1.149E-2	5.891E+5	3.41	-1.156E-2	5.552E+5	-2.55
-6.029E-3	5.715E+5	0.05	-1.197E-2	5.048E+5	-11.63	-1.206E-2	5.134E+5	-10.11
-6.002E-3	2.275E+5	-0.80	-1.242E-2	2.625E+5	14.44	-1.251E-2	2.630E+5	14.67
BLD-PANAMA			**BLM-PANAMA**			**BLA-PANAMA**		
Vertical Offsets (mm)	Reactions (N)	Diff (%)	Vertical Offsets (mm)	Reactions (N)	Diff (%)	Vertical Offsets (mm)	Reactions (N)	Diff (%)
6.067E-4	1.496E+6	-3.42	6.053E-4	1.497E+6	-3.34	6.023E-4	1.504E+6	-2.91
9.323E-4	2.516E+5	2.24	9.691E-4	2.523E+5	2.55	9.387E-4	2.508E+5	1.92
-2.024E-3	3.708E+5	0.62	-2.020E-3	3.700E+5	0.39	-2.061E-3	3.708E+5	0.61
-3.125E-3	4.833E+5	-0.19	-3.431E-3	4.833E+5	-0.18	-3.436E-3	4.822E+5	-0.40
-4.217E-3	4.999E+5	-1.85	-5.067E-3	5.005E+5	-1.73	-4.926E-3	5.025E+5	-1.33
-5.835E-3	4.565E+5	3.16	-7.864E-3	4.614E+5	4.28	-7.466E-3	4.557E+5	2.98
-5.863E-3	4.571E+5	18.71	-8.039E-3	4.562E+5	18.47	-7.608E-3	4.525E+5	17.49
-5.880E-3	4.743E+5	-3.03	-8.318E-3	4.300E+5	-12.09	-7.856E-3	4.268E+5	-12.73
-5.946E-3	4.936E+5	-13.35	-8.664E-3	5.424E+5	-4.78	-8.142E-3	5.547E+5	-2.62
-6.020E-3	5.718E+5	0.11	-8.998E-3	5.719E+5	0.14	-8.414E-3	5.742E+5	0.54
-6.005E-3	2.432E+5	6.04	-9.239E-3	2.339E+5	2.00	-8.596E-3	2.304E+5	0.47
16TDD			**16TAD**			**11TDS**		
Vertical Offsets (mm)	Reactions (N)	Diff (%)	Vertical Offsets (mm)	Reactions (N)	Diff (%)	Vertical Offsets (mm)	Reactions (N)	Diff (%)
6.137E-4	1.492E+6	-3.65	6.110E-4	1.497E+6	-3.36	6.056E-4	1.526E+6	-1.49
9.759E-4	2.611E+5	6.10	9.595E-4	2.531E+5	2.88	9.975E-4	2.001E+5	-18.66
-2.310E-3	3.663E+5	-0.61	-2.092E-3	3.692E+5	0.18	-6.177E-4	3.921E+5	6.41
-3.915E-3	4.848E+5	0.14	-3.317E-3	4.854E+5	0.26	-4.037E-4	4.928E+5	1.78
-4.930E-3	4.830E+5	-5.16	-4.039E-3	4.854E+5	-4.69	-4.496E-4	4.633E+5	-9.04
-5.963E-3	5.669E+5	28.11	-4.809E-3	5.605E+5	26.66	-8.671E-4	6.728E+5	52.05
-5.997E-3	3.353E+5	-12.93	-4.805E-3	3.252E+5	-15.56	-9.070E-4	2.583E+5	-32.91
-6.141E-3	4.430E+5	-9.43	-4.888E-3	4.538E+5	-7.21	-1.072E-3	4.258E+5	-12.94
-6.302E-3	5.633E+5	-1.12	-4.988E-3	5.667E+5	-0.52	-1.252E-3	5.647E+5	-0.88
-6.453E-3	5.758E+5	0.82	-5.075E-3	5.772E+5	1.06	-1.424E-3	5.762E+5	0.88
-6.521E-3	2.256E+5	-1.65	-5.087E-3	2.240E+5	-2.31	-1.514E-3	2.253E+5	-1.74

TABLE 5.8: Bearing reaction forces and vertical offsets for each studied loading condition. (continue)

11TAS			16TDS			16TAS		
Vertical Offsets (mm)	Reactions (N)	Diff (%)	Vertical Offsets (mm)	Reactions (N)	Diff (%)	Vertical Offsets (mm)	Reactions (N)	Diff (%)
6.057E-4	1.525E+6	-1.53	6.117E-4	1.496E+6	-3.40	6.127E-4	1.502E+6	-3.02
1.029E-3	2.012E+5	-18.22	9.625E-4	2.562E+5	4.12	9.171E-4	2.453E+5	-0.30
-5.844E-4	3.924E+5	6.48	-2.173E-3	3.643E+5	-1.14	-1.974E-3	3.693E+5	0.21
-3.930E-4	4.918E+5	1.57	-3.410E-3	4.907E+5	1.35	-2.891E-3	4.912E+5	1.45
-3.978E-4	4.630E+5	-9.09	-4.258E-3	4.714E+5	-7.44	-3.516E-3	4.702E+5	-7.68
-8.061E-4	6.766E+5	52.90	-5.283E-3	6.096E+5	37.77	-4.363E-3	6.272E+5	41.75
-8.509E-4	2.573E+5	-33.17	-5.360E-3	3.322E+5	-13.73	-4.427E-3	3.084E+5	-19.93
-1.023E-3	4.285E+5	-12.38	-5.580E-3	4.187E+5	-14.39	-4.625E-3	4.225E+5	-13.61
-1.219E-3	5.576E+5	-2.12	-5.826E-3	5.541E+5	-2.73	-4.844E-3	5.567E+5	-2.27
-1.400E-3	5.779E+5	1.18	-6.062E-3	5.761E+5	0.86	-5.049E-3	5.778E+5	1.16
-1.498E-3	2.259E+5	-1.51	-6.213E-3	2.278E+5	-0.66	-5.170E-3	2.266E+5	-1.20

MAX		
Vertical Offsets (mm)	Reactions (N)	Diff (%)
6.106E-4	1.499E+6	-3.19
9.167E-4	2.506E+5	1.86
-2.111E-3	3.669E+5	-0.44
-3.125E-3	4.898E+5	1.17
-3.693E-3	4.758E+5	-6.58
-4.341E-3	6.091E+5	37.64
-4.359E-3	2.951E+5	-23.36
-4.484E-3	4.510E+5	-7.79
-4.635E-3	5.560E+5	-2.40
-4.768E-3	5.777E+5	1.14
-4.816E-3	2.259E+5	-1.48

TABLE 5.9: Minimum film thickness, maximum pressure of the lubricant and power loss estimation for each studied loading condition.

DOCK2			BLD			BLD-S11.1		
Minimum Film Thickness (m)	Maximum Oil Pressure (Pa)	Power Loss (kW)	Minimum Film Thickness (m)	Maximum Oil Pressure (Pa)	Power Loss (kW)	Minimum Film Thickness (m)	Maximum Oil Pressure (Pa)	Power Loss (kW)
2.767E-4	1.975E+6	15.663	2.835E-4	1.746E+6	17.667	2.826E-4	1.767E+6	17.241
2.320E-4	5.525E+5	6.010	2.332E-4	5.579E+5	7.001	2.327E-4	5.574E+5	6.806
1.271E-4	1.095E+6	5.498	1.312E-4	1.090E+6	6.431	1.310E-4	1.099E+6	6.258
1.188E-4	1.515E+6	5.755	1.229E-4	1.500E+6	6.707	1.230E-4	1.501E+6	6.528
1.194E-4	1.604E+6	5.834	1.303E-4	1.570E+6	6.817	1.306E-4	1.596E+6	6.655
7.422E-5	8.221E+5	19.889	8.733E-5	8.044E+5	23.970	8.760E-5	8.033E+5	23.266
8.136E-5	8.422E+5	16.528	9.322E-5	1.067E+6	20.231	9.500E-5	9.371E+5	19.478
8.653E-5	2.077E+6	3.008	1.018E-4	1.801E+6	3.419	1.159E-4	2.613E+6	3.568
8.340E-5	2.460E+6	3.140	1.018E-4	2.777E+6	3.711	1.002E-4	2.063E+6	3.411
8.303E-5	2.476E+6	3.145	9.858E-5	2.366E+6	3.601	9.983E-5	2.565E+6	3.564
9.048E-5	8.544E+5	2.569	9.214E-5	9.844E+5	3.066	9.251E-5	9.845E+5	2.977
BLD-PANAMA			**BLM-PANAMA**			**BLA-PANAMA**		
Minimum Film Thickness (m)	Maximum Oil Pressure (Pa)	Power Loss (kW)	Minimum Film Thickness (m)	Maximum Oil Pressure (Pa)	Power Loss (kW)	Minimum Film Thickness (m)	Maximum Oil Pressure (Pa)	Power Loss (kW)
2.840E-4	1.736E+6	17.948	2.831E-4	1.758E+6	17.522	2.820E-4	1.504E+6	17.164
2.334E-4	5.548E+5	7.117	2.328E-4	5.577E+5	6.928	2.329E-4	5.554E+5	6.751
1.302E-4	1.085E+6	6.532	1.283E-4	1.085E+6	6.346	1.294E-4	1.091E+6	6.189
1.218E-4	1.485E+6	6.798	1.210E-4	1.483E+6	6.605	1.206E-4	1.483E+6	6.438
1.267E-4	1.546E+6	6.892	1.246E-4	1.560E+6	6.701	1.225E-4	1.570E+6	6.534
8.530E-5	8.056E+5	24.389	8.005E-5	8.065E+5	23.433	7.725E-5	8.009E+5	22.690
9.052E-5	1.116E+6	20.499	8.806E-5	1.034E+6	19.646	8.675E-5	1.031E+6	19.053
1.155E-4	1.482E+6	3.365	1.164E-4	1.886E+6	3.414	9.751E-5	1.806E+6	3.297
1.016E-4	3.040E+6	3.843	9.532E-5	2.417E+6	3.588	9.094E-5	2.433E+6	3.509
9.191E-5	2.347E+6	3.665	8.905E-5	2.512E+6	3.621	8.728E-5	2.500E+6	3.528
9.039E-5	9.165E+5	3.087	8.954E-5	8.725E+5	2.978	8.922E-5	8.609E+5	2.894
16TDD			**16TAD**			**11TDS**		
Minimum Film Thickness (m)	Maximum Oil Pressure (Pa)	Power Loss (kW)	Minimum Film Thickness (m)	Maximum Oil Pressure (Pa)	Power Loss (kW)	Minimum Film Thickness (m)	Maximum Oil Pressure (Pa)	Power Loss (kW)
2.900E-4	1.629E+6	20.880	2.887E-4	1.652E+6	20.269	2.915E-4	1.646E+6	22.697
2.346E-4	5.675E+5	8.478	2.343E-4	5.484E+5	8.143	2.306E-4	4.126E+5	8.778
1.317E-4	1.056E+6	7.766	1.281E-4	1.066E+6	7.473	1.215E-4	1.134E+6	8.377
1.219E-4	1.464E+6	8.018	1.211E-4	1.469E+6	7.742	1.209E-4	1.479E+6	8.710
1.211E-4	1.456E+6	7.996	1.207E-4	1.470E+6	7.735	1.213E-4	1.374E+6	8.609
7.503E-5	1.016E+6	28.851	7.510E-5	1.005E+6	27.794	7.821E-5	1.215E+6	31.812
7.405E-5	7.440E+5	23.605	7.346E-5	7.220E+5	22.719	6.582E-5	5.641E+5	25.622
9.207E-5	1.771E+6	4.058	9.043E-5	1.823E+6	3.933	9.317E-5	1.677E+6	4.373
8.857E-5	2.355E+6	4.306	8.728E-5	2.378E+6	4.168	8.964E-5	2.346E+6	4.669
8.753E-5	2.410E+6	4.323	8.662E-5	2.420E+6	4.183	8.855E-5	2.392E+6	4.683
8.745E-5	8.345E+5	3.638	8.798E-5	8.290E+5	3.511	8.676E-5	8.309E+5	3.971

TABLE 5.9: Minimum film thickness, maximum pressure of the lubricant and power loss estimation for each studied loading condition. (continue)

11TAS			16TDS			16TAS		
Minimum Film Thickness (m)	Maximum Oil Pressure (Pa)	Power Loss (kW)	Minimum Film Thickness (m)	Maximum Oil Pressure (Pa)	Power Loss (kW)	Minimum Film Thickness (m)	Maximum Oil Pressure (Pa)	Power Loss (kW)
2.914E-4	1.647E+6	22.605	2.891E-4	1.599E+6	22.547	2.919E-4	1.616E+6	22.224
2.306E-4	4.153E+5	8.745	2.349E-4	5.501E+5	9.175	2.348E-4	5.236E+5	8.944
1.216E-4	1.135E+6	8.342	1.279E-4	1.038E+6	8.408	1.260E-4	1.053E+6	8.243
1.209E-4	1.476E+6	8.670	1.216E-4	1.471E+6	8.717	1.212E-4	1.476E+6	8.564
1.213E-4	1.374E+6	8.572	1.214E-4	1.403E+6	8.641	1.212E-4	1.401E+6	8.487
7.848E-5	1.222E+6	31.680	7.665E-5	1.091E+6	31.712	7.724E-5	1.126E+6	31.148
6.589E-5	5.595E+5	25.501	7.327E-5	7.314E+5	25.852	7.124E-5	6.773E+5	25.293
9.350E-5	1.699E+6	4.368	9.637E-5	1.662E+6	4.392	9.441E-5	1.676E+6	4.311
9.006E-5	2.310E+6	4.637	9.240E-5	2.308E+6	4.667	9.124E-5	2.317E+6	4.586
8.854E-5	2.402E+6	4.669	8.938E-5	2.404E+6	4.695	8.873E-5	2.410E+6	4.616
8.682E-5	8.341E+5	3.954	8.704E-5	8.410E+5	3.976	8.699E-5	8.369E+5	3.902

MAX		
Minimum Film Thickness (m)	Maximum Oil Pressure (Pa)	Power Loss (kW)
2.890E-4	1.604E+6	22.563
2.350E-4	5.361E+5	9.138
1.268E-4	1.045E+6	8.396
1.213E-4	1.468E+6	8.707
1.211E-4	1.418E+6	8.652
7.556E-5	1.093E+6	31.648
6.908E-5	6.503E+5	25.707
9.191E-5	1.788E+6	4.413
8.925E-5	2.294E+6	4.641
8.806E-5	2.392E+6	4.679
8.694E-5	8.331E+5	3.973

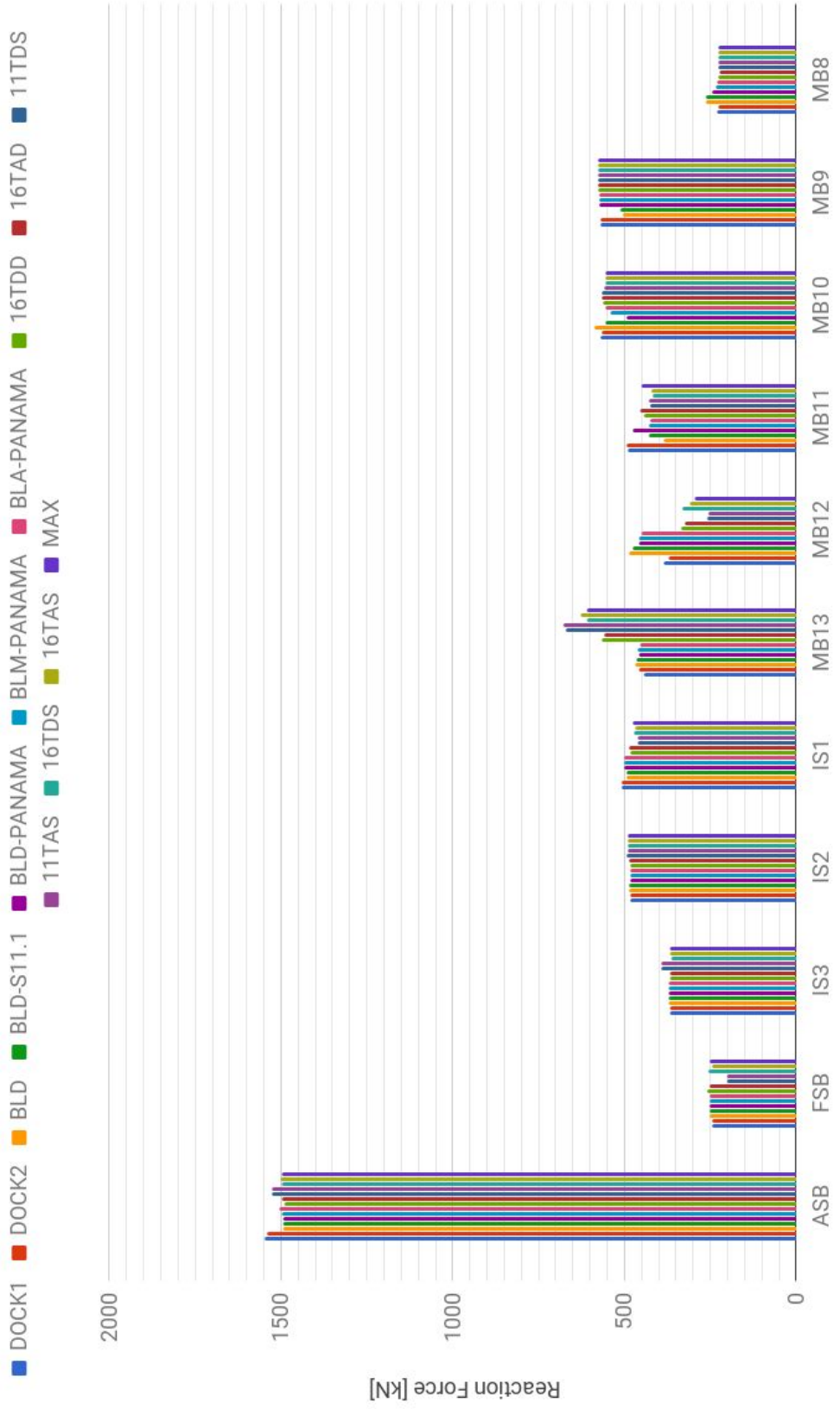

FIGURE 5.29: Bearing reaction forces for each loading condition of the vessel.

5.5.2. Loading Condition "DOCK1"

The following assumptions have been made for the calculations presented in this section:

- The M/E is running at 66.1 rpm,
- The M/E is in hot condition and M/E bearings are offset by an additional 0.41 mm relative to other conditions where the M/E is not running,
- Hull deformations are zero,
- The propeller and parts of the propeller shaft are immersed in water. Thus, their weight is partially supported by the bearings and the water.

TABLE 5.10: Loading Condition "DOCK1": Detailed calculation results.

Bearing	Reaction (N)	Mean Pressure (Pa)	Total Offsets (m)	Initial Offsets (m)	Hull Deform. (m)	Support Elastic Deformation (m)	Minimum FIlm Thickness (m)
ASB	1.549E+6	7.211E+5	5.827E-4	7.500E-4	0.000E+0	-4.425E-4	2.752E-4
FSB	2.461E+5	2.510E+5	9.135E-4	7.500E-4	0.000E+0	-7.030E-5	2.338E-4
IS3	3.685E+5	5.224E+5	-2.057E-3	-2.000E-3	0.000E+0	-1.843E-4	1.270E-4
IS2	4.842E+5	6.863E+5	-3.124E-3	-3.000E-3	0.000E+0	-2.421E-4	1.184E-4
IS1	5.093E+5	7.219E+5	-4.136E-3	-4.000E-3	0.000E+0	-2.546E-4	1.187E-4
MB13	4.425E+5	4.121E+5	-5.605E-3	-5.590E-3	0.000E+0	-8.850E-5	7.393E-5
MB12	3.851E+5	4.381E+5	-5.584E-3	-5.590E-3	0.000E+0	-7.702E-5	8.290E-5
MB11	4.891E+5	9.672E+5	-5.602E-3	-5.590E-3	0.000E+0	-9.782E-5	8.607E-5
MB10	5.697E+5	1.127E+6	-5.621E-3	-5.590E-3	0.000E+0	-1.139E-4	8.259E-5
MB9	5.712E+5	1.129E+6	-5.622E-3	-5.590E-3	0.000E+0	-1.142E-4	8.265E-5
MB8	2.293E+5	4.535E+5	-5.544E-3	-5.590E-3	0.000E+0	-4.587E-5	9.174E-5

In the rest of the tables, the condition of the M/E is incorporated in the initial offsets column where, M/E heat expansion offsets are equal to +0.41 mm.

Maximum permissible mean pressure:

- The limit is 0.8 MPa for the aft stern tube bearing and the value observed is 0.72 MPa,
- The limit is 0.8 MPa for the fore stern tube bearing and the value observed is 0.25 MPa,
- The limit is 1.0 MPa for the I/M shaft bearings and the value observed is 0.52 MPa, 0.69 MPa and 0.72 MPa respectively,
- No crankshaft bearing mean pressure value exceeds 3 MPa (as prescribed in manufacturer's manual).

5.5.3. Loading Condition "DOCK2"

The following assumptions have been made for the calculations presented in this section:

- The M/E is running at 67.3 rpm,
- The M/E is in hot condition and M/E bearings are offset by an additional 0.41 mm relative to other conditions where the M/E is not running,
- Hull deformations are not zero,
- The propeller and parts of the propeller shaft are immersed in water. Thus, their weight is partially supported by the bearings and the water.

TABLE 5.11: Loading Condition "DOCK2": Detailed calculation results.

Bearing	Reaction (N)	Mean Pressure (Pa)	Total Offsets (m)	Initial Offsets (m)	Hull Deform. (m)	Support Elastic Deformation (m)	Minimum FIlm Thickness (m)
ASB	1.542E+6	7.179E+5	5.862E-4	7.500E-4	0.000E+0	-4.405E-4	2.767E-4
FSB	2.467E+5	2.517E+5	9.324E-4	7.500E-4	2.084E-5	-7.049E-5	2.320E-4
IS3	3.684E+5	5.223E+5	-2.025E-3	-2.000E-3	3.170E-5	-1.842E-4	1.271E-4
IS2	4.847E+5	6.870E+5	-3.128E-3	-3.000E-3	-4.920E-6	-2.423E-4	1.188E-4
IS1	5.072E+5	7.189E+5	-4.228E-3	-4.000E-3	-9.420E-5	-2.536E-4	1.194E-4
MB13	4.590E+5	4.275E+5	-5.847E-3	-5.590E-3	-2.393E-4	-9.180E-5	7.422E-5
MB12	3.698E+5	4.207E+5	-5.855E-3	-5.590E-3	-2.721E-4	-7.396E-5	8.136E-5
MB11	4.936E+5	9.761E+5	-5.913E-3	-5.590E-3	-3.107E-4	-9.872E-5	8.653E-5
MB10	5.672E+5	1.122E+6	-5.979E-3	-5.590E-3	-3.593E-4	-1.134E-4	8.340E-5
MB9	5.715E+5	1.130E+6	-6.029E-3	-5.590E-3	-4.080E-4	-1.143E-4	8.303E-5
MB8	2.275E+5	4.499E+5	-6.002E-3	-5.590E-3	-4.566E-4	-4.550E-5	9.048E-5

Maximum permissible mean pressure:

- The limit is 0.8 MPa for the aft stern tube bearing and the value observed is 0.72 MPa,
- The limit is 0.8 MPa for the fore stern tube bearing and the value observed is 0.25 MPa,
- The limit is 1.0 MPa for the I/M shaft bearings and the value observed is 0.52 MPa, 0.69 MPa and 0.72 MPa respectively,
- No crankshaft bearing mean pressure value exceeds 3 MPa.

5.5.4. Loading Condition "BLD"

The following assumptions have been made for the calculations presented in this section:

- The M/E is running at 73.2 rpm,
- The M/E is in hot condition and M/E bearings are offset by an additional 0.41 mm relative to other conditions where the M/E is not running,
- Hull deformations are not zero,
- The propeller and parts of the propeller shaft are immersed in water. Thus, their weight is partially supported by the bearings and the water.

TABLE 5.12: Loading Condition "BLD": Detailed calculation results.

Bearing	Reaction (N)	Mean Pressure (Pa)	Total Offsets (m)	Initial Offsets (m)	Hull Deform. (m)	Support Elastic Deformation (m)	Minimum FIlm Thickness (m)
ASB	1.495E+6	6.959E+5	6.064E-4	7.500E-4	0.000E+0	-4.270E-4	2.835E-4
FSB	2.527E+5	2.578E+5	9.402E-4	7.500E-4	2.916E-5	-7.219E-5	2.332E-4
IS3	3.699E+5	5.243E+5	-2.155E-3	-2.000E-3	-1.017E-4	-1.850E-4	1.312E-4
IS2	4.866E+5	6.898E+5	-3.955E-3	-3.000E-3	-8.351E-4	-2.433E-4	1.229E-4
IS1	4.935E+5	6.996E+5	-6.342E-3	-4.000E-3	-2.226E-3	-2.468E-4	1.303E-4
MB13	4.697E+5	4.374E+5	-1.020E-2	-5.590E-3	-4.600E-3	-9.394E-5	8.733E-5
MB12	4.873E+5	5.543E+5	-1.049E-2	-5.590E-3	-4.900E-3	-9.745E-5	9.322E-5
MB11	3.873E+5	7.659E+5	-1.096E-2	-5.590E-3	-5.391E-3	-7.746E-5	1.018E-4
MB10	5.891E+5	1.165E+6	-1.149E-2	-5.590E-3	-5.880E-3	-1.178E-4	1.018E-4
MB9	5.048E+5	9.982E+5	-1.197E-2	-5.590E-3	-6.379E-3	-1.010E-4	9.858E-5
MB8	2.625E+5	5.190E+5	-1.242E-2	-5.590E-3	-6.868E-3	-5.249E-5	9.214E-5

Maximum permissible mean pressure:

- The limit is 0.8 MPa for the aft stern tube bearing and the value observed is 0.70 MPa,
- The limit is 0.8 MPa for the fore stern tube bearing and the value observed is 0.26 MPa,
- The limit is 1.0 MPa for the I/M shaft bearings and the value observed is 0.52 MPa, 0.69 MPa and 0.70 MPa respectively,
- No crankshaft bearing mean pressure value exceeds 3 MPa.

5.5.5. Loading Condition "BLD-S11.1"

The following assumptions have been made for the calculations presented in this section:

- The M/E is running at 72.1 rpm,
- The M/E is in hot condition and M/E bearings are offset by an additional 0.41 mm relative to other conditions where the M/E is not running,
- Hull deformations are not zero,
- The propeller and parts of the propeller shaft are immersed in water. Thus, their weight is partially supported by the bearings and the water.

TABLE 5.13: Loading Condition "BLD-S11.1": Detailed calculation results.

Bearing	Reaction (N)	Mean Pressure (Pa)	Total Offsets (m)	Initial Offsets (m)	Hull Deform. (m)	Support Elastic Deformation (m)	Minimum FIlm Thickness (m)
ASB	1.494E+6	6.958E+5	6.056E-4	7.500E-4	0.000E+0	-4.270E-4	2.826E-4
FSB	2.522E+5	2.574E+5	9.706E-4	7.500E-4	6.000E-5	-7.207E-5	2.327E-4
IS3	3.708E+5	5.256E+5	-2.074E-3	-2.000E-3	-2.000E-5	-1.854E-4	1.310E-4
IS2	4.864E+5	6.894E+5	-3.880E-3	-3.000E-3	-7.600E-4	-2.432E-4	1.230E-4
IS1	4.947E+5	7.012E+5	-6.337E-3	-4.000E-3	-2.220E-3	-2.474E-4	1.306E-4
MB13	4.637E+5	4.318E+5	-1.026E-2	-5.590E-3	-4.669E-3	-9.274E-5	8.760E-5
MB12	4.751E+5	5.404E+5	-1.056E-2	-5.590E-3	-4.972E-3	-9.502E-5	9.500E-5
MB11	4.291E+5	8.486E+5	-1.103E-2	-5.590E-3	-5.468E-3	-8.582E-5	1.159E-4
MB10	5.552E+5	1.098E+6	-1.156E-2	-5.590E-3	-5.961E-3	-1.110E-4	1.002E-4
MB9	5.134E+5	1.015E+6	-1.206E-2	-5.590E-3	-6.465E-3	-1.027E-4	9.983E-5
MB8	2.630E+5	5.201E+5	-1.251E-2	-5.590E-3	-6.959E-3	-5.260E-5	9.251E-5

Maximum permissible mean pressure:

- The limit is 0.8 MPa for the aft stern tube bearing and the value observed is 0.70 MPa,
- The limit is 0.8 MPa for the fore stern tube bearing and the value observed is 0.26 MPa,
- The limit is 1.0 MPa for the I/M shaft bearings and the value observed is 0.53 MPa, 0.69 MPa and 0.70 MPa respectively,
- No crankshaft bearing mean pressure value exceeds 3 MPa.

5.5.6. Loading Condition "BLD-PANAMA"

The following assumptions have been made for the calculations presented in this section:

- The M/E is running at 73.9 rpm,
- The M/E is in hot condition and M/E bearings are offset by an additional 0.41 mm relative to other conditions where the M/E is not running,
- Hull deformations are not zero,
- The propeller and parts of the propeller shaft are immersed in water. Thus, their weight is partially supported by the bearings and the water.

TABLE 5.14: Loading Condition "BLD-PANAMA": Detailed calculation results.

Bearing	Reaction (N)	Mean Pressure (Pa)	Total Offsets (m)	Initial Offsets (m)	Hull Deform. (m)	Support Elastic Deformation (m)	Minimum FIlm Thickness (m)
ASB	1.496E+6	6.964E+5	6.067E-4	7.500E-4	0.000E+0	-4.274E-4	2.840E-4
FSB	2.516E+5	2.567E+5	9.323E-4	7.500E-4	2.084E-5	-7.188E-5	2.334E-4
IS3	3.708E+5	5.256E+5	-2.024E-3	-2.000E-3	3.170E-5	-1.854E-4	1.302E-4
IS2	4.833E+5	6.850E+5	-3.125E-3	-3.000E-3	-4.920E-6	-2.416E-4	1.218E-4
IS1	4.999E+5	7.085E+5	-4.217E-3	-4.000E-3	-9.420E-5	-2.499E-4	1.267E-4
MB13	4.565E+5	4.251E+5	-5.835E-3	-5.590E-3	-2.393E-4	-9.129E-5	8.530E-5
MB12	4.571E+5	5.200E+5	-5.863E-3	-5.590E-3	-2.721E-4	-9.143E-5	9.052E-5
MB11	4.743E+5	9.379E+5	-5.880E-3	-5.590E-3	-3.107E-4	-9.486E-5	1.155E-4
MB10	4.936E+5	9.762E+5	-5.946E-3	-5.590E-3	-3.593E-4	-9.873E-5	1.016E-4
MB9	5.718E+5	1.131E+6	-6.020E-3	-5.590E-3	-4.080E-4	-1.144E-4	9.191E-5
MB8	2.432E+5	4.809E+5	-6.005E-3	-5.590E-3	-4.566E-4	-4.864E-5	9.039E-5

Maximum permissible mean pressure:

- The limit is 0.8 MPa for the aft stern tube bearing and the value observed is 0.70 MPa,
- The limit is 0.8 MPa for the fore stern tube bearing and the value observed is 0.26 MPa,
- The limit is 1.0 MPa for the I/M shaft bearings and the value observed is 0.53 MPa, 0.68 MPa and 0.71 MPa respectively,
- No crankshaft bearing mean pressure value exceeds 3 MPa.

5.5.7. Loading Condition "BLM-PANAMA"

The following assumptions have been made for the calculations presented in this section:

- The M/E is running at 72.8 rpm,
- The M/E is in hot condition and M/E bearings are offset by an additional 0.41 mm relative to other conditions where the M/E is not running,
- Hull deformations are not zero,
- The propeller and parts of the propeller shaft are immersed in water. Thus, their weight is partially supported by the bearings and the water.

TABLE 5.15: Loading Condition "BLM-PANAMA": Detailed calculation results.

Bearing	Reaction (N)	Mean Pressure (Pa)	Total Offsets (m)	Initial Offsets (m)	Hull Deform. (m)	Support Elastic Deformation (m)	Minimum FIlm Thickness (m)
ASB	1.497E+6	6.970E+5	6.053E-4	7.500E-4	0.000E+0	-4.277E-4	2.831E-4
FSB	2.523E+5	2.574E+5	9.691E-4	7.500E-4	5.833E-5	-7.209E-5	2.328E-4
IS3	3.700E+5	5.244E+5	-2.020E-3	-2.000E-3	3.660E-5	-1.850E-4	1.283E-4
IS2	4.833E+5	6.850E+5	-3.431E-3	-3.000E-3	-3.102E-4	-2.416E-4	1.210E-4
IS1	5.005E+5	7.094E+5	-5.067E-3	-4.000E-3	-9.416E-4	-2.502E-4	1.246E-4
MB13	4.614E+5	4.297E+5	-7.864E-3	-5.590E-3	-2.261E-3	-9.229E-5	8.005E-5
MB12	4.562E+5	5.190E+5	-8.039E-3	-5.590E-3	-2.446E-3	-9.124E-5	8.806E-5
MB11	4.300E+5	8.502E+5	-8.318E-3	-5.590E-3	-2.759E-3	-8.599E-5	1.164E-4
MB10	5.424E+5	1.073E+6	-8.664E-3	-5.590E-3	-3.061E-3	-1.085E-4	9.532E-5
MB9	5.719E+5	1.131E+6	-8.998E-3	-5.590E-3	-3.383E-3	-1.144E-4	8.905E-5
MB8	2.339E+5	4.626E+5	-9.239E-3	-5.590E-3	-3.692E-3	-4.678E-5	8.954E-5

Maximum permissible mean pressure:

- The limit is 0.8 MPa for the aft stern tube bearing and the value observed is 0.70 MPa,
- The limit is 0.8 MPa for the fore stern tube bearing and the value observed is 0.26 MPa,
- The limit is 1.0 MPa for the I/M shaft bearings and the value observed is 0.52 MPa, 0.69 MPa and 0.71 MPa respectively,
- No crankshaft bearing mean pressure value exceeds 3 MPa.

5.5.8. Loading Condition "BLA-PANAMA"

The following assumptions have been made for the calculations presented in this section:

- The M/E is running at 71.8 rpm,
- The M/E is in hot condition and M/E bearings are offset by an additional 0.41 mm relative to other conditions where the M/E is not running,
- Hull deformations are not zero,
- The propeller and parts of the propeller shaft are immersed in water. Thus, their weight is partially supported by the bearings and the water.

TABLE 5.16: Loading Condition "BLA-PANAMA": Detailed calculation results.

Bearing	Reaction (N)	Mean Pressure (Pa)	Total Offsets (m)	Initial Offsets (m)	Hull Deform. (m)	Support Elastic Deformation (m)	Minimum FIlm Thickness (m)
ASB	1.504E+6	7.001E+5	6.023E-4	7.500E-4	0.000E+0	-4.296E-4	2.820E-4
FSB	2.508E+5	2.559E+5	9.387E-4	7.500E-4	2.749E-5	-7.165E-5	2.329E-4
IS3	3.708E+5	5.255E+5	-2.061E-3	-2.000E-3	-5.100E-6	-1.854E-4	1.294E-4
IS2	4.822E+5	6.835E+5	-3.436E-3	-3.000E-3	-3.152E-4	-2.411E-4	1.206E-4
IS1	5.025E+5	7.123E+5	-4.926E-3	-4.000E-3	-7.974E-4	-2.513E-4	1.225E-4
MB13	4.557E+5	4.244E+5	-7.466E-3	-5.590E-3	-1.862E-3	-9.113E-5	7.725E-5
MB12	4.525E+5	5.147E+5	-7.608E-3	-5.590E-3	-2.014E-3	-9.049E-5	8.675E-5
MB11	4.268E+5	8.441E+5	-7.856E-3	-5.590E-3	-2.278E-3	-8.536E-5	9.751E-5
MB10	5.547E+5	1.097E+6	-8.142E-3	-5.590E-3	-2.532E-3	-1.109E-4	9.094E-5
MB9	5.742E+5	1.136E+6	-8.414E-3	-5.590E-3	-2.796E-3	-1.148E-4	8.728E-5
MB8	2.304E+5	4.557E+5	-8.596E-3	-5.590E-3	-3.049E-3	-4.608E-5	8.922E-5

Maximum permissible mean pressure:

- The limit is 0.8 MPa for the aft stern tube bearing and the value observed is 0.70 MPa,
- The limit is 0.8 MPa for the fore stern tube bearing and the value observed is 0.26 MPa,
- The limit is 1.0 MPa for the I/M shaft bearings and the value observed is 0.53 MPa, 0.68 MPa and 0.71 MPa respectively,
- No crankshaft bearing mean pressure value exceeds 3 MPa.

5.5.9. Loading Condition "16TDD"

The following assumptions have been made for the calculations presented in this section:

- The M/E is running at 81.1 rpm,
- The M/E is in hot condition and M/E bearings are offset by an additional 0.41 mm relative to other conditions where the M/E is not running,
- Hull deformations are not zero,
- The propeller and parts of the propeller shaft are immersed in water. Thus, their weight is partially supported by the bearings and the water.

TABLE 5.17: Loading Condition "16TDD": Detailed calculation results.

Bearing	Reaction (N)	Mean Pressure (Pa)	Total Offsets (m)	Initial Offsets (m)	Hull Deform. (m)	Support Elastic Deformation (m)	Minimum FIlm Thickness (m)
ASB	1.492E+6	6.948E+5	6.137E-4	7.500E-4	0.000E+0	-4.264E-4	2.900E-4
FSB	2.611E+5	2.664E+5	9.759E-4	7.500E-4	6.585E-5	-7.459E-5	2.346E-4
IS3	3.663E+5	5.192E+5	-2.310E-3	-2.000E-3	-2.581E-4	-1.831E-4	1.317E-4
IS2	4.848E+5	6.872E+5	-3.915E-3	-3.000E-3	-7.945E-4	-2.424E-4	1.219E-4
IS1	4.830E+5	6.846E+5	-4.930E-3	-4.000E-3	-8.094E-4	-2.415E-4	1.211E-4
MB13	5.669E+5	5.279E+5	-5.963E-3	-5.590E-3	-3.350E-4	-1.134E-4	7.503E-5
MB12	3.353E+5	3.814E+5	-5.997E-3	-5.590E-3	-4.145E-4	-6.706E-5	7.405E-5
MB11	4.430E+5	8.760E+5	-6.141E-3	-5.590E-3	-5.549E-4	-8.859E-5	9.207E-5
MB10	5.633E+5	1.114E+6	-6.302E-3	-5.590E-3	-6.884E-4	-1.127E-4	8.857E-5
MB9	5.758E+5	1.139E+6	-6.453E-3	-5.590E-3	-8.358E-4	-1.152E-4	8.753E-5
MB8	2.256E+5	4.461E+5	-6.521E-3	-5.590E-3	-9.732E-4	-4.511E-5	8.745E-5

Maximum permissible mean pressure:

- The limit is 0.8 MPa for the aft stern tube bearing and the value observed is 0.69 MPa,
- The limit is 0.8 MPa for the fore stern tube bearing and the value observed is 0.27 MPa,
- The limit is 1.0 MPa for the I/M shaft bearings and the value observed is 0.52 MPa, 0.69 MPa and 0.68 MPa respectively,
- No crankshaft bearing mean pressure value exceeds 3 MPa.

5.5.10. Loading Condition "16TAD"

The following assumptions have been made for the calculations presented in this section:

- The M/E is running at 79.6 rpm,
- The M/E is in hot condition and M/E bearings are offset by an additional 0.41 mm relative to other conditions where the M/E is not running,
- Hull deformations are not zero,
- The propeller and parts of the propeller shaft are immersed in water. Thus, their weight is partially supported by the bearings and the water.

TABLE 5.18: Loading Condition "16TAD": Detailed calculation results.

Bearing	Reaction (N)	Mean Pressure (Pa)	Total Offsets (m)	Initial Offsets (m)	Hull Deform. (m)	Support Elastic Deformation (m)	Minimum FIlm Thickness (m)
ASB	1.497E+6	6.968E+5	6.110E-4	7.500E-4	0.000E+0	-4.276E-4	2.887E-4
FSB	2.531E+5	2.583E+5	9.595E-4	7.500E-4	4.749E-5	-7.233E-5	2.343E-4
IS3	3.692E+5	5.233E+5	-2.092E-3	-2.000E-3	-3.510E-5	-1.846E-4	1.281E-4
IS2	4.854E+5	6.881E+5	-3.317E-3	-3.000E-3	-1.952E-4	-2.427E-4	1.211E-4
IS1	4.854E+5	6.880E+5	-4.039E-3	-4.000E-3	8.261E-5	-2.427E-4	1.207E-4
MB13	5.605E+5	5.219E+5	-4.809E-3	-5.590E-3	8.179E-4	-1.121E-4	7.510E-5
MB12	3.252E+5	3.699E+5	-4.805E-3	-5.590E-3	7.762E-4	-6.504E-5	7.346E-5
MB11	4.538E+5	8.974E+5	-4.888E-3	-5.590E-3	7.021E-4	-9.076E-5	9.043E-5
MB10	5.667E+5	1.121E+6	-4.988E-3	-5.590E-3	6.280E-4	-1.133E-4	8.728E-5
MB9	5.772E+5	1.141E+6	-5.075E-3	-5.590E-3	5.439E-4	-1.154E-4	8.662E-5
MB8	2.240E+5	4.430E+5	-5.087E-3	-5.590E-3	4.598E-4	-4.481E-5	8.798E-5

Maximum permissible mean pressure:

- The limit is 0.8 MPa for the aft stern tube bearing and the value observed is 0.70 MPa,
- The limit is 0.8 MPa for the fore stern tube bearing and the value observed is 0.26 MPa,
- The limit is 1.0 MPa for the I/M shaft bearings and the value observed is 0.52 MPa, 0.69 MPa and 0.69 MPa respectively,
- No crankshaft bearing mean pressure value exceeds 3 MPa.

5.5.11. Loading Condition "11TDS"

The following assumptions have been made for the calculations presented in this section:

- The M/E is running at 84.9 rpm,
- The M/E is in hot condition and M/E bearings are offset by an additional 0.41 mm relative to other conditions where the M/E is not running,
- Hull deformations are not zero,
- The propeller and parts of the propeller shaft are immersed in water. Thus, their weight is partially supported by the bearings and the water.

TABLE 5.19: Loading Condition "11TDS": Detailed calculation results.

Bearing	Reaction (N)	Mean Pressure (Pa)	Total Offsets (m)	Initial Offsets (m)	Hull Deform. (m)	Support Elastic Deformation (m)	Minimum FIlm Thickness (m)
ASB	1.526E+6	7.104E+5	6.056E-4	7.500E-4	0.000E+0	-4.359E-4	2.915E-4
FSB	2.001E+5	2.042E+5	9.975E-4	7.500E-4	7.404E-5	-5.718E-5	2.306E-4
IS3	3.921E+5	5.558E+5	-6.177E-4	-2.000E-3	1.457E-3	-1.961E-4	1.215E-4
IS2	4.928E+5	6.985E+5	-4.037E-4	-3.000E-3	2.722E-3	-2.464E-4	1.209E-4
IS1	4.633E+5	6.566E+5	-4.496E-4	-4.000E-3	3.661E-3	-2.316E-4	1.213E-4
MB13	6.728E+5	6.266E+5	-8.671E-4	-5.590E-3	4.779E-3	-1.346E-4	7.821E-5
MB12	2.583E+5	2.939E+5	-9.070E-4	-5.590E-3	4.669E-3	-5.167E-5	6.582E-5
MB11	4.258E+5	8.421E+5	-1.072E-3	-5.590E-3	4.510E-3	-8.516E-5	9.317E-5
MB10	5.647E+5	1.117E+6	-1.252E-3	-5.590E-3	4.361E-3	-1.129E-4	8.964E-5
MB9	5.762E+5	1.139E+6	-1.424E-3	-5.590E-3	4.193E-3	-1.152E-4	8.855E-5
MB8	2.253E+5	4.456E+5	-1.514E-3	-5.590E-3	4.034E-3	-4.507E-5	8.676E-5

Maximum permissible mean pressure:

- The limit is 0.8 MPa for the aft stern tube bearing and the value observed is 0.71 MPa,
- The limit is 0.8 MPa for the fore stern tube bearing and the value observed is 0.20 MPa,
- The limit is 1.0 MPa for the I/M shaft bearings and the value observed is 0.56 MPa, 0.70 MPa and 0.66 MPa respectively,
- No crankshaft bearing mean pressure value exceeds 3 MPa.

5.5.12. Loading Condition "11TAS"

The following assumptions have been made for the calculations presented in this section:

- The M/E is running at 84.7 rpm,
- The M/E is in hot condition and M/E bearings are offset by an additional 0.41 mm relative to other conditions where the M/E is not running,
- Hull deformations are not zero,
- The propeller and parts of the propeller shaft are immersed in water. Thus, their weight is partially supported by the bearings and the water.

TABLE 5.20: Loading Condition "11TAS": Detailed calculation results.

Bearing	Reaction (N)	Mean Pressure (Pa)	Total Offsets (m)	Initial Offsets (m)	Hull Deform. (m)	Support Elastic Deformation (m)	Minimum FIlm Thickness (m)
ASB	1.525E+6	7.100E+5	6.057E-4	7.500E-4	0.000E+0	-4.357E-4	2.914E-4
FSB	2.012E+5	2.053E+5	1.029E-3	7.500E-4	1.057E-4	-5.749E-5	2.306E-4
IS3	3.924E+5	5.562E+5	-5.844E-4	-2.000E-3	1.490E-3	-1.962E-4	1.216E-4
IS2	4.918E+5	6.970E+5	-3.930E-4	-3.000E-3	2.732E-3	-2.459E-4	1.209E-4
IS1	4.630E+5	6.563E+5	-3.978E-4	-4.000E-3	3.712E-3	-2.315E-4	1.213E-4
MB13	6.766E+5	6.301E+5	-8.061E-4	-5.590E-3	4.841E-3	-1.353E-4	7.848E-5
MB12	2.573E+5	2.927E+5	-8.509E-4	-5.590E-3	4.725E-3	-5.147E-5	6.589E-5
MB11	4.285E+5	8.475E+5	-1.023E-3	-5.590E-3	4.559E-3	-8.571E-5	9.350E-5
MB10	5.576E+5	1.103E+6	-1.219E-3	-5.590E-3	4.393E-3	-1.115E-4	9.006E-5
MB9	5.779E+5	1.143E+6	-1.400E-3	-5.590E-3	4.217E-3	-1.156E-4	8.854E-5
MB8	2.259E+5	4.467E+5	-1.498E-3	-5.590E-3	4.051E-3	-4.518E-5	8.682E-5

Maximum permissible mean pressure:

- The limit is 0.8 MPa for the aft stern tube bearing and the value observed is 0.71 MPa,
- The limit is 0.8 MPa for the fore stern tube bearing and the value observed is 0.21 MPa,
- The limit is 1.0 MPa for the I/M shaft bearings and the value observed is 0.56 MPa, 0.70 MPa and 0.66 MPa respectively,
- No crankshaft bearing mean pressure value exceeds 3 MPa.

5.5.13. Loading Condition "16TDS"

The following assumptions have been made for the calculations presented in this section:

- The M/E is running at 84.9 rpm,
- The M/E is in hot condition and M/E bearings are offset by an additional 0.41 mm relative to other conditions where the M/E is not running,
- Hull deformations are not zero,
- The propeller and parts of the propeller shaft are immersed in water. Thus, their weight is partially supported by the bearings and the water.

TABLE 5.21: Loading Condition "16TDS": Detailed calculation results.

Bearing	Reaction (N)	Mean Pressure (Pa)	Total Offsets (m)	Initial Offsets (m)	Hull Deform. (m)	Support Elastic Deformation (m)	Minimum FIlm Thickness (m)
ASB	1.496E+6	6.966E+5	6.117E-4	7.500E-4	0.000E+0	-4.275E-4	2.891E-4
FSB	2.562E+5	2.614E+5	9.625E-4	7.500E-4	5.080E-5	-7.320E-5	2.349E-4
IS3	3.643E+5	5.164E+5	-2.173E-3	-2.000E-3	-1.187E-4	-1.822E-4	1.279E-4
IS2	4.907E+5	6.955E+5	-3.410E-3	-3.000E-3	-2.858E-4	-2.453E-4	1.216E-4
IS1	4.714E+5	6.681E+5	-4.258E-3	-4.000E-3	-1.438E-4	-2.357E-4	1.214E-4
MB13	6.096E+5	5.677E+5	-5.283E-3	-5.590E-3	3.521E-4	-1.219E-4	7.665E-5
MB12	3.322E+5	3.779E+5	-5.360E-3	-5.590E-3	2.227E-4	-6.644E-5	7.327E-5
MB11	4.187E+5	8.280E+5	-5.580E-3	-5.590E-3	-2.290E-6	-8.374E-5	9.637E-5
MB10	5.541E+5	1.096E+6	-5.826E-3	-5.590E-3	-2.173E-4	-1.108E-4	9.240E-5
MB9	5.761E+5	1.139E+6	-6.062E-3	-5.590E-3	-4.463E-4	-1.152E-4	8.938E-5
MB8	2.278E+5	4.505E+5	-6.213E-3	-5.590E-3	-6.643E-4	-4.556E-5	8.704E-5

Maximum permissible mean pressure:

- The limit is 0.8 MPa for the aft stern tube bearing and the value observed is 0.72 MPa,
- The limit is 0.8 MPa for the fore stern tube bearing and the value observed is 0.25 MPa,
- The limit is 1.0 MPa for the I/M shaft bearings and the value observed is 0.52 MPa, 0.69 MPa and 0.72 MPa respectively,
- No crankshaft bearing mean pressure value exceeds 3 MPa.

5.5.14. Loading Condition "16TAS"

The following assumptions have been made for the calculations presented in this section:

- The M/E is running at 84.1 rpm,
- The M/E is in hot condition and M/E bearings are offset by an additional 0.41 mm relative to other conditions where the M/E is not running,
- Hull deformations are not zero,
- The propeller and parts of the propeller shaft are immersed in water. Thus, their weight is partially supported by the bearings and the water.

TABLE 5.22: Loading Condition "16TAS": Detailed calculation results.

Bearing	Reaction (N)	Mean Pressure (Pa)	Total Offsets (m)	Initial Offsets (m)	Hull Deform. (m)	Support Elastic Deformation (m)	Minimum FIlm Thickness (m)
ASB	1.502E+6	6.993E+5	6.127E-4	7.500E-4	0.000E+0	-4.292E-4	2.919E-4
FSB	2.453E+5	2.503E+5	9.171E-4	7.500E-4	2.437E-6	-7.009E-5	2.348E-4
IS3	3.693E+5	5.235E+5	-1.974E-3	-2.000E-3	8.427E-5	-1.846E-4	1.260E-4
IS2	4.912E+5	6.962E+5	-2.891E-3	-3.000E-3	2.334E-4	-2.456E-4	1.212E-4
IS1	4.702E+5	6.665E+5	-3.516E-3	-4.000E-3	5.983E-4	-2.351E-4	1.212E-4
MB13	6.272E+5	5.841E+5	-4.363E-3	-5.590E-3	1.275E-3	-1.254E-4	7.724E-5
MB12	3.084E+5	3.508E+5	-4.427E-3	-5.590E-3	1.153E-3	-6.167E-5	7.124E-5
MB11	4.225E+5	8.356E+5	-4.625E-3	-5.590E-3	9.547E-4	-8.451E-5	9.441E-5
MB10	5.567E+5	1.101E+6	-4.844E-3	-5.590E-3	7.660E-4	-1.113E-4	9.124E-5
MB9	5.778E+5	1.143E+6	-5.049E-3	-5.590E-3	5.674E-4	-1.156E-4	8.873E-5
MB8	2.266E+5	4.481E+5	-5.170E-3	-5.590E-3	3.787E-4	-4.532E-5	8.699E-5

Maximum permissible mean pressure:

- The limit is 0.8 MPa for the aft stern tube bearing and the value observed is 0.70 MPa,
- The limit is 0.8 MPa for the fore stern tube bearing and the value observed is 0.25 MPa,
- The limit is 1.0 MPa for the I/M shaft bearings and the value observed is 0.52 MPa, 0.70 MPa and 0.67 MPa respectively,
- No crankshaft bearing mean pressure value exceeds 3 MPa.

5.5.15. Loading Condition "MAX"

The following assumptions have been made for the calculations presented in this section:

- The M/E is running at 84.9 rpm,
- The M/E is in hot condition and M/E bearings are offset by an additional 0.41 mm relative to other conditions where the M/E is not running,
- Hull deformations are not zero,
- The propeller and parts of the propeller shaft are immersed in water. Thus, their weight is partially supported by the bearings and the water.

TABLE 5.23: Loading Condition "MAX": Detailed calculation results.

Bearing	Reaction (N)	Mean Pressure (Pa)	Total Offsets (m)	Initial Offsets (m)	Hull Deform. (m)	Support Elastic Deformation (m)	Minimum FIlm Thickness (m)
ASB	1.499E+6	6.981E+5	6.106E-4	7.500E-4	0.000E+0	-4.284E-4	2.890E-4
FSB	2.506E+5	2.557E+5	9.167E-4	7.500E-4	3.274E-6	-7.161E-5	2.350E-4
IS3	3.669E+5	5.200E+5	-2.111E-3	-2.000E-3	-5.402E-5	-1.834E-4	1.268E-4
IS2	4.898E+5	6.943E+5	-3.125E-3	-3.000E-3	-1.500E-6	-2.449E-4	1.213E-4
IS1	4.758E+5	6.744E+5	-3.693E-3	-4.000E-3	4.241E-4	-2.379E-4	1.211E-4
MB13	6.091E+5	5.672E+5	-4.341E-3	-5.590E-3	1.296E-3	-1.218E-4	7.556E-5
MB12	2.951E+5	3.357E+5	-4.359E-3	-5.590E-3	1.221E-3	-5.902E-5	6.908E-5
MB11	4.510E+5	8.919E+5	-4.484E-3	-5.590E-3	1.104E-3	-9.020E-5	9.191E-5
MB10	5.560E+5	1.100E+6	-4.635E-3	-5.590E-3	9.767E-4	-1.112E-4	8.925E-5
MB9	5.777E+5	1.142E+6	-4.768E-3	-5.590E-3	8.494E-4	-1.155E-4	8.806E-5
MB8	2.259E+5	4.468E+5	-4.816E-3	-5.590E-3	7.321E-4	-4.519E-5	8.694E-5

Maximum permissible mean pressure:

- The limit is 0.8 MPa for the aft stern tube bearing and the value observed is 0.70 MPa,
- The limit is 0.8 MPa for the fore stern tube bearing and the value observed is 0.26 MPa,
- The limit is 1.0 MPa for the I/M shaft bearings and the value observed is 0.52 MPa, 0.69 MPa and 0.67 MPa respectively,
- No crankshaft bearing mean pressure value exceeds 3 MPa.

5.6. Parameters Affecting Shaft Alignment

5.6.1. Accommodation Block

Although the shaft alignment procedure is not expected to start before the vessel stern blocks are fully welded and all of the stern structure is in place, sometimes this practice is overlooked [4]. In this test case, we investigate the effect of installation of the accomodation block on the shaft alignment plan. Let us assume that the initial shaft alignment plan was conducted in the same docking condition, but without the accomodation block being attached to the rest of the steel structure of the vessel. The accomodation block contributes to the lightship weight (~1000 t depending on the extent of the superstructure). When we subtract the accomodation block weight from the rest of the steel structure, we also alter the weight and buoyancy distribution; thus the hull exhibits offsets different than before. All things considered, it is obvious that the initial shaft alignment plan will not be accurate after installation of the accommodation block.

Figure 5.30 illustrates the vertical offsets of all bearings for all studied loading conditions, with the consideration that the reference condition is the one discussed above. No safe conclusions can be drawn from **Figure 5.30** alone. For this reason, we calculate the difference between the actual bearing offsets and the ones obtained through the above process. Then, we plot these differences for all bearings. **Figure 5.31** depicts the additional offsets the above mentioned case imposes to the system's bearings. A key point is that the additional offsets do not depend on the loading condition; they remain practically constant across the different conditions, but exhibit differences from the reference shaft alignment plan.

A quick glimpse on the bearing reactions (**Figure 5.32**) shows that the changes in bearing reaction forces, in the case that the accomodation block installation is performed after application of the shaft alignment plan, are moderate. The above conclusion can be further elaborated with the aid of **Table 5.24**. In particular, **Table 5.24** displays the percentage difference of bearing loads between the reference and studied case. M/E bearings MB10 and MB11 exhibit a maximum deviation in loading of approximately 20%. Although the absolute bearing loads are found to be within the limits, it is advisable that a careful consideration of such issues should be taken in the design stage.

Based on the above, it can be concluded that, in the case that the accommodation block is installed after the shaft alignment procedure, proper corrective actions should be taken to ensure that the final alignment status of the vessel is in compliance with Class rules. Further, it is advisable that bearing reaction measurements should be performed after the installation of the accommodation block, to verify proper operation of the bearings.

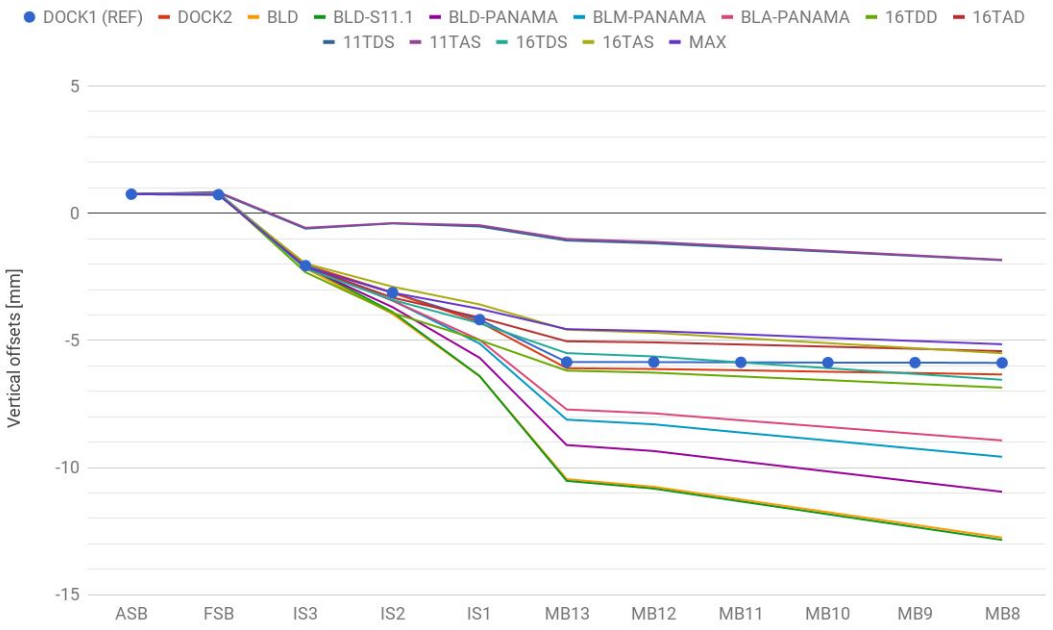

FIGURE 5.30: Hull induced additional vertical bearing offsets for different loading conditions of the studied vessel. The reference loading conditions refers to DOCK1 without the accomodation block being attached to the rest of the structure.

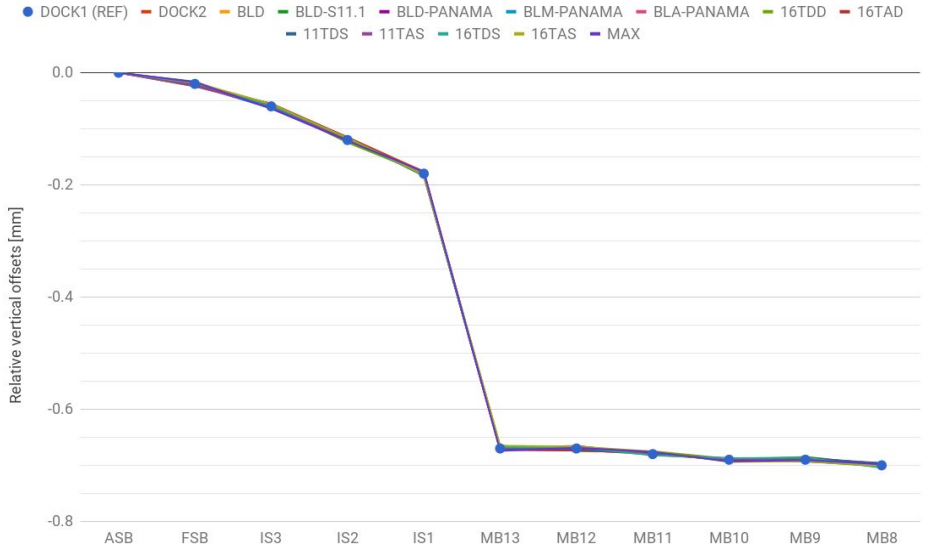

FIGURE 5.31: Relative vertical offsets of the bearings, for the loading conditions presented in **Figure 5.30**.

TABLE 5.24: Deviations of bearing reaction forces from the reference values, in case of installation of the accommodation block after completion of shaft alignment procedure.

Bearing	BLD	BLD-S11.1
ASB	-0.31%	-0.30%
FSB	0.01%	-0.06%
IS3	0.16%	0.22%
IS2	-0.29%	-0.32%
IS1	0.76%	0.74%
MB13	-2.53%	-2.01%
MB12	-5.99%	-7.51%
MB11	18.56%	19.00%
MB10	-14.71%	-21.02%
MB9	4.73%	7.46%
MB8	-0.53%	-2.29%

FIGURE 5.32: Bearing reaction forces for each loading condition of the vessel, in case of installation of the accommodation block after completion of shaft alignment procedure.

5.6.2. Voyage

As the vessel is en route from the departure port to the arrival port, consumables such as fuels and lubricants reduce in volume. It is reasonable that the loading and buoyancy distribution change and consequently, the hull would react with different hull deflections. **Figure 5.33** illustrates the vertical bearing offsets for a panama loading condition (from departure to arrival).

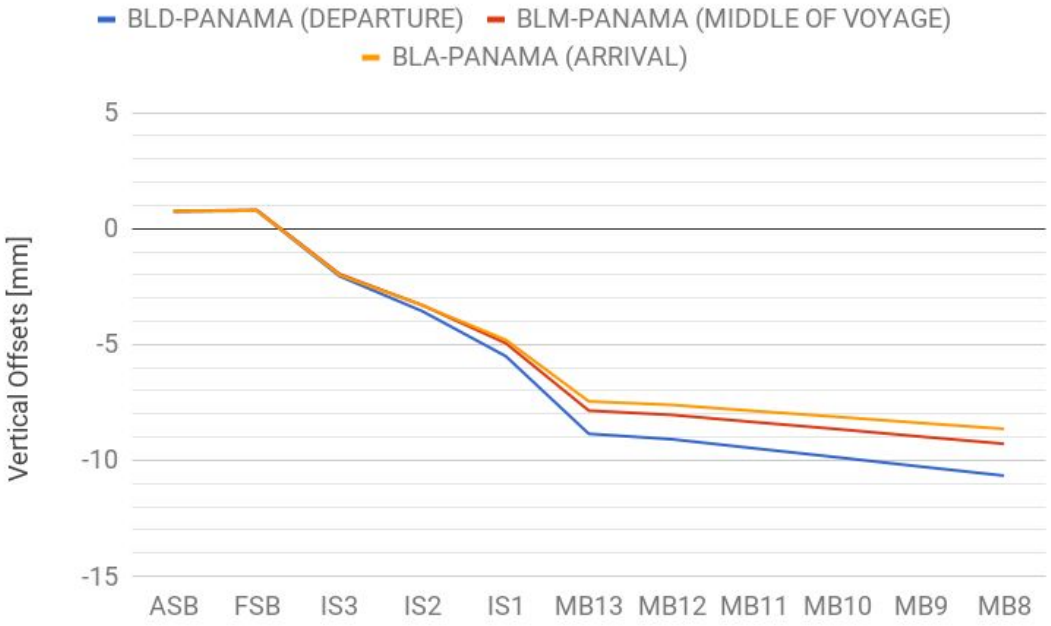

FIGURE 5.33: Bearing vertical offsets for a panama loading condition at departure, middle of voyage and arrival.

Figure 5.34 depicts the bearing reaction forces for the three considered loading conditions. All bearing reaction forces are found to be within limits, but bearings MB10 and MB11 exhibit the maximum deviation. In particular, MB10 reaction forces range from 494 kN to 555 kN (10% deviation), while reaction forces for MB11 range from MB11 427 kN to 474 kN (10% deviation). It can be concluded that, although relevant changes are not pronounced, attention should be given to assess bearing performance throughout a voyage to ensure proper bearing operation.

TABLE 5.25: Bearing reaction forces and maximum deviation for a panama loading condition at departure, middle of voyage and arrival.

Bearing	BLD-PANAMA	BLM-PANAMA	BLA-PANAMA	Maximum Deviation (%)
ASB	1.496E+6	1.497E+6	1.504E+6	0.53
FSB	2.516E+5	2.523E+5	2.508E+5	0.62
IS3	3.708E+5	3.700E+5	3.708E+5	0.23
IS2	4.833E+5	4.833E+5	4.822E+5	0.21
IS1	4.999E+5	5.005E+5	5.025E+5	0.53
MB13	4.565E+5	4.614E+5	4.557E+5	1.25
MB12	4.571E+5	4.562E+5	4.525E+5	1.02
MB11	4.743E+5	4.300E+5	4.268E+5	10.01
MB10	4.936E+5	5.424E+5	5.547E+5	11.01
MB9	5.718E+5	5.719E+5	5.742E+5	0.43
MB8	2.432E+5	2.339E+5	2.304E+5	5.25

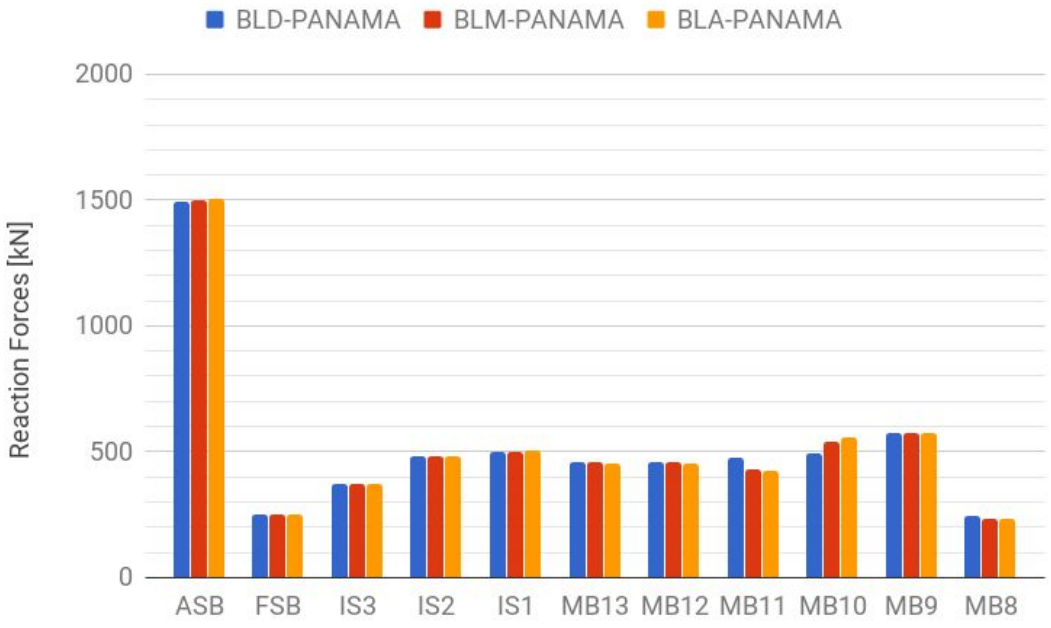

FIGURE 5.34: Bearing reaction forces for a panama loading condition at departure, middle of voyage and arrival.

5.6.3 Shaft Rigidity

In the present work, the shaft line is modelled as as series of beam elements with appropriate geometric and material properties. The shaft line contributes to the bending of the whole aft ship structure. Therefore, it is essential to model the shaft line for accurate prediction of hull deformations at the aft region of the vessel. To assess the effect of inclusion of the shaft in the finite element calculations, an additional FE model has been generated using beam elements with zero elastic properties; only the weight of the shaft is considered. **Figure 5.35** and **Figure 5.36** depict the absolute and relative vertical offsets with respect to the reference alignment condition. The effect of shaft rigidity on the shaft alignment plan is not obvious through examination of the vertical offsets of the bearings, as they do not show any repeating pattern.

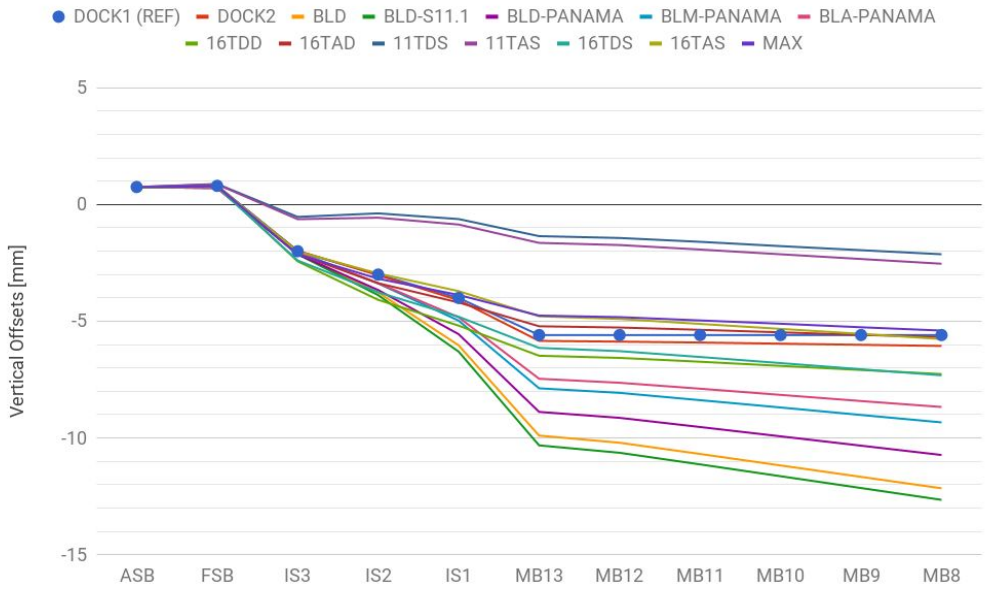

FIGURE 5.35: Effect of shaft stiffness on the bearing vertical offsets for different loading conditions of the vessel.

Figure 5.37 depicts the bearing reaction forces for all loading conditions for the case where shaft stiffness is neglected. The behaviour M/E bearings MB9-MB12 for the loading condition “BLD-S11.1” are of particular interest. Specifically, MB11 and MB9 are being unloaded, while MB12 and MB10 are overloaded, with MB10 being the most loaded of all.

Quantitatively, the percentage difference of the bearing reaction forces between the reference condition and the studied case, regarding loading condition “BLD-S11.1”, is demonstrated in **Table 5.26**. Bearing MB11 exhibits a 50% decrease of supported load, while bearing MB10 shows a 25% increase of supported load. Although the bearing loads are within limits, this analysis shows that shaft modelling in the FE model of the vessel may be crucial for accurate calculations of bearing offsets due to hull deflections.

TABLE 5.26: Effect of shaft stiffness on the bearing reaction forces for loading condition "BLD-S11.1".

Bearing	Reaction Forces w/ Shaft Rigidity (N)	Reaction Forces w/o Shaft Rigidity (N)	Diff (%)
ASB	1.494E+6	1.490E+6	-0.30
FSB	2.522E+5	2.520E+5	-0.09
IS3	3.708E+5	3.700E+5	-0.22
IS2	4.864E+5	4.870E+5	0.12
IS1	4.947E+5	4.910E+5	-0.75
MB13	4.637E+5	4.930E+5	5.94
MB12	4.751E+5	4.890E+5	2.84
MB11	4.291E+5	2.870E+5	-49.52
MB10	5.552E+5	7.380E+5	24.78
MB9	5.134E+5	4.130E+5	-24.31
MB8	2.630E+5	2.830E+5	7.07

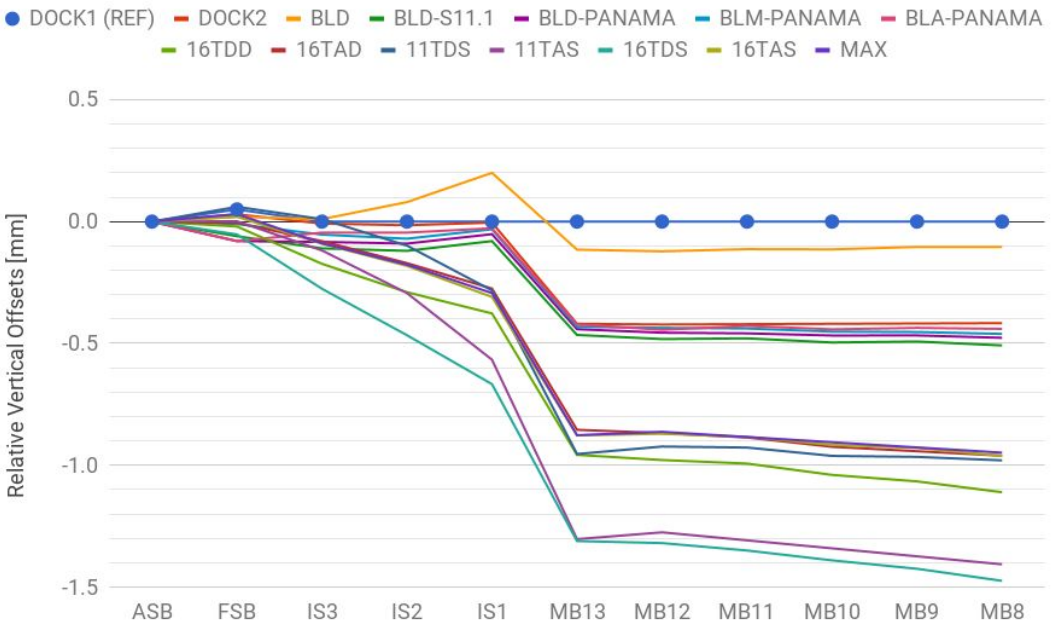

FIGURE 5.36: Effect of shaft stiffness: Relative vertical bearing offsets with respect to the reference calculations for different loading conditions of the vessel.

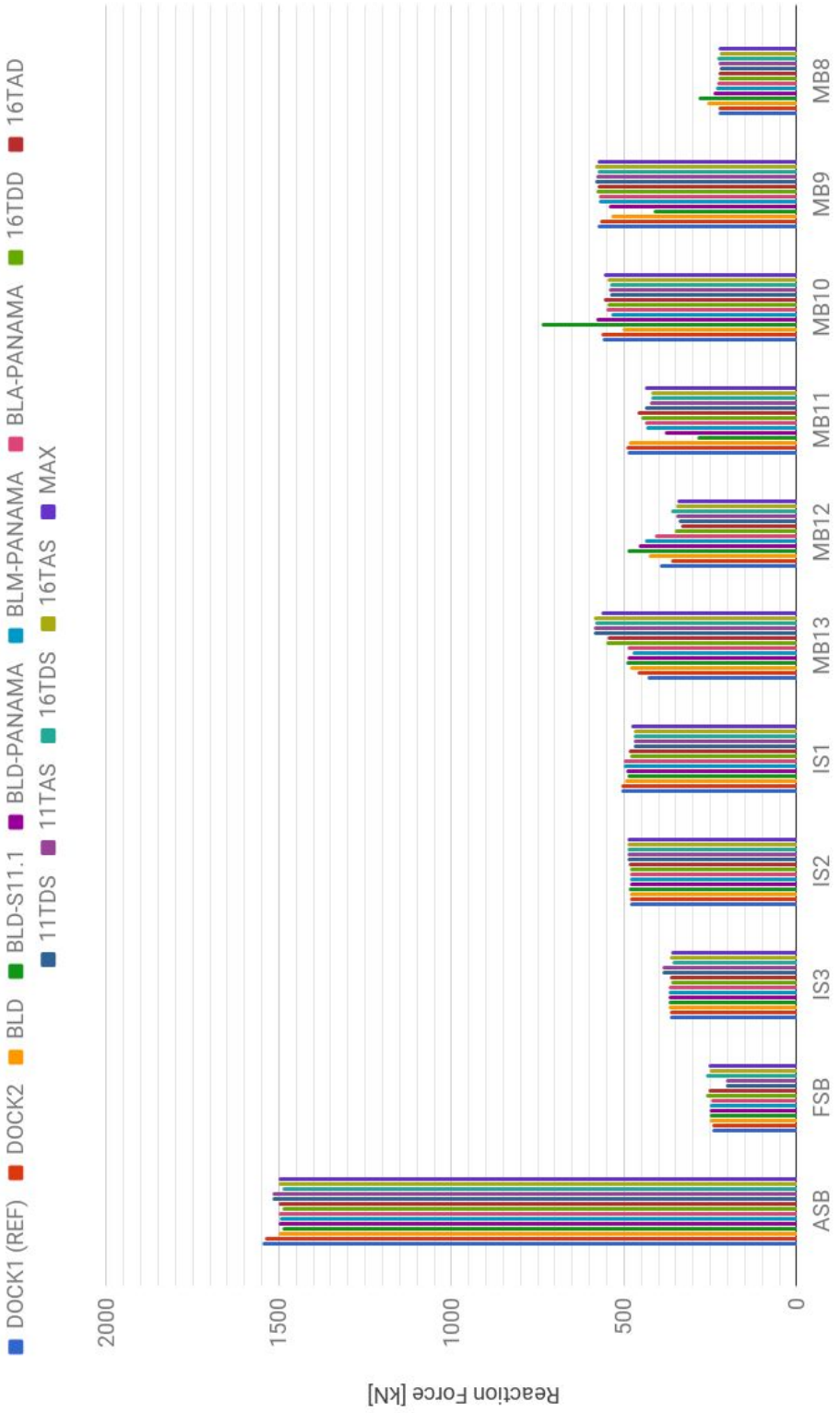

FIGURE 5.37: Bearing reaction forces for different loading conditions of the vessel when shaft stiffness is not considered in the FE model of the vessel.

5.6.4. Bearing Foundation Stiffness

In the present shaft alignment calculations, bearing foundation stiffness has been taken into consideration for estimating bearing reaction forces. The bearing is, thus, assumed to behave as a linear spring, which will deflect under the action of a load applied to the bearing. In this section, the effect of including bearing foundation stiffness in the calculation of bearing reaction forces is assessed. To this end, additional calculations have been performed assuming that bearing foundations are rigid, and the resulting bearing reactions are compared against those of the reference calculations. Relevant calculations are performed for different loading conditions of the vessel. **Figure 5.38** depicts the bearing reaction forces for all studied loading conditions.

The most obvious point of this analysis is that, for a set of loading conditions, the rigid support modelling leads to calculation of negative bearing loads, which would not be acceptable. In particular, M/E bearing MB12 is being either unloaded or, worse, negatively loaded at different loading conditions. As a result, adjacent bearings (mostly the first M/E bearing) are also influenced, experiencing increased loads (~30% with respect to the reference conditions).

Figure 5.39 illustrates the difference in bearing reaction forces for a specific loading condition (11TAS) when bearing foundation stiffness is considered or not. Interestingly, when the rigid support is considered, the shaft alignment plan fails to yield trustworthy results. In fact, the present results justify the use of elastic support modelling, even if a small number of loading conditions of the vessel are affected, in terms of bearing reaction forces.

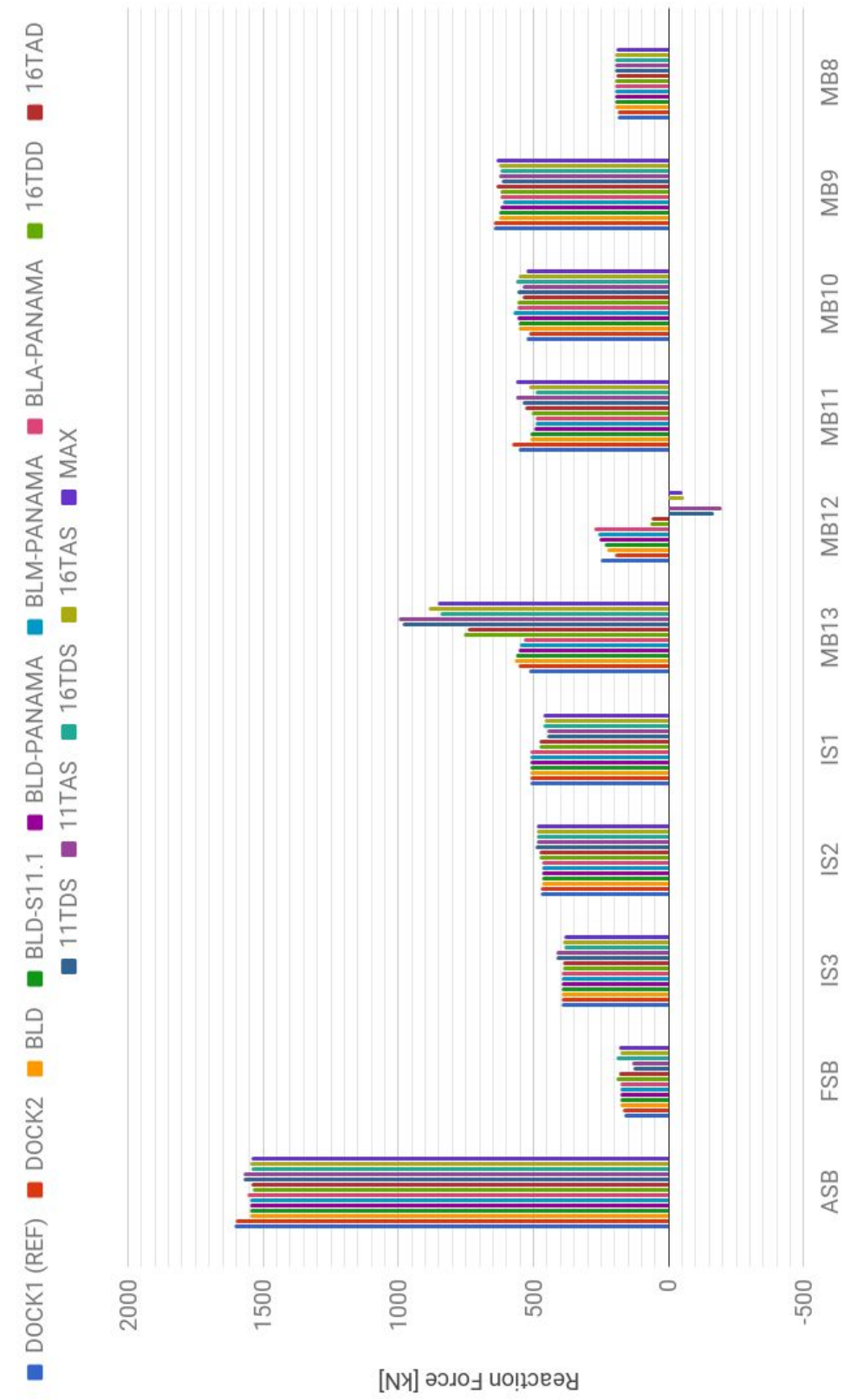

FIGURE 5.38: Bearing reaction forces for different loading conditions of the vessel when rigid bearing foundations are assumed.

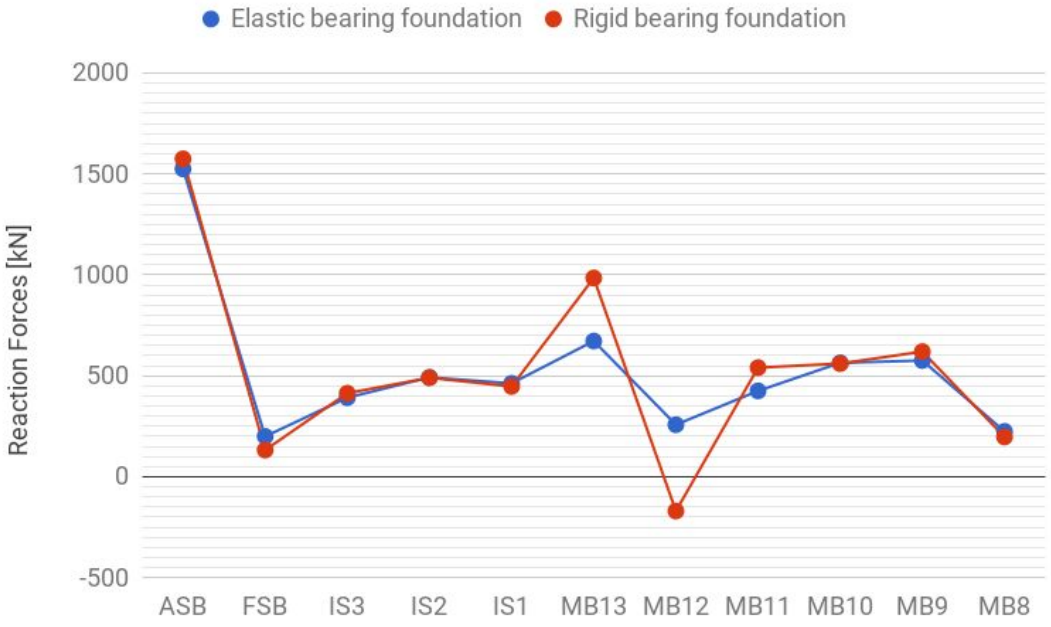

FIGURE 5.39: Loading Condition “11TAS”: Bearing reaction forces for (a) elastic bearing foundation, and (b) rigid bearing foundation.

5.7. Power Loss Estimation

Friction forces develop in the lubricant domain during bearing operation; these can be calculated through equation **EQ. 4.6**. Given the friction forces, the friction coefficient of each bearing can be calculated as the ratio of total friction force to the total hydrodynamic load. Finally, friction torque and friction power loss can be estimated using the above results. **Figure 5.40** illustrates the calculated power loss of the bearings for all the studied loading conditions. Remarkably, M/E bearing MB12 and MB13 exhibit maximum power losses among all the other bearings. The increased diameter and length of these bearings along with the relatively smaller value of minimum oil film thickness are the key reason for this behavior.

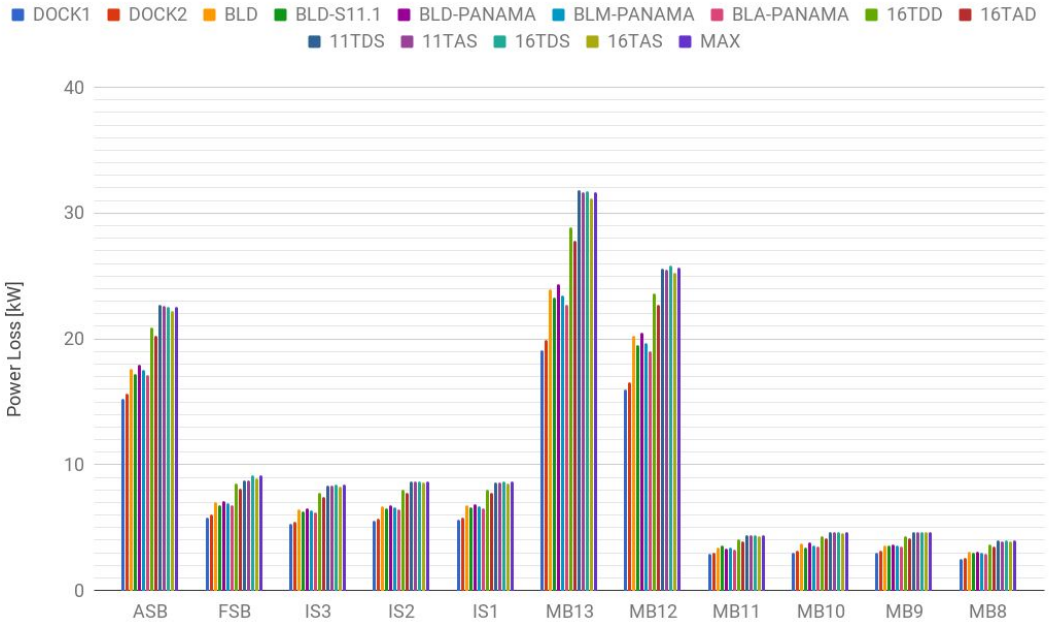

FIGURE 5.40: Power loss estimation for all loading conditions.

The figure most widely believed to accurately represent shafting power losses is 0.5~1.0% of the M/E's BHP at M.C.R. This is an estimate very commonly found in literature. It is evident that the results presented in this section, neither confirm that belief, nor strongly contradict it. **Table 5.27** summarises the results displayed in **Table 5.9b**, also presenting a comparison with the respective break horse power. A mean value, of power losses, of 0.285% BHP is observed for the bearings under consideration.

TABLE 5.27a: Power loss estimation for all bearings and loading conditions in kW.

#	ASB	FSB	IS3	IS2	IS1	SUM1	MB13	MB12	MB11	MB10	MB9	MB8	SUM2
LC1	15.2	5.8	5.3	5.6	5.6	37.5	19.1	16.0	2.9	3.0	3.0	2.5	46.5
LC2	15.7	6.0	5.5	5.8	5.8	38.8	19.9	16.5	3.0	3.1	3.1	2.6	48.3
LC3	17.7	7.0	6.4	6.7	6.8	44.6	24.0	20.2	3.4	3.7	3.6	3.1	58.0
LC4	17.2	6.8	6.3	6.5	6.7	43.5	23.3	19.5	3.6	3.4	3.6	3.0	56.3
LC5	17.9	7.1	6.5	6.8	6.9	45.3	24.4	20.5	3.4	3.8	3.7	3.1	58.8
LC6	17.5	6.9	6.3	6.6	6.7	44.1	23.4	19.6	3.4	3.6	3.6	3.0	56.7
LC7	17.2	6.8	6.2	6.4	6.5	43.1	22.7	19.1	3.3	3.5	3.5	2.9	55.0
LC8	20.9	8.5	7.8	8.0	8.0	53.1	28.9	23.6	4.1	4.3	4.3	3.6	68.8
LC9	20.3	8.1	7.5	7.7	7.7	51.4	27.8	22.7	3.9	4.2	4.2	3.5	66.3
LC10	22.7	8.8	8.4	8.7	8.6	57.2	31.8	25.6	4.4	4.7	4.7	4.0	75.1
LC11	22.6	8.7	8.3	8.7	8.6	56.9	31.7	25.5	4.4	4.6	4.7	4.0	74.8
LC12	22.5	9.2	8.4	8.7	8.6	57.5	31.7	25.9	4.4	4.7	4.7	4.0	75.3
LC13	22.2	8.9	8.2	8.6	8.5	56.5	31.1	25.3	4.3	4.6	4.6	3.9	73.9
LC14	22.6	9.1	8.4	8.7	8.7	57.5	31.6	25.7	4.4	4.6	4.7	4.0	75.1

TABLE 5.27b: Power loss estimation for all bearings and loading conditions in kW (continue).

#	Total Power Losses	Engine Power	Total % Engine Power
LC1	84.1	24876	0.338
LC2	87.0	26269	0.331
LC3	102.6	33723	0.304
LC4	99.8	32219	0.310
LC5	104.1	34731	0.300
LC6	100.8	33177	0.304
LC7	98.0	31890	0.307
LC8	121.9	45900	0.266
LC9	117.7	43447	0.271
LC10	132.3	52733	0.251
LC11	131.7	52351	0.252
LC12	132.8	52732	0.252
LC13	130.3	51238	0.254
LC14	132.5	52735	0.251

6. Conclusions - Future Work

6.1. Conclusions

In the present work, the shaft alignment of a typical 10,000 containership has been thoroughly investigated. The propulsion shaft of the ship has been modelled as a statically indeterminate, multi-supported beam, and solved using matrix analysis. A detailed finite element model of the aft end structure of the ship has been generated, to accurately calculate hull deformations. For normal ship operation, the oil film thickness and the stiffness of the bearing foundations have been taken into account.

First, considering the afloat dock condition of the ship, a reference shaft alignment plan has been assumed, and a quasi-static equilibrium of the shaft has been calculated, yielding the reaction forces at the shaft bearings. Next, fourteen (14) representative loading conditions of the vessel, corresponding to, ballast, design and scantling conditions have been simulated. The corresponding hull deflections have been computed, the offset of the bearings due to hull deflections have been determined, and the bearing reaction forces have been calculated.

The results demonstrate that the initial shaft alignment plan of the studied vessel is satisfactory, as all bearing reaction forces are positive and within manufacturer's limits for all studied loading conditions. In detail, the reaction force of the aft stern tube bearing displays a maximum deviation of approximately 3.7%. The first two main engine bearings (MB13 and MB12) exhibit the most pronounced deviations in reaction forces (34.6% and 47.2% respectively), without raising any concerns for the reliability of the shafting system.

Next, a comparative analysis of the key parameters affecting the shaft alignment is conducted. First, the effect of performing the shaft alignment plan without having the accommodation block in place is examined. Although the bearing reaction forces are within limits, a maximum deviation of 20.0% is displayed. Second, the voyage effect over the shafting system is considered. In this scenario, bearing reaction forces are found to be within limits and a maximum deviation of 10.0% is exhibited. Next, the effect of shaft rigidity on the shaft alignment plan is analysed. In this case, some bearings exhibit a deviation near 25.0% and up to 50.0%. Last, the effect of bearing foundation stiffness is examined. In particular, calculations performed excluding the effect of bearing foundation stiffness reveal that the predicted bearing reaction forces may be substantially different for several bearings of the system, while some of the main engine bearings are calculated with negative loading, which would lead to wrong conclusions about the validity of the proposed shaft alignment plan. The results of the present study strengthen the conclusions drawn by other researchers in the recent literature, and show that bearing foundation stiffness has a non-detrimental effect on the calculated bearing reactions, and should therefore be taken into consideration during relevant calculations.

6.2. Future Work

The finite element analysis conducted in the present work opens up the path to extend our knowledge and comprehension of the various parameters that play a key role in the shaft alignment calculations. Future work aiming at this direction is suggested below.

6.2.1. Hull Deflections due to Sea Swell

An important parameter to be considered is the hull deformations due to sea swell. In addition to the deformations of the hull structure caused by the different loading conditions, the deformations of hull structure due to hydrodynamic loads / waves could be included in elastic shaft alignment calculations. Sea swell wave characteristics are to be defined for maximizing the double-bottom relative deformation in terms of shaft line supports.

6.2.2. Hydrodynamic Propeller Loads

Classification Societies suggest hydrodynamic propeller loads should be included in the shaft alignment calculations. In our analysis, only static phenomena have been taken into consideration. It is essential that propeller thrust be part of the investigation of the shafting behavior. A hybrid analysis could be conducted where the static model incorporates the dynamic loads as quasi-static. Finally, a purely dynamic analysis could be ordered in case any problems emerge by the hybrid analysis, for obtaining a more accurate assessment of shaft status.

6.2.3. Detailed Aft Stern Tube Bearing Modelling

In the present work, the aft stern tube bearing has been modelled as a single support point. BV, in their rule notation, state that the aftermost bearing is to be modeled with at least five supporting points in order to have detailed results at each section of the bearing. To this end, shaft alignment calculations should be reevaluated with a more sophisticated shaft model, so as to simulate shaft-bearing interaction in the aft stern-tube bearing, which is a critical bearing of the system, since it supports the radial load of the overhanged propeller. It is expected that more detailed modeling of bearing and shaft interaction in the aft stern tube bearing will increase the accuracy of calculation of bearing forces in the stern tube region.

6.2.4. Hull Deflections due to Thermal Expansion

It is common practice for the yards to perform application of the shaft alignment plan during night time. This procedure is selected so that ambient temperature is close to the sea water temperature, and hull expansion due to thermal effects is minimized. The effect of thermal expansion of the vessel hull could be evaluated by performing coupled thermal-structural analysis of the system using FEA. The effects of hull deformation due to thermal expansion could thus be evaluated, leading to appropriate corrections, in the case of alignment plan application during day-time.

6.2.5. Optimisation of Shaft Alignment Plan

Complementary to the analysis presented in this work, an optimisation process can be carried out for a number of shafting plan parameters. Having considered hydrodynamic propeller loads, as well as hull deflections due to the different loading conditions and sea swell, an engineer can propose an optimised initial shaft alignment plan. The target of an optimization procedure can include:

- Optimal distribution of reaction forces,
- Minimisation of shaft bending moments,
- Maximization of the minimum oil film thickness of bearings,
- Minimisation of the power loss of the shafting system.

7. Literature - References

[1] Harrington, R. (1992). *Marine engineering.*

[2] Devanney, J., Kennedy, M. (2003). *The down ratchet and the deterioration of tanker newbuilding standards.* Center for Tankship Excellence.

[3] Šverko, D. (2003). *Design concerns in propulsion shafting alignment.* Proceedings of the ICMES Conference 2003. Helsinki.

[4] American Bureau of Shipping. (2014). *Guidance notes on propulsion shafting alignment.*

[5] Šverko, D. (2006). *A solution to robust shaft alignment design.* ABS Technical Papers.

[6] Dahler, G. et al. (2004). *A study on flexible hulls, flexible engines, crankshaft deflections and engine bearing loads for VLCC propulsion machinery.* CIMAC Congress. Paper 48. Kyoto.

[7] Murawski, L. (2005). *Shaft line alignment analysis taking ship construction flexibility and deformations into consideration.* Marine Structures. 18(1). pp. 62–84.

[8] Korbetis G., Vlachos, O., Charitopoulos, A.G., Papadopoulos, C.I. (2014). *Effects of hull deformation on the static shaft alignment characteristics of VLCCs: a case study.* Proceedings of the 13th International Conference on Computer Applications and Information Technology in the Maritime Industries. 12-14 May 2014. Redworth/UK.

[9] Bureau Veritas. (2015). *Elastic Shaft Alignment (ESA).*

[10] American Bureau of Shipping. (2015). *Enhanced Shaft Alignment (ESA).*

[11] Vlachos, O. (2015). *Elastic Shaft Alignment.* Diploma thesis.

[12] Servis, D. et al. (2004). *Finite element modelling and strength analysis of hold no. 1 of bulk carriers.* Marine Structures. 16(8). pp. 601–626.

[13] Det Norske Veritas. (2006). *Casualty Information.*

[14] Bureau Veritas. (2017). *Rules for the Classification of Steel Ships (NR467).*

[15] American Bureau of Shipping. (2018). *Rules for building and classing steel vessels.*

[16] Cameron, A. (1983). *Basic Lubrication Theory.*

[17] Frangopoulos, C. A. (2005). *Ship Energy Systems, Volume C: Propulsion Shaft Alignment (in Greek).*

[18] Paik, J. K. (2003). *Ultimate Limit State Design of Steel-Plated Structures.*

[19] Frangopoulos, C. A. (1989). *Torsional Vibrations (in Greek).*

APPENDIX A

A/A	Name	Position [m]	Length [m]	Diameter [m]
1	Shaft	0.000	0.570	0.695
2	Connector	0.570	0.000	-
3	Shaft	0.570	1.035	0.916
4	Propeller mass	1.605	0.000	-
5	Shaft	1.605	0.925	0.965
6	Shaft	2.530	0.615	0.988
7	Bearing element	3.145	1.087	0.988
8	ASB	4.232	0.000	-
9	Bearing element	4.232	1.087	0.988
10	Shaft	5.319	0.481	0.988
11	Shaft	5.800	0.100	0.957
12	Shaft	5.900	4.110	0.925
13	Shaft	10.010	0.100	0.958
14	Shaft	10.110	0.377	0.990
15	Bearing element	10.487	0.495	0.990
16	FSB	10.982	0.000	-
17	Bearing element	10.982	0.495	0.990
18	Shaft	11.477	0.175	0.990
19	Shaft	11.652	0.558	0.990
20	Shaft	12.210	0.100	0.990
21	Shaft	12.310	1.230	0.898
22	Flange	13.540	0.170	1.660
23	Flange	13.710	0.170	1.660
24	Shaft	13.880	1.830	0.805
25	Shaft	15.710	4.330	0.805
26	Shaft	20.040	0.040	0.818
27	Shaft	20.080	0.391	0.830
28	Bearing element	20.471	0.425	0.830
29	ISB3	20.896	0.000	-
30	Bearing element	20.896	0.425	0.830
31	Shaft	21.321	0.391	0.830
32	Shaft	21.712	0.040	0.818
33	Shaft	21.752	0.144	0.805
34	Shaft	21.896	4.444	0.805
35	Flange	26.340	0.170	1.660
36	Flange	26.510	0.170	1.660
37	Shaft	26.680	3.625	0.805
38	Shaft	30.305	0.040	0.818
39	Shaft	30.345	0.391	0.830
40	Bearing element	30.736	0.425	0.830
41	ISB2	31.161	0.000	-
42	Bearing element	31.161	0.425	0.830
43	Shaft	31.586	0.391	0.830

A/A	Name	Position [m]	Length [m]	Diameter [m]
44	Shaft	31.977	0.040	0.830
45	Shaft	32.017	0.144	0.805
46	Shaft	32.161	5.149	0.805
47	Shaft	37.310	1.830	0.805
48	Flange	39.140	0.170	1.660
49	Flange	39.310	0.170	1.660
50	Shaft	39.480	2.118	0.805
51	Shaft	41.598	0.040	0.818
52	Shaft	41.638	0.391	0.830
53	Bearing element	42.029	0.425	0.830
54	ISB1	42.454	0.000	-
55	Bearing element	42.454	0.425	0.830
56	Shaft	42.879	0.391	0.830
57	Shaft	43.270	0.040	0.818
58	Shaft	43.310	0.144	0.805
59	Shaft	43.454	4.856	0.805
60	Shaft	48.310	3.630	0.805
61	Flange	51.940	0.170	1.830
62	Engine flange	52.110	0.140	1.830
63	Flywheel	52.250	0.000	-
64	Shaft	52.250	0.100	2.190
65	Bearing element	52.350	0.585	1.180
66	MB13	52.935	0.000	-
67	Bearing element	52.935	0.325	1.180
68	Shaft	53.260	0.090	2.290
69	Shaft	53.350	0.180	1.930
70	Shaft	53.530	0.090	2.290
71	Bearing element	53.620	0.325	1.180
72	MB12	53.945	0.000	-
73	Bearing element	53.945	0.420	0.602
74	Shaft	54.365	0.375	0.602
75	Load	54.740	0.000	-
76	Shaft	54.740	0.375	0.602
77	Bearing element	55.115	0.420	0.602
78	MB11	55.535	0.000	-
79	Bearing element	55.535	0.420	0.602
80	Shaft	55.955	0.375	0.602
81	Load	56.330	0.000	-
82	Shaft	56.330	0.375	0.602
83	Bearing element	56.705	0.420	0.602
84	MB10	57.125	0.000	-
85	Bearing element	57.125	0.420	0.602
86	Shaft	57.545	0.375	0.602
87	Load	57.920	0.000	-
88	Shaft	57.920	0.375	0.602

A/A	Name	Position [m]	Length [m]	Diameter [m]
89	Bearing element	58.295	0.420	0.602
90	MB9	58.715	0.000	-
91	Bearing element	58.715	0.420	0.602
92	Shaft	59.135	0.375	0.602
93	Load	59.510	0.000	-
94	Shaft	59.510	0.375	0.602
95	Bearing element	59.885	0.420	0.602
96	MB8	60.305	0.000	-
97	Bearing element	60.305	0.420	0.602

A/A	Name	Position [m]	Load [N]
2	Connector	0.570	6.525E+4
4	Propeller mass	1.605	9.402E+5
63	Flywheel	52.250	8.342E+4
75	Load	54.740	5.466E+5
81	Load	56.330	5.466E+5
87	Load	57.920	5.466E+5
93	Load	59.510	5.466E+5

APPENDIX B

LOAD: DOCK1 : NORMAL DOCKING

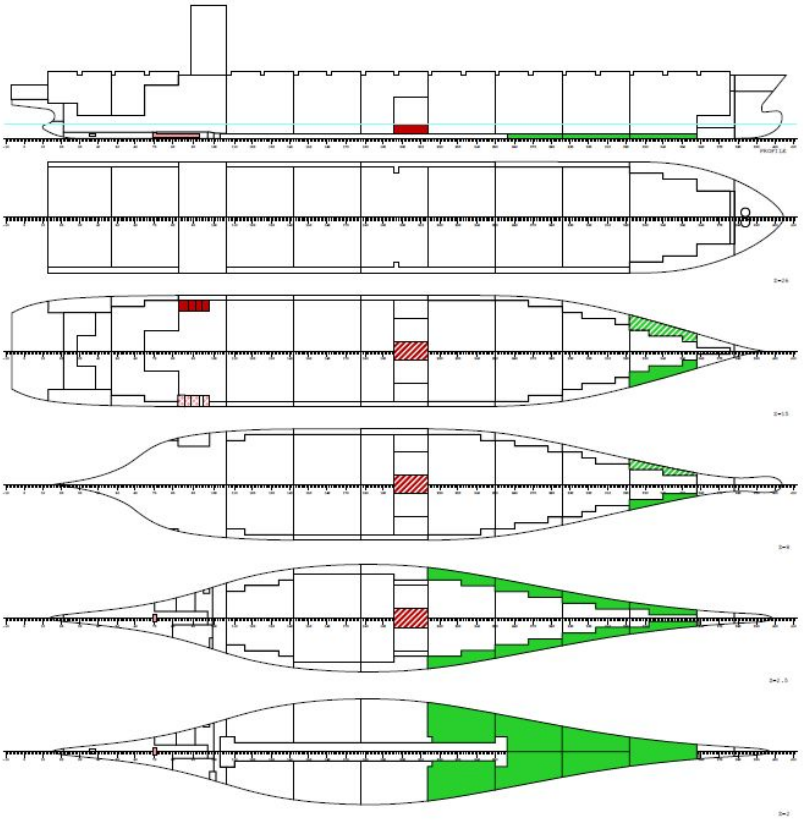

XFRAM m	#	BEND tm	REL %	BMMX tm	BMMN tm	RELSH t	REL %	SHMX t	SHMN t	TORS tm	REL %	TMMX tm	TMMN tm
10.40	13	14993	33.3	45028	-19086	1749	43.0	4065	-801	942	4.2	22432	-22432
16.91	21	28666	32.1	89337	-39357	2465	42.1	5861	-1652	935	4.2	22432	-22432
23.00	29	45218	32.7	138272	-58310	2957	40.9	7229	-2448	921	4.1	22432	-22432
37.55	47	95261	34.0	280510	-103841	3853	40.3	9569	-4350	891	4.0	22432	-22432
52.10	65	155175	35.2	440575	-150045	4291	38.2	11231	-6063	866	3.9	22432	-22432
57.85	72	180463	35.7	504815	-168356	4565	39.8	11464	-6494	891	4.0	22432	-22432
66.65	83	226495	37.8	599292	-196327	5838	50.2	11623	-6848	729	3.3	22432	-22432
78.50	96	308116	43.2	713937	-234032	8260	73.8	11191	-6962	9426	42.0	22432	-22432
87.50	106	387365	48.9	791423	-262669	9264	83.6	11075	-6962	11318	50.5	22432	-22432
102.0	124	512522	58.4	878094	-308632	7708	72.7	10606	-6887	11316	50.4	22432	-22432
116.6	142	609234	66.6	915087	-353413	5522	66.5	8298	-6550	11286	50.3	22432	-22432
131.1	160	671863	70.7	950587	-396375	3050	49.0	6223	-6223	11254	50.2	22432	-22432
145.7	178	697370	73.4	950587	-396375	441	7.1	6223	-8086	11218	50.0	22432	-22432
160.2	196	684698	72.5	945001	-396375	-2177	26.1	6223	-8354	11179	49.8	22432	-22432
174.8	214	637840	69.8	914398	-396333	-4234	50.4	6223	-8397	11136	49.6	22432	-22432
189.3	232	569371	65.4	871062	-395751	-5174	60.9	6237	-8498	11113	49.5	22432	-22432
203.9	250	488677	60.5	808296	-394958	-5918	65.0	6548	-9102	11110	49.5	22432	-22432
218.4	268	398845	56.9	700417	-362651	-6329	63.3	7012	-10005	11109	49.5	22432	-22432
233.0	286	306612	54.7	560467	-310689	-6342	60.8	7230	-10429	11107	49.5	22432	-22432
247.6	304	216057	51.5	419892	-258730	-6098	62.4	7230	-9766	11107	49.5	22432	-22432
262.1	322	130925	44.7	292602	-206773	-5597	64.6	7230	-8664	11106	49.5	22432	-22432
276.7	340	63854	33.0	193763	-154818	-3601	55.1	6618	-6532	4534	20.2	22432	-22432
291.2	358	27166	23.5	115648	-99620	-1564	39.1	4327	-3999	-57	0.3	22432	-22432
307.5	378	6994	15.5	45089	-45553	-785	44.9	1901	-1749	-35	0.2	22432	-22432

LOAD: DOCK2 : DOCKING WITH 12000t CARGO

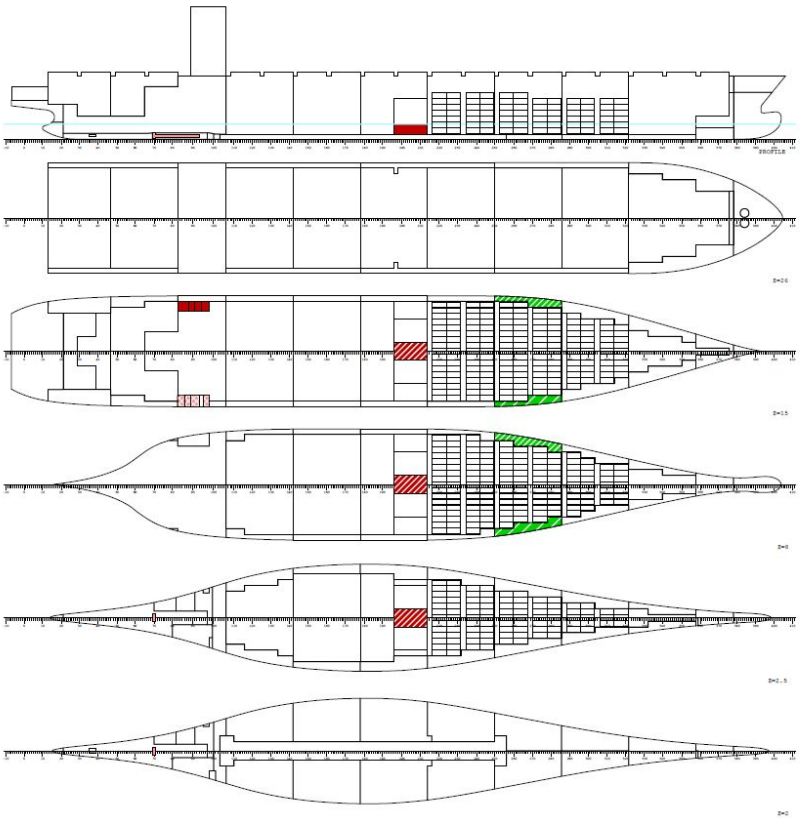

XFRAM m	#	BEND tm	REL %	BMMX tm	BMMN tm	RELSHREL t	%	SHMX t	SHMN t	TORS tm	REL %	TMMX tm	TMMN tm
10.40	13	14978	33.3	45028	-19086	1749	43.0	4065	-801	902	4.0	22432	-22432
16.91	21	28635	32.1	89337	-39357	2461	42.0	5861	-1652	879	3.9	22432	-22432
23.00	29	45136	32.6	138272	-58310	2945	40.7	7229	-2448	850	3.8	22432	-22432
37.55	47	94748	33.8	280510	-103841	3801	39.7	9569	-4350	784	3.5	22432	-22432
52.10	65	153321	34.8	440575	-150045	4150	37.0	11231	-6063	722	3.2	22432	-22432
57.85	72	177638	35.2	504815	-168356	4368	38.1	11464	-6494	733	3.3	22432	-22432
66.65	83	221434	36.9	599292	-196327	5523	47.5	11623	-6848	550	2.5	22432	-22432
78.50	96	298152	41.8	713937	-234032	7743	69.2	11191	-6962	9217	41.1	22432	-22432
87.50	106	371977	47.0	791423	-262669	8575	77.4	11075	-6962	11087	49.4	22432	-22432
102.0	124	484962	55.2	878094	-308632	6723	63.4	10606	-6887	11049	49.3	22432	-22432
116.6	142	565096	61.8	915087	-353413	4228	51.0	8298	-6550	10983	49.0	22432	-22432
131.1	160	606627	63.8	950587	-396375	1444	23.2	6223	-6223	10914	48.7	22432	-22432
145.7	178	606490	63.8	950587	-396375	-1477	18.3	6223	-8086	10842	48.3	22432	-22432
160.2	196	563643	59.6	945001	-396375	-4406	52.7	6223	-8354	10767	48.0	22432	-22432
174.8	214	482104	52.7	914398	-396333	-6771	80.6	6223	-8397	10688	47.6	22432	-22432
189.3	232	382030	43.9	871062	-395751	-6592	77.6	6237	-8498	10628	47.4	22432	-22432
203.9	250	286083	35.4	808296	-394958	-6201	68.1	6548	-9102	10590	47.2	22432	-22432
218.4	268	205208	29.3	700417	-362651	-4561	45.6	7012	-10005	5339	23.8	22432	-22432
233.0	286	147736	26.4	560467	-310689	-3022	29.0	7230	-10429	188	0.8	22432	-22432
247.6	304	106512	25.4	419892	-258730	-2418	24.8	7230	-9766	151	0.7	22432	-22432
262.1	322	74966	25.6	292602	-206773	-1737	20.0	7230	-8664	115	0.5	22432	-22432
276.7	340	49175	25.4	193763	-154818	-1752	26.8	6618	-6532	79	0.4	22432	-22432
291.2	358	25494	22.0	115648	-99620	-1460	36.5	4327	-3999	43	0.2	22432	-22432
307.5	378	6533	14.5	45089	-45553	-735	42.0	1901	-1749	25	0.1	22432	-22432

LOAD: BLD : BALLAST DEP.

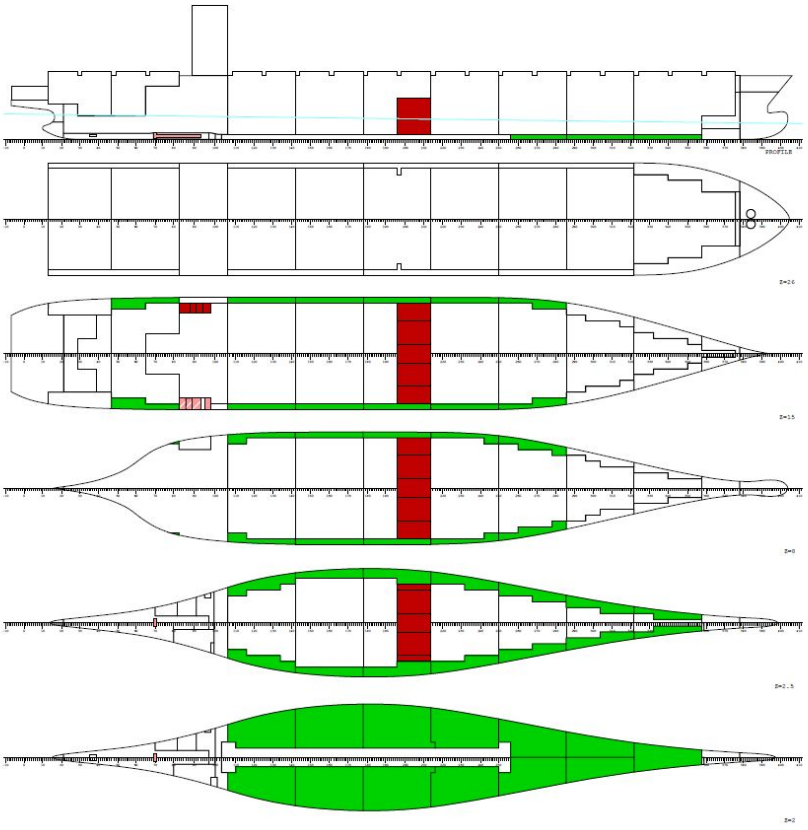

XFRAM m	#	BEND tm	REL %	BMMX tm	BMMN tm	RELSHREL t	%	SHMX t	SHMN t	TORS tm	REL %	TMMX tm	TMMN tm
10.40	13	15270	49.3	30997	-238	1746	43.5	4019	-528	855	3.8	22432	-22432
16.91	21	29022	48.2	60230	-490	2444	43.4	5633	-1088	812	3.6	22432	-22432
23.00	29	45397	47.6	95457	-725	2870	42.1	6813	-1613	765	3.4	22432	-22432
37.55	47	91663	44.5	206184	-1502	3277	37.9	8656	-2866	656	2.9	22432	-22432
52.10	65	140401	41.8	335725	-3008	3173	32.4	9786	-3919	550	2.5	22432	-22432
57.85	72	158071	40.7	387938	-3639	2985	30.5	9786	-4077	543	2.4	22432	-22432
66.65	83	186948	40.3	463885	-4605	3468	36.0	9646	-4077	334	1.5	22432	-22432
78.50	96	231534	41.9	552831	-5906	4291	47.2	9092	-4077	1553	6.9	22432	-22432
87.50	106	270758	44.4	610295	-6894	4575	51.0	8970	-4077	1491	6.6	22432	-22432
102.0	124	327422	49.4	662589	-8142	2944	34.6	8499	-4077	1410	6.3	22432	-22432
116.6	142	354752	53.5	662589	-8155	629	10.2	6167	-4077	1300	5.8	22432	-22432
131.1	160	346676	52.3	662589	-8155	-1760	43.2	4077	-4077	1188	5.3	22432	-22432
145.7	178	304872	46.0	662589	-8155	-4006	66.4	4077	-6038	1072	4.8	22432	-22432
160.2	196	231423	35.2	656706	-8155	-6109	96.7	4077	-6320	953	4.2	22432	-22432
174.8	214	195264	31.3	624486	-8111	1102	27.0	4077	-6365	831	3.7	22432	-22432
189.3	232	199800	34.5	578875	-7499	-472	7.3	4077	-6465	728	3.2	22432	-22432
203.9	250	184586	36.0	512809	-6664	-1571	22.6	4077	-6962	646	2.9	22432	-22432
218.4	268	158552	37.2	426647	-5809	-1899	24.6	4077	-7705	564	2.5	22432	-22432
233.0	286	133235	41.1	323839	-4975	-1527	19.0	4077	-8053	483	2.2	22432	-22432
247.6	304	106867	48.5	220372	-4144	-2088	28.4	4077	-7355	403	1.8	22432	-22432
262.1	322	75944	58.0	130890	-3315	-2159	34.9	4077	-6195	323	1.4	22432	-22432
276.7	340	46135	64.7	71356	-2488	-1897	45.2	3732	-4199	243	1.1	22432	-22432
291.2	358	22796	62.1	36697	-1950	-1327	53.2	2480	-2493	164	0.7	22432	-22432
307.5	378	5590	59.6	9378	-1862	-684	63.8	1072	-1072	96	0.4	22432	-22432

LOAD: BLD-S11.1 : BALLAST DEP.(URS11.1)

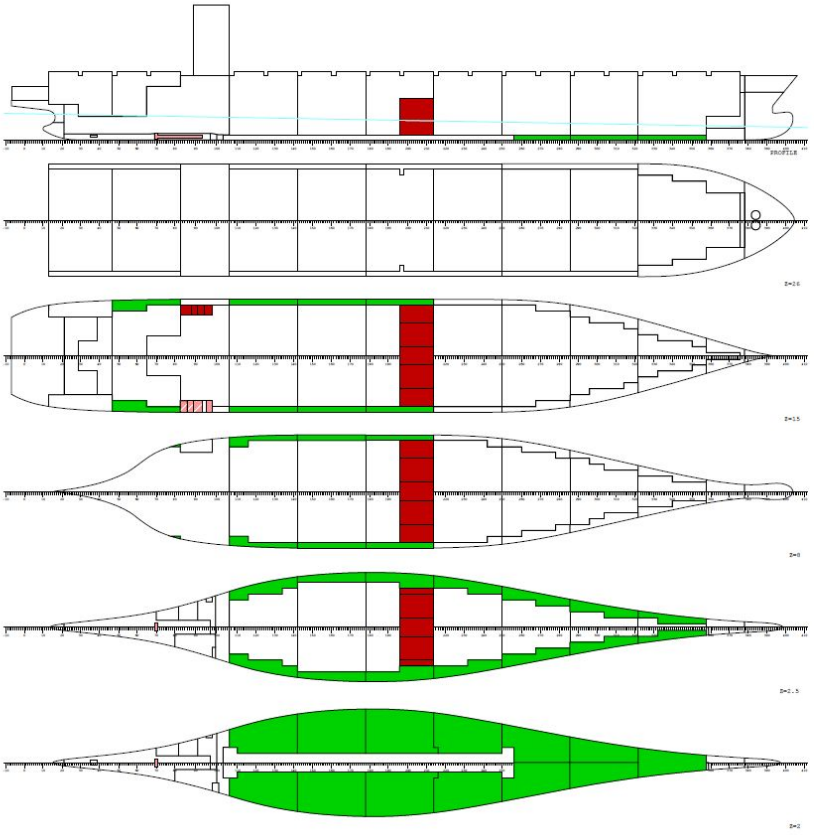

XFRAM m	#	BEND tm	REL %	BMMX tm	BMMN tm	RELSHREL t	%	SHMX t	SHMN t	TORS tm	REL %	TMMX tm	TMMN tm
10.40	13	15397	49.7	30997	-238	1746	43.4	4019	-528	855	3.8	22432	-22432
16.91	21	29199	48.5	60230	-490	2443	43.4	5633	-1088	812	3.6	22432	-22432
23.00	29	45606	47.8	95457	-725	2865	42.1	6813	-1613	765	3.4	22432	-22432
37.55	47	91715	44.5	206184	-1502	3235	37.4	8656	-2866	656	2.9	22432	-22432
52.10	65	139572	41.6	335725	-3008	3081	31.5	9786	-3919	550	2.5	22432	-22432
57.85	72	156731	40.4	387938	-3639	2884	29.5	9786	-4077	543	2.4	22432	-22432
66.65	83	184774	39.8	463885	-4605	3366	34.9	9646	-4077	334	1.5	22432	-22432
78.50	96	228402	41.3	552831	-5906	4220	46.4	9092	-4077	1554	6.9	22432	-22432
87.50	106	267266	43.8	610295	-6894	4552	50.7	8970	-4077	1491	6.6	22432	-22432
102.0	124	324550	49.0	662589	-8142	3045	35.8	8499	-4077	1410	6.3	22432	-22432
116.6	142	354718	53.5	662589	-8155	911	14.8	6167	-4077	1300	5.8	22432	-22432
131.1	160	352517	53.2	662589	-8155	-1241	30.4	4077	-4077	1188	5.3	22432	-22432
145.7	178	320438	48.4	662589	-8155	-3196	52.9	4077	-6038	1072	4.8	22432	-22432
160.2	196	261377	39.8	656706	-8155	-4950	78.3	4077	-6320	953	4.2	22432	-22432
174.8	214	245133	39.3	624486	-8111	2665	65.4	4077	-6365	831	3.7	22432	-22432
189.3	232	268029	46.3	578875	-7499	447	11.0	4077	-6465	728	3.2	22432	-22432
203.9	250	261437	51.0	512809	-6664	-1369	19.7	4077	-6962	646	2.9	22432	-22432
218.4	268	231939	54.4	426647	-5809	-2600	33.7	4077	-7705	564	2.5	22432	-22432
233.0	286	189916	58.6	323839	-4975	-3188	39.6	4077	-8053	483	2.2	22432	-22432
247.6	304	142798	64.8	220372	-4144	-3306	45.0	4077	-7355	403	1.8	22432	-22432
262.1	322	97097	74.2	130890	-3315	-3002	48.5	4077	-6195	323	1.4	22432	-22432
276.7	340	57421	80.5	71356	-2488	-2441	58.1	3732	-4199	243	1.1	22432	-22432
291.2	358	27955	76.2	36697	-1950	-1655	66.4	2480	-2493	164	0.7	22432	-22432
307.5	378	6955	74.2	9378	-1862	-848	79.1	1072	-1072	96	0.4	22432	-22432

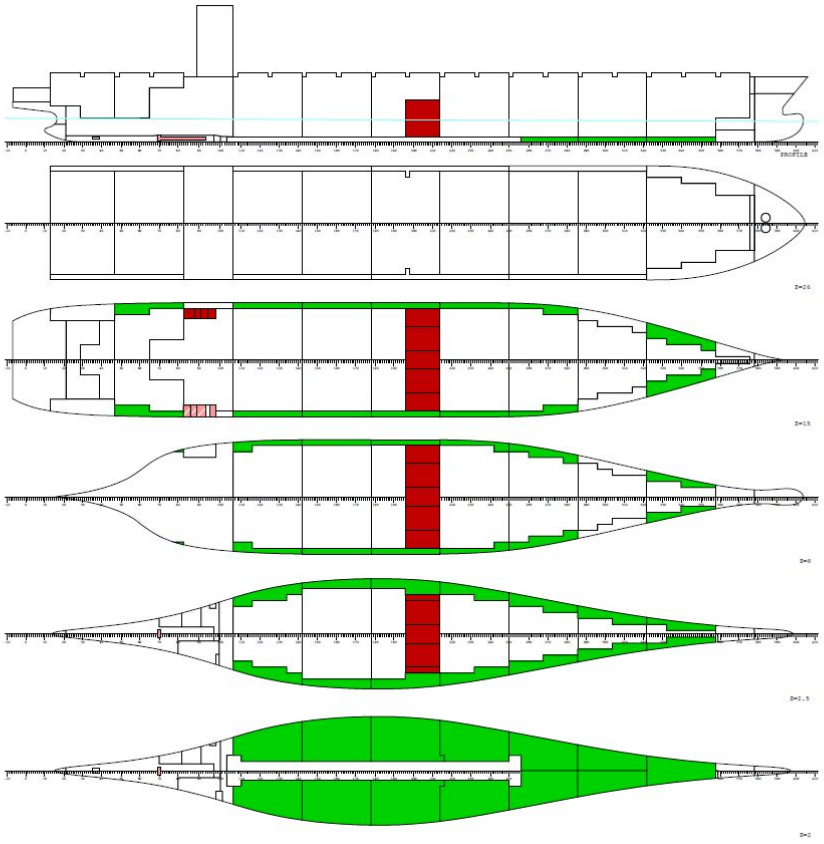

XFRAM m	#	BEND tm	REL %	BMMX tm	BMMN tm	RELSHREL t	%	SHMX t	SHMN t	TORS tm	REL %	TMMX tm	TMMN tm
10.40	13	15060	48.6	30997	-238	1747	43.5	4019	-528	855	3.8	22432	-22432
16.91	21	28729	47.7	60230	-490	2447	43.4	5633	-1088	812	3.6	22432	-22432
23.00	29	45069	47.2	95457	-725	2885	42.4	6813	-1613	765	3.4	22432	-22432
37.55	47	91987	44.6	206184	-1502	3409	39.4	8656	-2866	656	2.9	22432	-22432
52.10	65	144480	43.0	335725	-3008	3596	36.7	9786	-3919	550	2.5	22432	-22432
57.85	72	164850	42.5	387938	-3639	3528	36.0	9786	-4077	543	2.4	22432	-22432
66.65	83	199128	42.9	463885	-4605	4178	43.3	9646	-4077	334	1.5	22432	-22432
78.50	96	253137	45.8	552831	-5906	5191	57.1	9092	-4077	1553	6.9	22432	-22432
87.50	106	300856	49.3	610295	-6894	5585	62.3	8970	-4077	1491	6.6	22432	-22432
102.0	124	372945	56.3	662589	-8142	4067	47.9	8499	-4077	1410	6.3	22432	-22432
116.6	142	416720	62.9	662589	-8155	1780	28.9	6167	-4077	1300	5.8	22432	-22432
131.1	160	424859	64.1	662589	-8155	-668	16.4	4077	-4077	1188	5.3	22432	-22432
145.7	178	397785	60.0	662589	-8155	-3060	50.7	4077	-6038	1072	4.8	22432	-22432
160.2	196	336325	51.2	656706	-8155	-5394	85.3	4077	-6320	953	4.2	22432	-22432
174.8	214	308077	49.3	624486	-8111	1500	36.8	4077	-6365	831	3.7	22432	-22432
189.3	232	315373	54.5	578875	-7499	-477	7.4	4077	-6465	728	3.2	22432	-22432
203.9	250	296504	57.8	512809	-6664	-2051	29.5	4077	-6962	646	2.9	22432	-22432
218.4	268	259494	60.8	426647	-5809	-2905	37.7	4077	-7705	564	2.5	22432	-22432
233.0	286	215448	66.5	323839	-4975	-3067	38.1	4077	-8053	483	2.2	22432	-22432
247.6	304	162735	73.8	220372	-4144	-4135	56.2	4077	-7355	403	1.8	22432	-22432
262.1	322	98496	75.3	130890	-3315	-4653	75.1	4077	-6195	323	1.4	22432	-22432
276.7	340	43041	60.3	71356	-2488	-2916	69.4	3732	-4199	243	1.1	22432	-22432
291.2	358	16258	44.3	36697	-1950	-920	36.9	2480	-2493	164	0.7	22432	-22432
307.5	378	3767	40.2	9378	-1862	-473	44.1	1072	-1072	96	0.4	22432	-22432

LOAD: BLM-PANAMA : BALLAST AFT. MID.-PANAMA

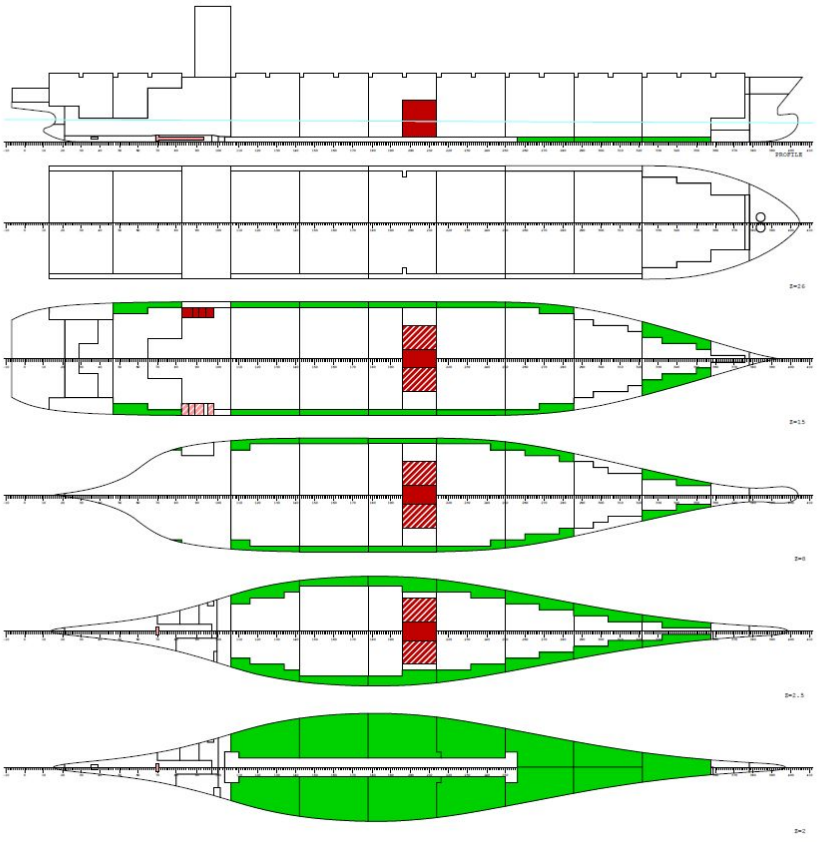

XFRAM m	#	BEND tm	REL %	BMMX tm	BMMN tm	RELSHREL t	%	SHMX t	SHMN t	TORS tm	REL %	TMMX tm	TMMN tm
10.40	13	15068	48.6	30997	-238	1747	43.5	4019	-528	610	2.7	22432	-22432
16.91	21	28743	47.7	60230	-490	2449	43.5	5633	-1088	466	2.1	22432	-22432
23.00	29	45112	47.3	95457	-725	2894	42.5	6813	-1613	326	1.5	22432	-22432
37.55	47	92493	44.9	206184	-1502	3479	40.2	8656	-2866	-8	0.0	22432	-22432
52.10	65	147372	43.9	335725	-3008	3878	39.6	9786	-3919	-337	1.5	22432	-22432
57.85	72	169687	43.7	387938	-3639	3922	40.1	9786	-4077	-433	1.9	22432	-22432
66.65	83	208239	44.9	463885	-4605	4758	49.3	9646	-4077	-778	3.5	22432	-22432
78.50	96	269401	48.7	552831	-5906	5836	64.2	9092	-4077	4472	19.9	22432	-22432
87.50	106	322479	52.8	610295	-6894	6002	66.9	8970	-4077	5250	23.4	22432	-22432
102.0	124	403151	60.8	662589	-8142	4831	56.8	8499	-4077	4944	22.0	22432	-22432
116.6	142	460611	69.5	662589	-8155	2897	47.0	6167	-4077	4611	20.6	22432	-22432
131.1	160	487599	73.6	662589	-8155	806	19.8	4077	-4077	4274	19.1	22432	-22432
145.7	178	484580	73.1	662589	-8155	-1227	20.3	4077	-6038	3934	17.5	22432	-22432
160.2	196	452419	68.9	656706	-8155	-3200	50.6	4077	-6320	3591	16.0	22432	-22432
174.8	214	423884	67.9	624486	-8111	-732	11.5	4077	-6365	3245	14.5	22432	-22432
189.3	232	401369	69.3	578875	-7499	-2343	36.2	4077	-6465	2918	13.0	22432	-22432
203.9	250	357977	69.8	512809	-6664	-3558	51.1	4077	-6962	2611	11.6	22432	-22432
218.4	268	301555	70.7	426647	-5809	-4071	52.8	4077	-7705	2306	10.3	22432	-22432
233.0	286	242809	75.0	323839	-4975	-3929	48.8	4077	-8053	2001	8.9	22432	-22432
247.6	304	179505	81.5	220372	-4144	-4738	64.4	4077	-7355	1696	7.6	22432	-22432
262.1	322	108065	82.6	130890	-3315	-5049	81.5	4077	-6195	1392	6.2	22432	-22432
276.7	340	48038	67.3	71356	-2488	-3157	75.2	3732	-4199	1088	4.8	22432	-22432
291.2	358	18562	50.6	36697	-1950	-1057	42.4	2480	-2493	785	3.5	22432	-22432
307.5	378	4454	47.5	9378	-1862	-541	50.4	1072	-1072	465	2.1	22432	-22432

LOAD: BLA-PANAMA : BALLAST ARR.-PANAMA

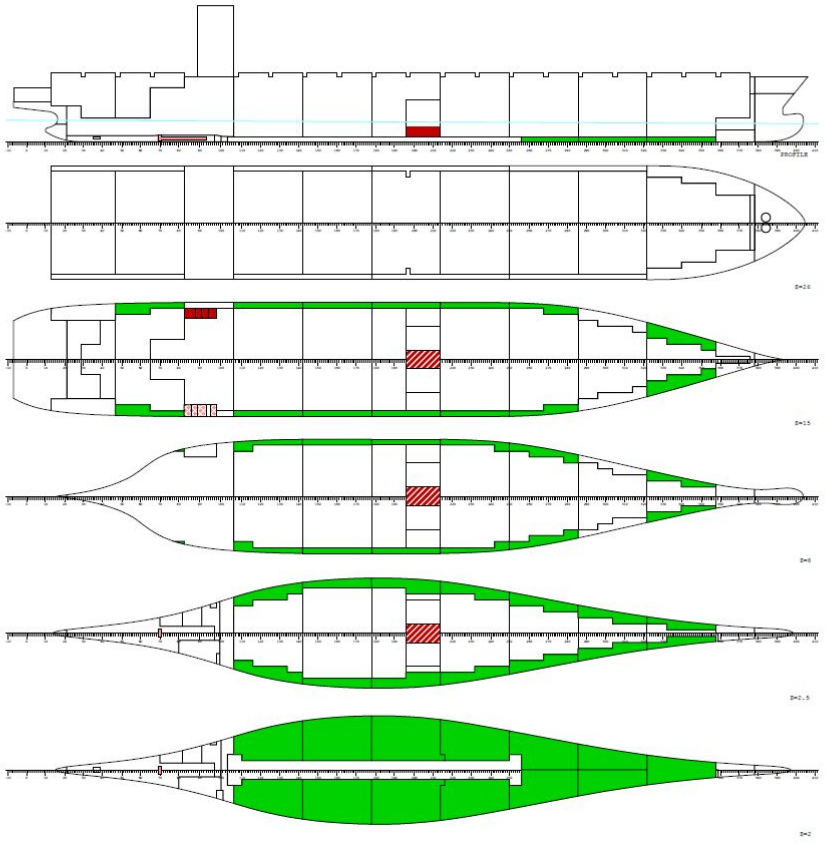

XFRAM m	#	BEND tm	REL %	BMMX tm	BMMN tm	RELSHREL t	%	SHMX t	SHMN t	TORS tm	REL %	TMMX tm	TMMN tm
10.40	13	15076	48.6	30997	-238	1748	43.5	4019	-528	415	1.9	22432	-22432
16.91	21	28755	47.7	60230	-490	2450	43.5	5633	-1088	192	0.9	22432	-22432
23.00	29	45146	47.3	95457	-725	2900	42.6	6813	-1613	-23	0.1	22432	-22432
37.55	47	92888	45.1	206184	-1502	3532	40.8	8656	-2866	-535	2.4	22432	-22432
52.10	65	149499	44.5	335725	-3008	4085	41.7	9786	-3919	-1043	4.6	22432	-22432
57.85	72	173262	44.7	387938	-3639	4219	43.1	9786	-4077	-1208	5.4	22432	-22432
66.65	83	215085	46.4	463885	-4605	5206	54.0	9646	-4077	-1661	7.4	22432	-22432
78.50	96	281816	51.0	552831	-5906	6345	69.8	9092	-4077	6644	29.6	22432	-22432
87.50	106	339256	55.6	610295	-6894	6313	70.4	8970	-4077	8237	36.7	22432	-22432
102.0	124	426546	64.4	662589	-8142	5430	63.9	8499	-4077	7753	34.6	22432	-22432
116.6	142	494858	74.7	662589	-8155	3789	61.4	6167	-4077	7242	32.3	22432	-22432
131.1	160	536982	81.0	662589	-8155	1993	48.9	4077	-4077	6727	30.0	22432	-22432
145.7	178	553402	83.5	662589	-8155	257	6.3	4077	-6038	6209	27.7	22432	-22432
160.2	196	545005	83.0	656706	-8155	-1418	22.4	4077	-6320	5688	25.4	22432	-22432
174.8	214	516369	82.7	624486	-8111	-2526	39.7	4077	-6365	5164	23.0	22432	-22432
189.3	232	469941	81.2	578875	-7499	-3838	59.4	4077	-6465	4658	20.8	22432	-22432
203.9	250	406950	79.4	512809	-6664	-4760	68.4	4077	-6962	4174	18.6	22432	-22432
218.4	268	335064	78.5	426647	-5809	-4999	64.9	4077	-7705	3690	16.4	22432	-22432
233.0	286	264632	81.7	323839	-4975	-4613	57.3	4077	-8053	3207	14.3	22432	-22432
247.6	304	192915	87.5	220372	-4144	-5217	70.9	4077	-7355	2724	12.1	22432	-22432
262.1	322	115749	88.4	130890	-3315	-5365	86.6	4077	-6195	2241	10.0	22432	-22432
276.7	340	52070	73.0	71356	-2488	-3351	79.8	3732	-4199	1759	7.8	22432	-22432
291.2	358	20426	55.7	36697	-1950	-1168	46.8	2480	-2493	1278	5.7	22432	-22432
307.5	378	5004	53.4	9378	-1862	-596	55.6	1072	-1072	758	3.4	22432	-22432

LOAD: 16TDD : 16T/TEU DEP. AT DESIGN DRAFT

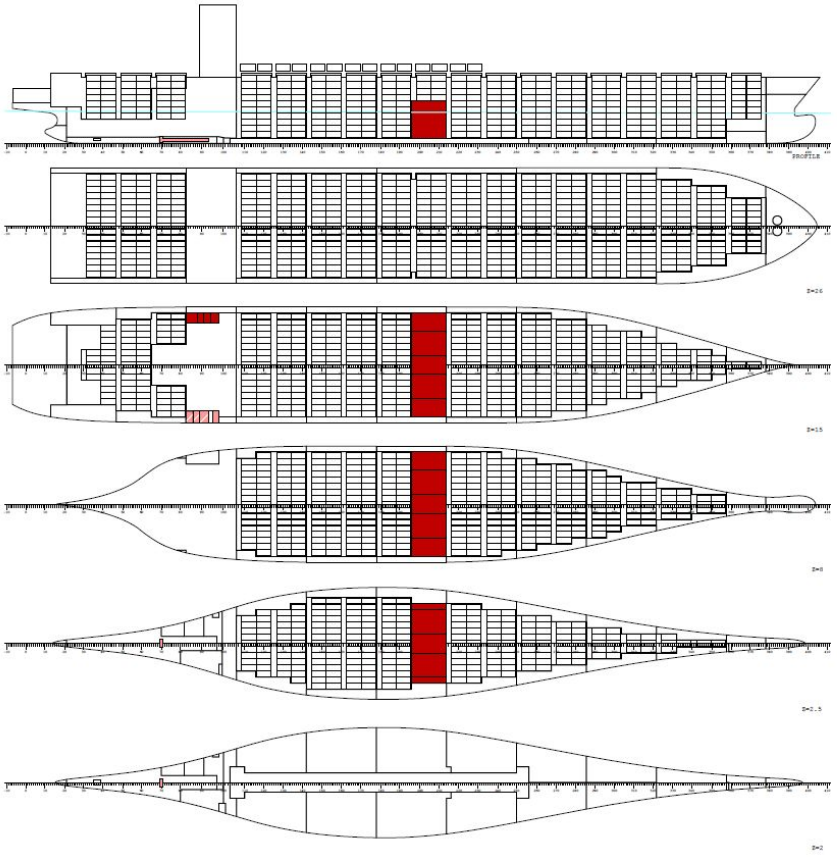

XFRAM m	#	BEND tm	REL %	BMMX tm	BMMN tm	RELSHREL t	%	SHMX t	SHMN t	TORS tm	REL %	TMMX tm	TMMN tm
10.40	13	15023	48.5	30997	-238	1730	43.0	4019	-528	886	4.0	22432	-22432
16.91	21	28266	46.9	60230	-490	2306	40.9	5633	-1088	857	3.8	22432	-22432
23.00	29	42977	45.0	95457	-725	2460	36.1	6813	-1613	822	3.7	22432	-22432
37.55	47	93406	45.3	206184	-1502	4622	53.4	8656	-2866	742	3.3	22432	-22432
52.10	65	164204	48.9	335725	-3008	5282	54.0	9786	-3919	665	3.0	22432	-22432
57.85	72	192176	49.5	387938	-3639	4762	48.7	9786	-4077	670	3.0	22432	-22432
66.65	83	236881	51.1	463885	-4605	5253	54.5	9646	-4077	478	2.1	22432	-22432
78.50	96	291713	52.8	552831	-5906	4244	46.7	9092	-4077	1720	7.7	22432	-22432
87.50	106	323888	53.1	610295	-6894	3073	34.3	8970	-4077	1677	7.5	22432	-22432
102.0	124	359008	54.2	662589	-8142	2290	26.9	8499	-4077	1625	7.2	22432	-22432
116.6	142	377799	57.0	662589	-8155	1005	16.3	6167	-4077	1544	6.9	22432	-22432
131.1	160	376631	56.8	662589	-8155	-432	10.6	4077	-4077	1461	6.5	22432	-22432
145.7	178	353542	53.4	662589	-8155	-1984	32.9	4077	-6038	1374	6.1	22432	-22432
160.2	196	307820	46.9	656706	-8155	-3522	55.7	4077	-6320	1284	5.7	22432	-22432
174.8	214	286722	45.9	624486	-8111	993	24.4	4077	-6365	1192	5.3	22432	-22432
189.3	232	286627	49.5	578875	-7499	-237	3.7	4077	-6465	465	2.1	22432	-22432
203.9	250	266866	52.0	512809	-6664	-1751	25.1	4077	-6962	391	1.7	22432	-22432
218.4	268	228118	53.5	426647	-5809	-2836	36.8	4077	-7705	338	1.5	22432	-22432
233.0	286	178083	55.0	323839	-4975	-3341	41.5	4077	-8053	286	1.3	22432	-22432
247.6	304	124919	56.7	220372	-4144	-3319	45.1	4077	-7355	235	1.0	22432	-22432
262.1	322	76009	58.1	130890	-3315	-2826	45.6	4077	-6195	184	0.8	22432	-22432
276.7	340	37559	52.6	71356	-2488	-2034	48.4	3732	-4199	133	0.6	22432	-22432
291.2	358	12506	34.1	36697	-1950	-1081	43.4	2480	-2493	83	0.4	22432	-22432
307.5	378	778	8.3	9378	-1862	-177	16.5	1072	-1072	48	0.2	22432	-22432

LOAD: 16TAD : 16T/TEU ARR. AT DESIGN DRAFT

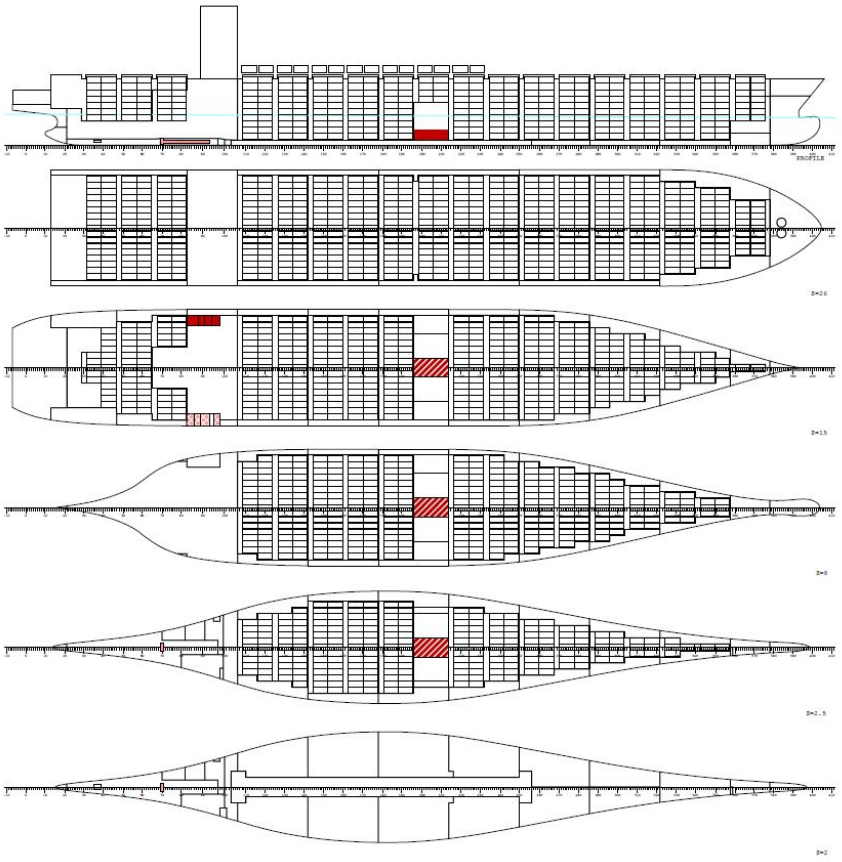

XFRAM m	#	BEND tm	REL %	BMMX tm	BMMN tm	RELSHREL t	%	SHMX t	SHMN t	TORS tm	REL %	TMMX tm	TMMN tm
10.40	13	15147	48.9	30997	-238	1745	43.4	4019	-528	447	2.0	22432	-22432
16.91	21	28797	47.8	60230	-490	2413	42.8	5633	-1088	237	1.1	22432	-22432
23.00	29	44567	46.7	95457	-725	2692	39.5	6813	-1613	34	0.2	22432	-22432
37.55	47	101008	49.0	206184	-1502	5216	60.3	8656	-2866	-449	2.0	22432	-22432
52.10	65	183507	54.7	335725	-3008	6290	64.3	9786	-3919	-928	4.1	22432	-22432
57.85	72	217813	56.1	387938	-3639	5944	60.7	9786	-4077	-1082	4.8	22432	-22432
66.65	83	274158	59.1	463885	-4605	6708	69.5	9646	-4077	-1517	6.8	22432	-22432
78.50	96	346265	62.6	552831	-5906	5725	63.0	9092	-4077	6811	30.4	22432	-22432
87.50	106	390803	64.0	610295	-6894	4049	45.1	8970	-4077	8423	37.6	22432	-22432
102.0	124	443864	67.0	662589	-8142	3771	44.4	8499	-4077	7968	35.5	22432	-22432
116.6	142	488104	73.7	662589	-8155	3013	48.9	6167	-4077	7486	33.4	22432	-22432
131.1	160	520186	78.5	662589	-8155	2122	52.1	4077	-4077	7000	31.2	22432	-22432
145.7	178	538447	81.3	662589	-8155	1136	27.9	4077	-6038	6511	29.0	22432	-22432
160.2	196	542471	82.6	656706	-8155	186	4.6	4077	-6320	6019	26.8	22432	-22432
174.8	214	516752	82.7	624486	-8111	-3357	52.7	4077	-6365	5524	24.6	22432	-22432
189.3	232	457997	79.1	578875	-7499	-3959	61.2	4077	-6465	4395	19.6	22432	-22432
203.9	250	388843	75.8	512809	-6664	-4829	69.4	4077	-6962	3919	17.5	22432	-22432
218.4	268	310114	72.7	426647	-5809	-5268	68.4	4077	-7705	3464	15.4	22432	-22432
233.0	286	229333	70.8	323839	-4975	-5155	64.0	4077	-8053	3010	13.4	22432	-22432
247.6	304	154014	69.9	220372	-4144	-4576	62.2	4077	-7355	2556	11.4	22432	-22432
262.1	322	90416	69.1	130890	-3315	-3617	58.4	4077	-6195	2103	9.4	22432	-22432
276.7	340	43307	60.7	71356	-2488	-2464	58.7	3732	-4199	1650	7.4	22432	-22432
291.2	358	14040	38.3	36697	-1950	-1262	50.6	2480	-2493	1197	5.3	22432	-22432
307.5	378	844	9.0	9378	-1862	-211	19.7	1072	-1072	711	3.2	22432	-22432

LOAD: 11TDS : 11T/TEU DEP. AT SCANTLING DRAFT

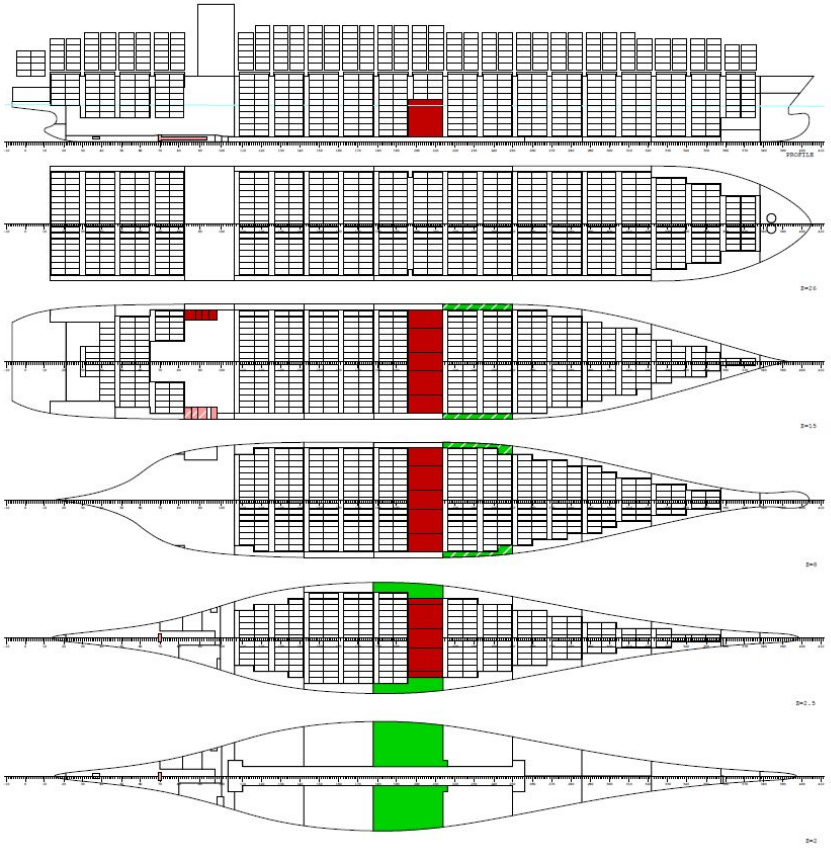

XFRAM m	#	BEND tm	REL %	BMMX tm	BMMN tm	RELSH t	REL %	SHMX t	SHMN t	TORS tm	REL %	TMMX tm	TMMN tm
10.40	13	22056	71.2	30997	-238	2448	60.9	4019	-528	965	4.3	22432	-22432
16.91	21	44794	74.4	60230	-490	4402	78.2	5633	-1088	967	4.3	22432	-22432
23.00	29	76333	80.0	95457	-725	5883	86.3	6813	-1613	962	4.3	22432	-22432
37.55	47	176614	85.7	206184	-1502	8140	94.0	8656	-2866	954	4.3	22432	-22432
52.10	65	297518	88.6	335725	-3008	8738	89.3	9786	-3919	949	4.2	22432	-22432
57.85	72	345123	89.0	387938	-3639	8240	84.2	9786	-4077	982	4.4	22432	-22432
66.65	83	420689	90.7	463885	-4605	8869	91.9	9646	-4077	834	3.7	22432	-22432
78.50	96	511468	92.5	552831	-5906	6643	73.1	9092	-4077	2134	9.5	22432	-22432
87.50	106	560976	91.9	610295	-6894	4513	50.3	8970	-4077	2136	9.5	22432	-22432
102.0	124	608199	91.8	662589	-8142	2562	30.1	8499	-4077	3341	14.9	22432	-22432
116.6	142	623980	94.2	662589	-8155	337	5.5	6167	-4077	4325	19.3	22432	-22432
131.1	160	606339	91.5	662589	-8155	-2029	49.8	4077	-4077	4313	19.2	22432	-22432
145.7	178	553223	83.5	662589	-8155	-4516	74.8	4077	-6038	4298	19.2	22432	-22432
160.2	196	474618	72.3	656706	-8155	-5518	87.3	4077	-6320	4280	19.1	22432	-22432
174.8	214	434585	69.6	624486	-8111	492	12.1	4077	-6365	4259	19.0	22432	-22432
189.3	232	424146	73.3	578875	-7499	-1166	18.0	4077	-6465	1998	8.9	22432	-22432
203.9	250	392095	76.5	512809	-6664	-2410	34.6	4077	-6962	-238	1.1	22432	-22432
218.4	268	339115	79.5	426647	-5809	-4076	52.9	4077	-7705	-219	1.0	22432	-22432
233.0	286	267468	82.6	323839	-4975	-4982	61.9	4077	-8053	-199	0.9	22432	-22432
247.6	304	188881	85.7	220372	-4144	-5049	68.6	4077	-7355	-179	0.8	22432	-22432
262.1	322	115413	88.2	130890	-3315	-4438	71.6	4077	-6195	-158	0.7	22432	-22432
276.7	340	55156	77.3	71356	-2488	-3260	77.6	3732	-4199	-137	0.6	22432	-22432
291.2	358	16036	43.7	36697	-1950	-1631	65.4	2480	-2493	-115	0.5	22432	-22432
307.5	378	366	3.9	9378	-1862	-113	10.5	1072	-1072	-70	0.3	22432	-22432

LOAD: 11TAS : 11T/TEU ARR. AT SCANTLING DRAFT

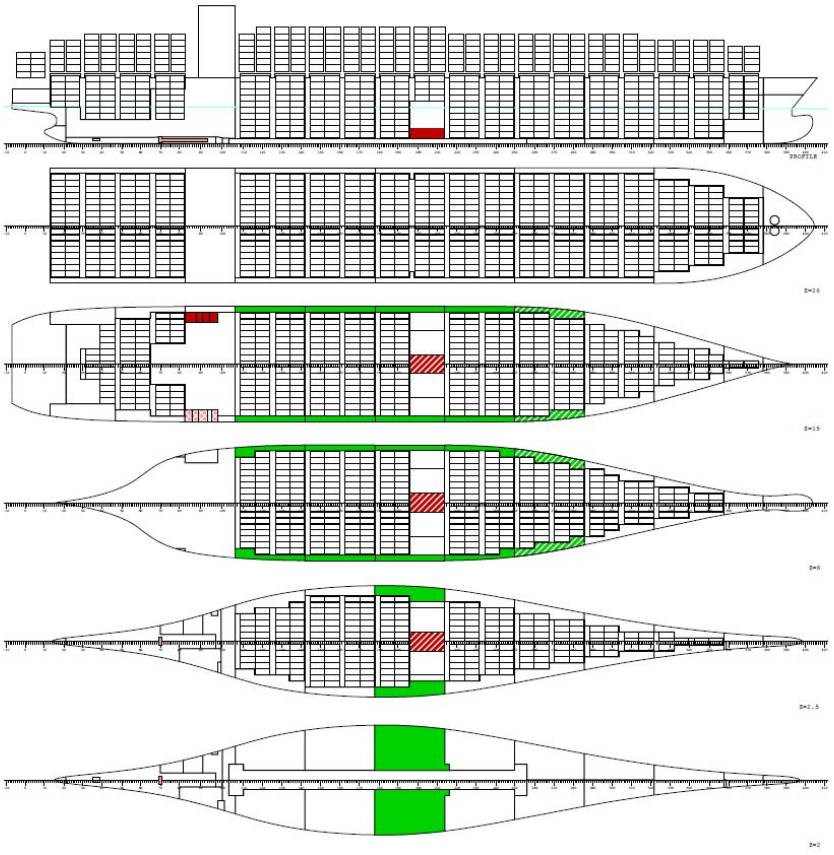

XFRAM m	#	BEND tm	REL %	BMMX tm	BMMN tm	RELSHR t	REL %	SHMX t	SHMN t	TORS tm	REL %	TMMX tm	TMMN tm
10.40	13	21836	70.4	30997	-238	2405	59.8	4019	-528	856	3.8	22432	-22432
16.91	21	44303	73.6	60230	-490	4345	77.1	5633	-1088	813	3.6	22432	-22432
23.00	29	75511	79.1	95457	-725	5815	85.4	6813	-1613	767	3.4	22432	-22432
37.55	47	174785	84.8	206184	-1502	8055	93.1	8656	-2866	659	2.9	22432	-22432
52.10	65	294538	87.7	335725	-3008	8650	88.4	9786	-3919	554	2.5	22432	-22432
57.85	72	341693	88.1	387938	-3639	8155	83.3	9786	-4077	548	2.4	22432	-22432
66.65	83	416620	89.8	463885	-4605	8793	91.2	9646	-4077	339	1.5	22432	-22432
78.50	96	504405	91.2	552831	-5906	6229	68.5	9092	-4077	8972	40.0	22432	-22432
87.50	106	547978	89.8	610295	-6894	3313	36.9	8970	-4077	10815	48.2	22432	-22432
102.0	124	588181	88.8	662589	-8142	2716	32.0	8499	-4077	11922	53.1	22432	-22432
116.6	142	614239	92.7	662589	-8155	1478	24.0	6167	-4077	12805	57.1	22432	-22432
131.1	160	621530	93.8	662589	-8155	247	6.1	4077	-4077	12694	56.6	22432	-22432
145.7	178	610066	92.1	662589	-8155	-1080	17.9	4077	-6038	12579	56.1	22432	-22432
160.2	196	590116	89.9	656706	-8155	-906	14.3	4077	-6320	12461	55.6	22432	-22432
174.8	214	562867	90.1	624486	-8111	-2378	37.4	4077	-6365	12341	55.0	22432	-22432
189.3	232	513544	88.7	578875	-7499	-3655	56.5	4077	-6465	12238	54.6	22432	-22432
203.9	250	448269	87.4	512809	-6664	-4502	64.7	4077	-6962	12157	54.2	22432	-22432
218.4	268	370408	86.8	426647	-5809	-5401	70.1	4077	-7705	5747	25.6	22432	-22432
233.0	286	284754	87.9	323839	-4975	-5576	69.2	4077	-8053	476	2.1	22432	-22432
247.6	304	198834	90.2	220372	-4144	-5481	74.5	4077	-7355	397	1.8	22432	-22432
262.1	322	120301	91.9	130890	-3315	-4722	76.2	4077	-6195	317	1.4	22432	-22432
276.7	340	56963	79.8	71356	-2488	-3421	81.5	3732	-4199	239	1.1	22432	-22432
291.2	358	16335	44.5	36697	-1950	-1700	68.2	2480	-2493	161	0.7	22432	-22432
307.5	378	212	2.3	9378	-1862	-124	11.6	1072	-1072	95	0.4	22432	-22432

LOAD: 16TDS : 16T/TEU DEP. AT SCANTLING DRAFT

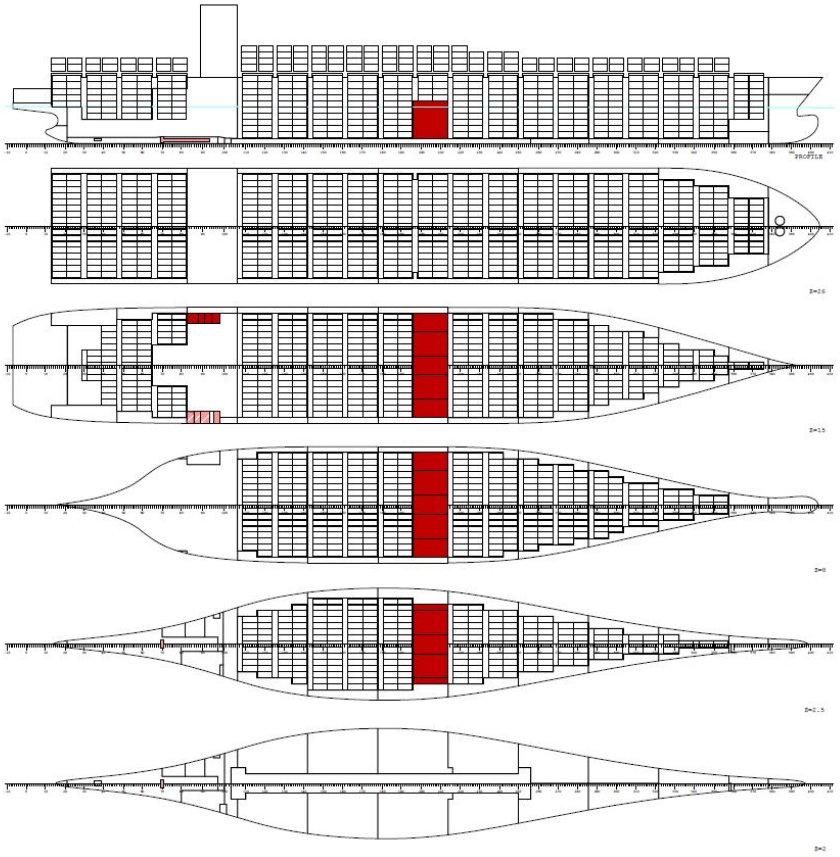

XFRAM m	#	BEND tm	REL %	BMMX tm	BMMN tm	RELSHEAR t	REL %	SHMX t	SHMN t	TORS tm	REL %	TMMX tm	TMMN tm
10.40	13	8886	28.7	30997	-238	821	20.4	4019	-528	911	4.1	22432	-22432
16.91	21	20881	34.7	60230	-490	2785	49.4	5633	-1088	891	4.0	22432	-22432
23.00	29	42604	44.6	95457	-725	4252	62.4	6813	-1613	866	3.9	22432	-22432
37.55	47	116751	56.6	206184	-1502	6196	71.6	8656	-2866	807	3.6	22432	-22432
52.10	65	207645	61.8	335725	-3008	6582	67.3	9786	-3919	753	3.4	22432	-22432
57.85	72	242309	62.5	387938	-3639	5885	60.1	9786	-4077	767	3.4	22432	-22432
66.65	83	296204	63.9	463885	-4605	6250	64.8	9646	-4077	588	2.6	22432	-22432
78.50	96	355714	64.3	552831	-5906	4009	44.1	9092	-4077	1849	8.2	22432	-22432
87.50	106	381516	62.5	610295	-6894	1884	21.0	8970	-4077	1819	8.1	22432	-22432
102.0	124	399611	60.3	662589	-8142	1346	15.8	8499	-4077	1789	8.0	22432	-22432
116.6	142	405310	61.2	662589	-8155	328	5.3	6167	-4077	1731	7.7	22432	-22432
131.1	160	394870	59.6	662589	-8155	-850	20.9	4077	-4077	1669	7.4	22432	-22432
145.7	178	366217	55.3	662589	-8155	-2152	35.6	4077	-6038	1605	7.2	22432	-22432
160.2	196	318526	48.5	656706	-8155	-3447	54.5	4077	-6320	1538	6.9	22432	-22432
174.8	214	298932	47.9	624486	-8111	1304	32.0	4077	-6365	1467	6.5	22432	-22432
189.3	232	302943	52.3	578875	-7499	38	0.9	4077	-6465	1415	6.3	22432	-22432
203.9	250	286688	55.9	512809	-6664	-1493	21.4	4077	-6962	233	1.0	22432	-22432
218.4	268	248170	58.2	426647	-5809	-2938	38.1	4077	-7705	166	0.7	22432	-22432
233.0	286	193597	59.8	323839	-4975	-3726	46.3	4077	-8053	136	0.6	22432	-22432
247.6	304	132788	60.3	220372	-4144	-3836	52.2	4077	-7355	107	0.5	22432	-22432
262.1	322	75845	57.9	130890	-3315	-3255	52.5	4077	-6195	78	0.3	22432	-22432
276.7	340	32466	45.5	71356	-2488	-2120	50.5	3732	-4199	49	0.2	22432	-22432
291.2	358	8618	23.5	36697	-1950	-681	27.3	2480	-2493	22	0.1	22432	-22432
307.5	378	429	4.6	9378	-1862	-112	10.4	1072	-1072	12	0.1	22432	-22432

LOAD: 16TAS : 16T/TEU ARR. AT SCANTLING DRAFT

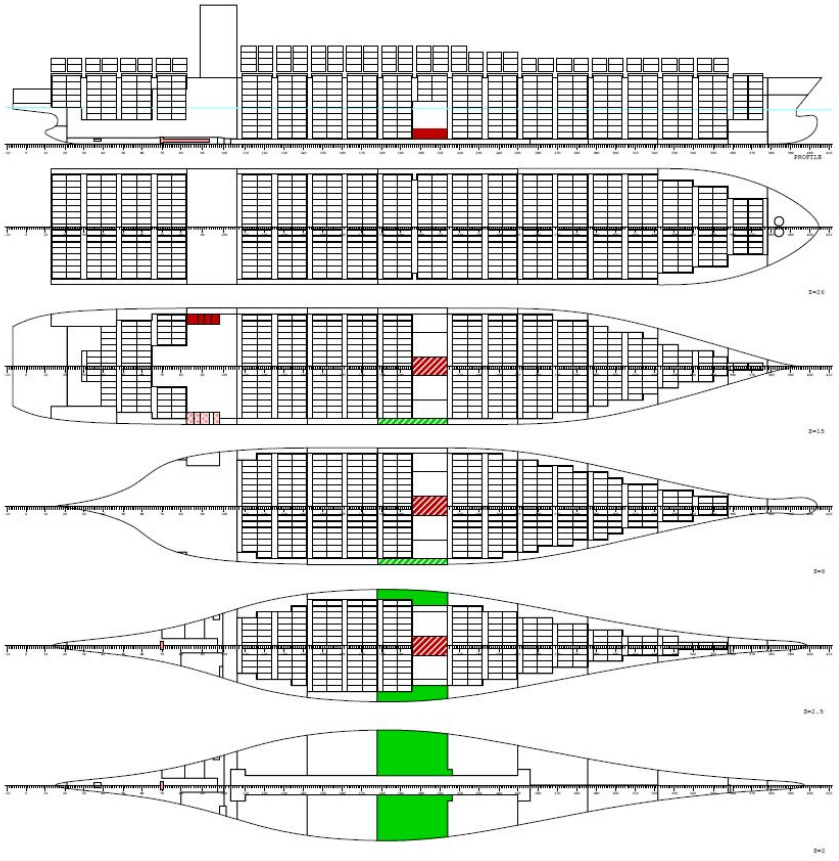

XFRAM		BEND	REL	BMMX	BMMN	RELSHREL		SHMX	SHMN	TORS	REL	TMMX	TMMN
m	#	tm	%	tm	tm	t	%	t	t	tm	%	tm	tm
10.40	13	10471	33.8	30997	-238	1015	25.3	4019	-528	933	4.2	22432	-22432
16.91	21	24070	40.0	60230	-490	3071	54.5	5633	-1088	922	4.1	22432	-22432
23.00	29	47845	50.1	95457	-725	4627	67.9	6813	-1613	905	4.0	22432	-22432
37.55	47	129212	62.7	206184	-1502	6802	78.6	8656	-2866	867	3.9	22432	-22432
52.10	65	230812	68.8	335725	-3008	7437	76.0	9786	-3919	833	3.7	22432	-22432
57.85	72	270730	69.8	387938	-3639	6843	69.9	9786	-4077	855	3.8	22432	-22432
66.65	83	333818	72.0	463885	-4605	7370	76.4	9646	-4077	689	3.1	22432	-22432
78.50	96	405720	73.4	552831	-5906	5000	55.0	9092	-4077	9379	41.8	22432	-22432
87.50	106	438915	71.9	610295	-6894	2245	25.0	8970	-4077	11266	50.2	22432	-22432
102.0	124	464538	70.1	662589	-8142	2009	23.6	8499	-4077	11256	50.2	22432	-22432
116.6	142	482256	72.8	662589	-8155	1307	21.2	6167	-4077	11219	50.0	22432	-22432
131.1	160	488538	73.7	662589	-8155	459	11.3	4077	-4077	11178	49.8	22432	-22432
145.7	178	481522	72.7	662589	-8155	-498	8.2	4077	-6038	11134	49.6	22432	-22432
160.2	196	472955	72.0	656706	-8155	260	6.4	4077	-6320	6135	27.3	22432	-22432
174.8	214	459274	73.5	624486	-8111	-1629	25.6	4077	-6365	1248	5.6	22432	-22432
189.3	232	423815	73.2	578875	-7499	-2484	38.4	4077	-6465	1216	5.4	22432	-22432
203.9	250	373872	72.9	512809	-6664	-3613	51.9	4077	-6962	55	0.2	22432	-22432
218.4	268	307598	72.1	426647	-5809	-4647	60.3	4077	-7705	8	0.0	22432	-22432
233.0	286	231231	71.4	323839	-4975	-5029	62.4	4077	-8053	-2	0.0	22432	-22432
247.6	304	154363	70.0	220372	-4144	-4760	64.7	4077	-7355	-11	0.0	22432	-22432
262.1	322	86548	66.1	130890	-3315	-3848	62.1	4077	-6195	-19	0.1	22432	-22432
276.7	340	36649	51.4	71356	-2488	-2448	58.3	3732	-4199	-27	0.1	22432	-22432
291.2	358	9609	26.2	36697	-1950	-818	32.8	2480	-2493	-35	0.2	22432	-22432
307.5	378	371	4.0	9378	-1862	-134	12.5	1072	-1072	-22	0.1	22432	-22432

LOAD: MAX : HOMOGENEOUS 14T TEU AT 15.2m DRAFT

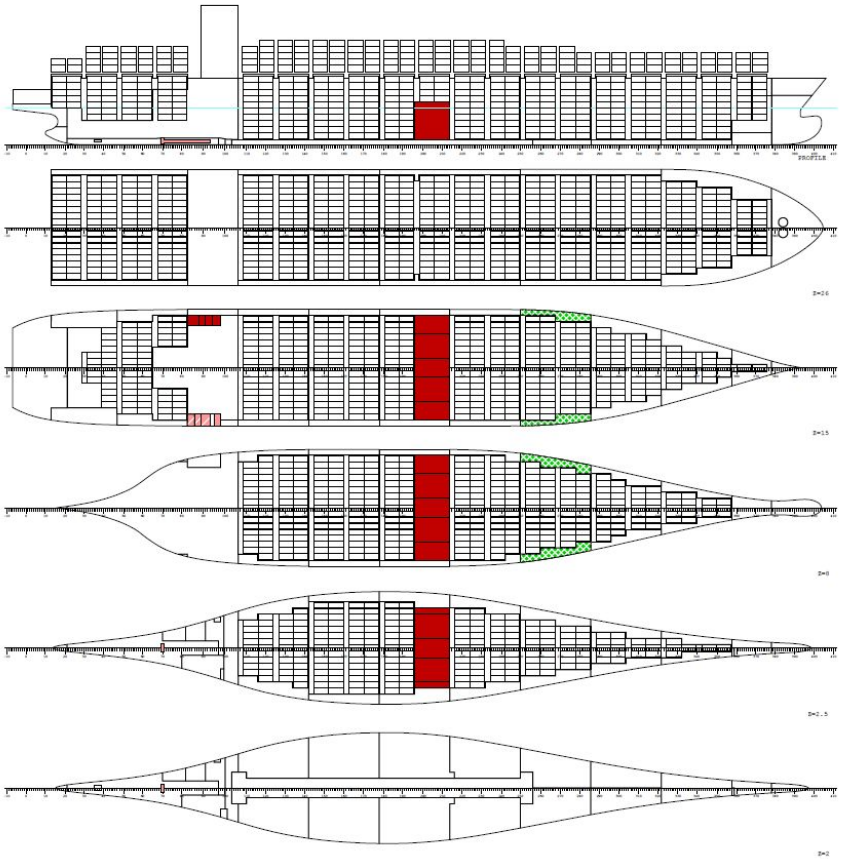

XFRAM		BEND	REL	BMMX	BMMN	RELSHREL		SHMX	SHMN	TORS	REL	TMMX	TMMN
m	#	tm	%	tm	tm	t	%	t	t	tm	%	tm	tm
10.40	13	9832	31.7	30997	-238	954	23.7	4019	-528	915	4.1	22432	-22432
16.91	21	22020	36.6	60230	-490	2730	48.5	5633	-1088	896	4.0	22432	-22432
23.00	29	42791	44.8	95457	-725	4012	58.9	6813	-1613	873	3.9	22432	-22432
37.55	47	117529	57.0	206184	-1502	6580	76.0	8656	-2866	818	3.6	22432	-22432
52.10	65	217918	64.9	335725	-3008	7549	77.1	9786	-3919	768	3.4	22432	-22432
57.85	72	258711	66.7	387938	-3639	7104	72.6	9786	-4077	783	3.5	22432	-22432
66.65	83	324947	70.0	463885	-4605	7885	81.7	9646	-4077	606	2.7	22432	-22432
78.50	96	404248	73.1	552831	-5906	5715	62.9	9092	-4077	1870	8.3	22432	-22432
87.50	106	445494	73.0	610295	-6894	3625	40.4	8970	-4077	1843	8.2	22432	-22432
102.0	124	484032	73.1	662589	-8142	2455	28.9	8499	-4077	1816	8.1	22432	-22432
116.6	142	503369	76.0	662589	-8155	1039	16.8	6167	-4077	1762	7.9	22432	-22432
131.1	160	500530	75.5	662589	-8155	-570	14.0	4077	-4077	1704	7.6	22432	-22432
145.7	178	473101	71.4	662589	-8155	-2318	38.4	4077	-6038	1643	7.3	22432	-22432
160.2	196	420028	64.0	656706	-8155	-4074	64.5	4077	-6320	1579	7.0	22432	-22432
174.8	214	390720	62.6	624486	-8111	599	14.7	4077	-6365	1512	6.7	22432	-22432
189.3	232	382194	66.0	578875	-7499	-854	13.2	4077	-6465	1464	6.5	22432	-22432
203.9	250	353710	69.0	512809	-6664	-2280	32.8	4077	-6962	1437	6.4	22432	-22432
218.4	268	305605	71.6	426647	-5809	-3433	44.6	4077	-7705	1856	8.3	22432	-22432
233.0	286	245086	75.7	323839	-4975	-4160	51.7	4077	-8053	2191	9.8	22432	-22432
247.6	304	176395	80.0	220372	-4144	-4491	61.1	4077	-7355	2165	9.7	22432	-22432
262.1	322	108859	83.2	130890	-3315	-4052	65.4	4077	-6195	2140	9.5	22432	-22432
276.7	340	53317	74.7	71356	-2488	-2997	71.4	3732	-4199	1713	7.6	22432	-22432
291.2	358	16223	44.2	36697	-1950	-1605	64.4	2480	-2493	857	3.8	22432	-22432
307.5	378	583	6.2	9378	-1862	-103	9.6	1072	-1072	6	0.0	22432	-22432

APPENDIX C

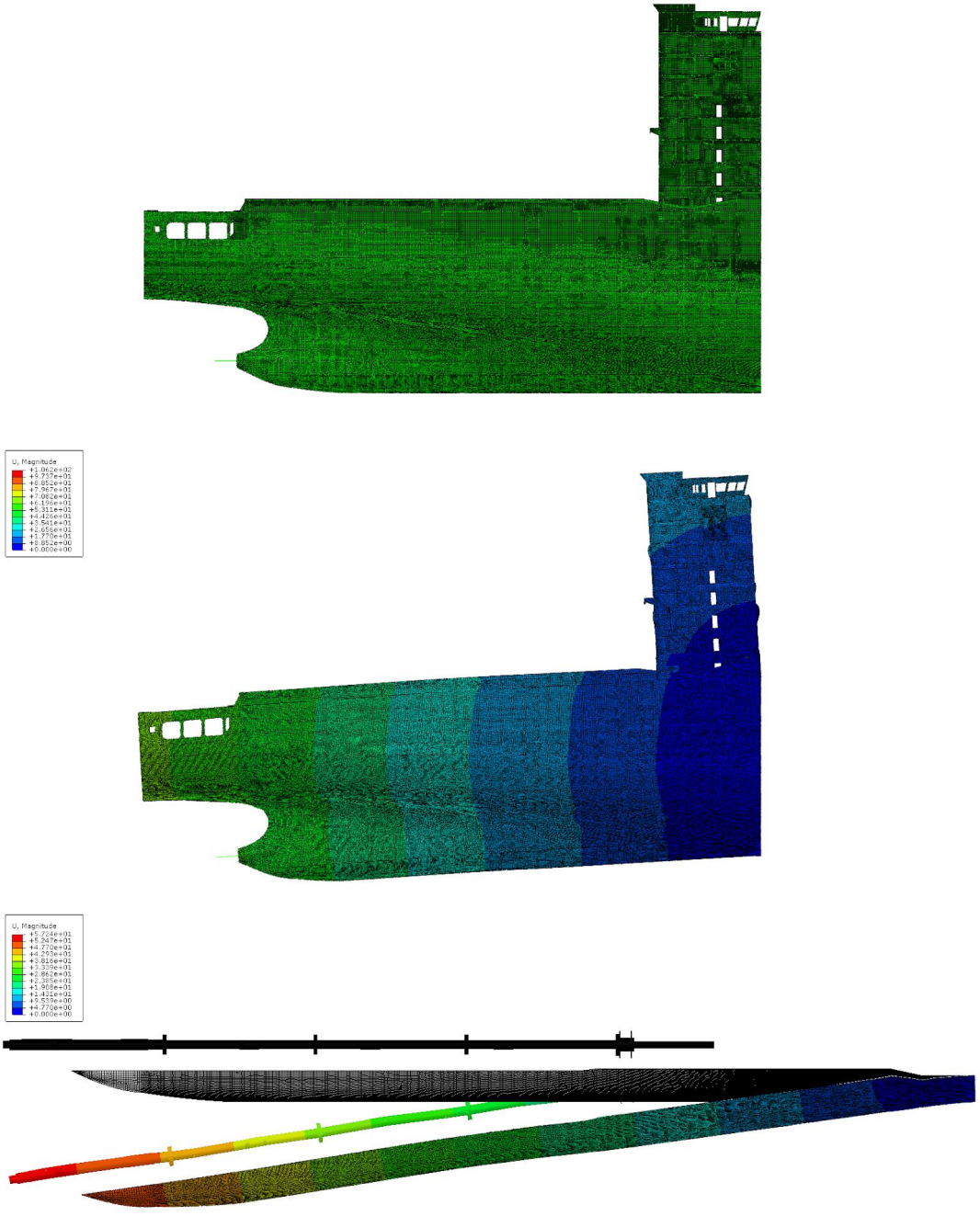

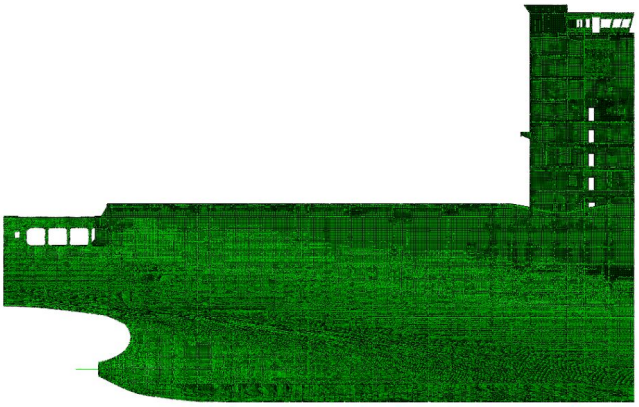

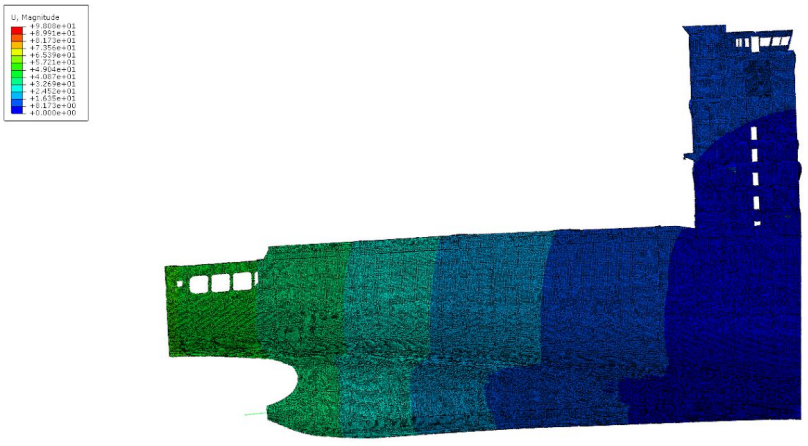
U, Magnitude
+9.808e+01
+8.991e+01
+8.173e+01
+7.356e+01
+6.539e+01
+5.721e+01
+4.904e+01
+4.087e+01
+3.269e+01
+2.452e+01
+1.635e+01
+8.173e+00
+0.000e+00

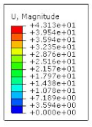
U, Magnitude
+4.313e+01
+3.954e+01
+3.594e+01
+3.235e+01
+2.876e+01
+2.516e+01
+2.157e+01
+1.797e+01
+1.438e+01
+1.078e+01
+7.189e+00
+3.594e+00
+0.000e+00

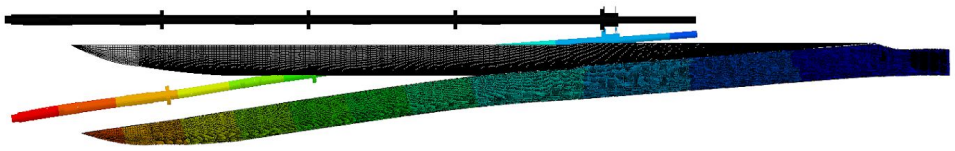

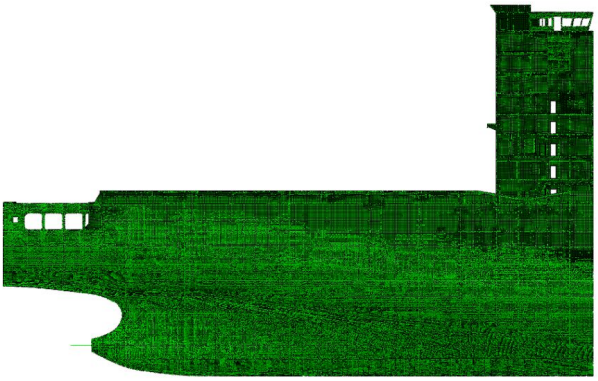

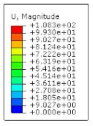
U, Magnitude
+1.083e+02
+9.930e+01
+9.027e+01
+8.124e+01
+7.222e+01
+6.319e+01
+5.416e+01
+4.514e+01
+3.611e+01
+2.709e+01
+1.806e+01
+9.027e+00
+0.000e+00

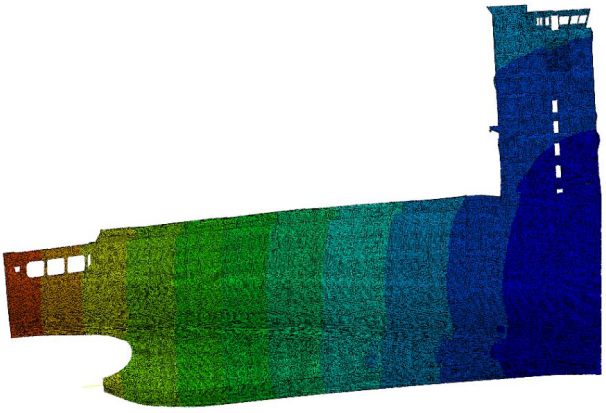

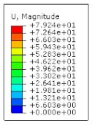
U, Magnitude
+7.904e+01
+7.264e+01
+6.623e+01
+5.983e+01
+5.283e+01
+4.622e+01
+3.962e+01
+3.302e+01
+2.641e+01
+1.981e+01
+1.321e+01
+6.603e+00
+0.000e+00

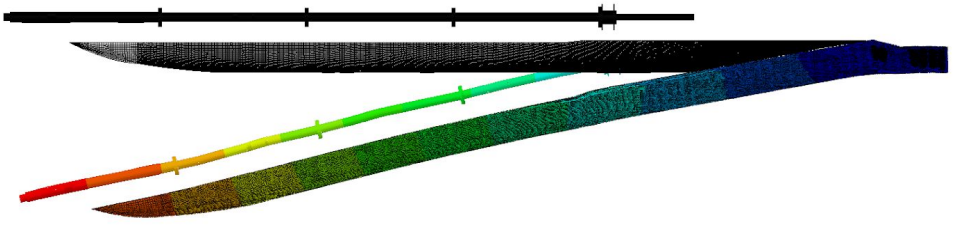

APPENDIX D

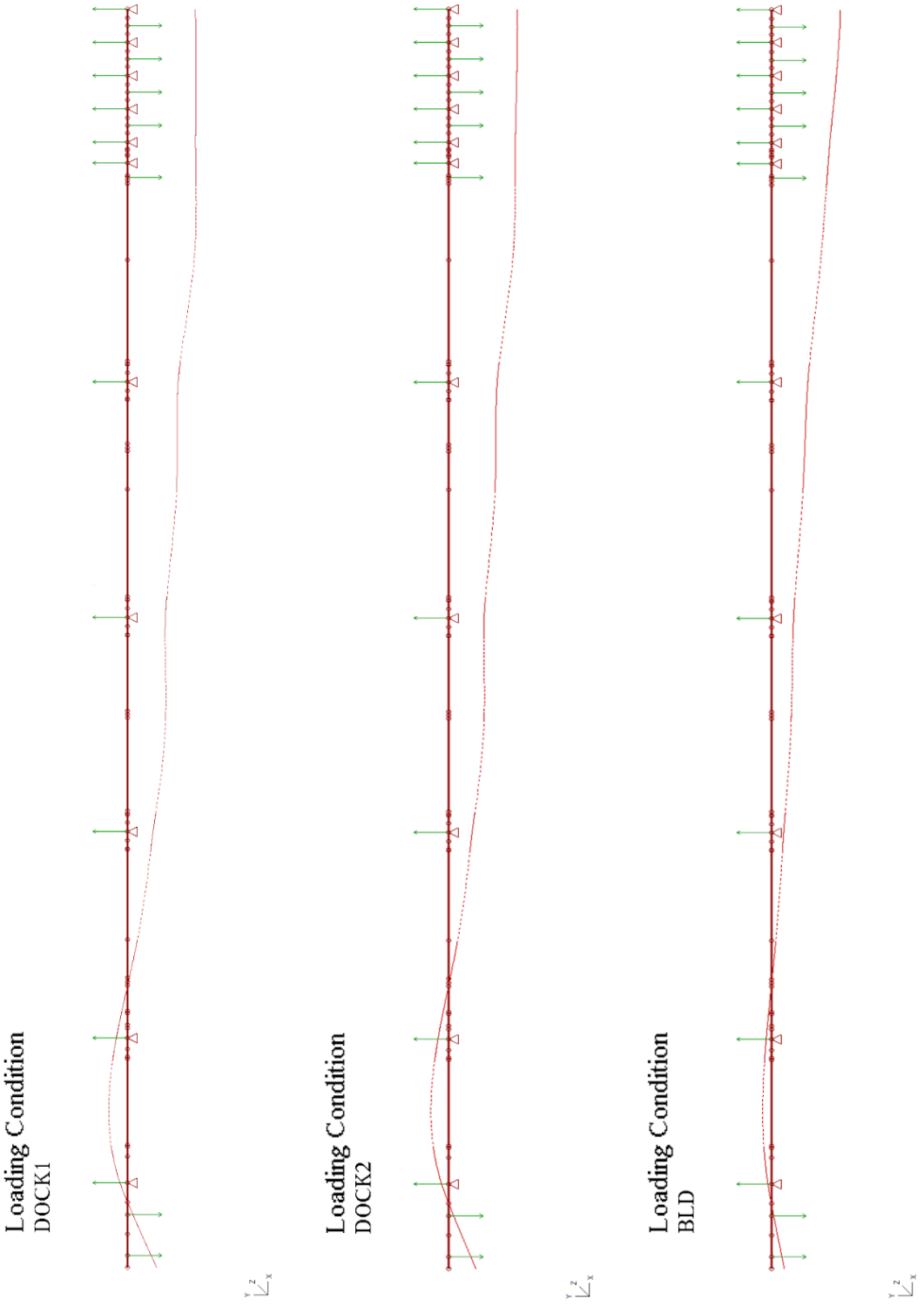
Loading Condition
DOCK1
Loading Condition
DOCK2
Loading Condition
BLD

Loading Condition
BLD-S11.1

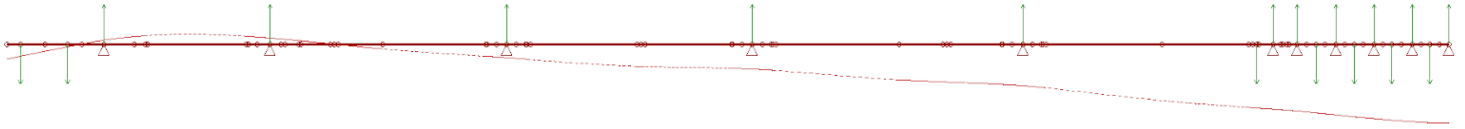

Loading Condition
BLD-PANAMA

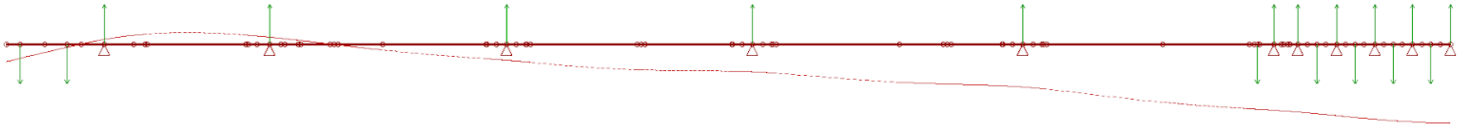

Loading Condition
BLM-PANAMA

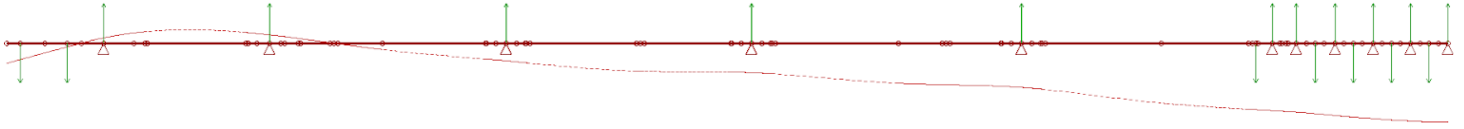

Loading Condition
BLA-PANAMA

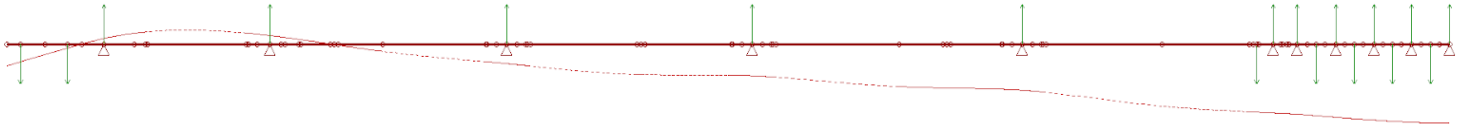

Loading Condition
16TDD

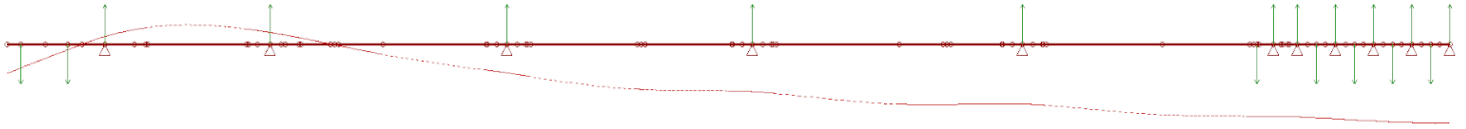

Loading Condition
16TAD

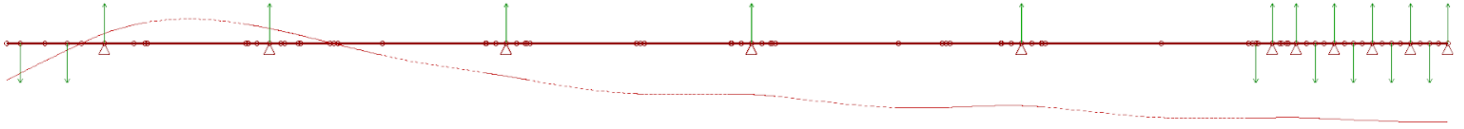

Loading Condition
11TDS

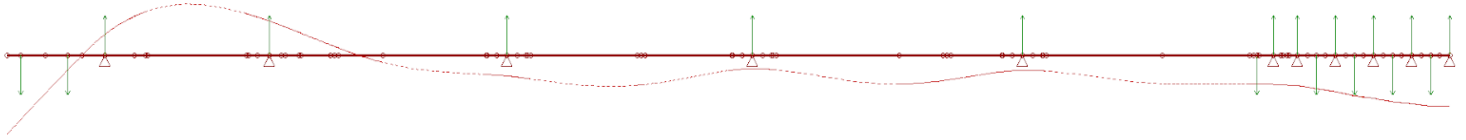

Loading Condition
11TAS

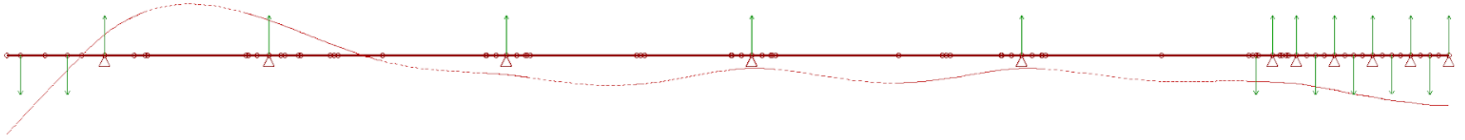

Loading Condition
16TDS

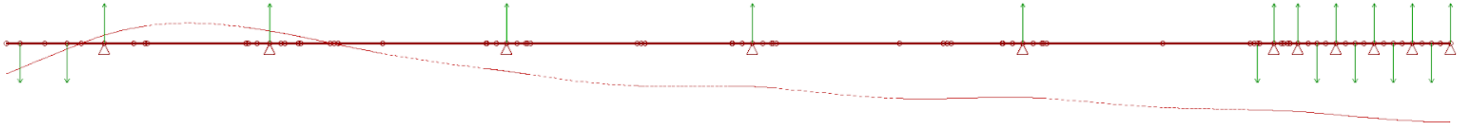

Loading Condition
16TAS

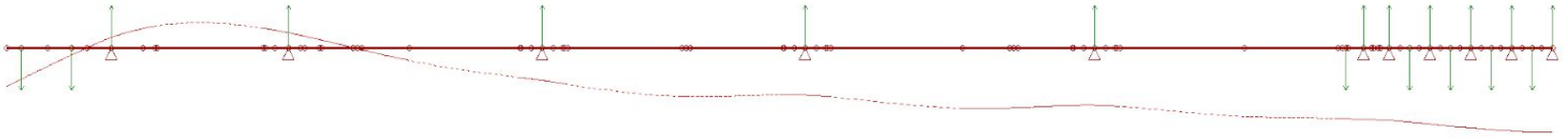

Loading Condition
MAX